Transcriptional Regulation of Synapse Remodeling in C. elegans

Dissertation Advisor: Prof Joshua M. Kaplan Author: Katherine L. Thompson-Peer

Transcriptional Regulation of Synapse Remodeling in *C. elegans*

ABSTRACT

The ability of a neuron to alter its synaptic connections during development is essential to circuit assembly. Synapse remodeling or refinement has been observed in many species and many neuronal circuits, yet the mechanisms defining which neurons undergo remodeling are unclear. Moreover, the molecules that execute the process of remodeling are also obscure. To address this issue, we sought to identify targets of the transcription factor *unc-55* COUP-TF, which acts as a cell-specific repressor of synapse remodeling in *C. elegans. unc-55* COUP-TF is expressed in VD neurons, where it prevents synapse remodeling. DD neurons can remodel synapses because they do not express *unc-55* COUP-TF. Ectopic expression of *unc-55* COUP-TF in DD neurons prevents remodeling.

We identified the transcription factor Hunchback-like *hbl-1* as a target of UNC-55 COUP-TF repression. Differential expression of *hbl-1* explains the cell-type specificity of remodeling. *hbl-1* is expressed in the DD neurons that are capable of remodeling, and is not expressed in the VD neurons that do not remodel. In *unc-55* mutants, *hbl-1* expression increases in VD neurons where it promotes ectopic remodeling. Moreover, *hbl-1* expression levels bidirectionally regulate the timing of DD remodeling, as increases in *hbl-1* cause precocious remodeling while decreases in *hbl-1* cause remodeling delays. Finally, *hbl-1* coordinates heterochronic microRNA and neuronal activity pathways to regulate the timing of remodeling. Increases or decreases in circuit activity cause increases or decreases in *hbl-1* expression, and consequently early or delayed remodeling. Thus,

convergent regulation of *hbl-1* expression defines a genetic mechanism that patterns activity-dependent synaptic remodeling across cell types and across developmental time.

We identified other targets of UNC-55 COUP-TF regulation using gene expression profiling, and implicate some of these factors in the regulation of remodeling using functional genomic screens. Our work suggests roles for conserved networks of transcription factors in the regulation of remodeling. We propose a model in which *hbl-1* and other targets of *unc-55* COUP-TF transcriptional repression are responsible for regulating synapse remodeling in *C. elegans.*

TABLE OF CONTENTS

Title Page *i*
Abstract *iii*
Table of Contents *v*
List of Figures and Tables *vii*
Acknowledgements *ix*

Chapter 1: Introduction ***1***
Overview *2*
A brief introduction to synaptogenesis *3*
Topics in synapse elimination *7*
Remodeling coordinates synapse formation and elimination *9*
Regulation of developmental time *15*
Synapse remodeling in *C. elegans* *17*
Outline of Dissertation *20*

Chapter 2: HBL-1 patterns synapse remodeling in *C. elegans* ***21***
Abstract *22*
Introduction *23*
Results *26*
VD neurons undergo ectopic synaptic remodeling in *unc-55* mutants *26*
UNC-55 inhibits *hbl-1* expression in VD neurons *31*
hbl-1 is required for ectopic remodeling of VD synapses in *unc-55* mutants *35*
DD remodeling occurs during a precise time window and is patterned spatially *42*
DD remodeling is delayed in *hbl-1* mutants *43*
DD remodeling occurs earlier in *mir-84* mutants *47*
Changes in GABA release do not alter the timing of DD plasticity *50*
Circuit activity regulates *hbl-1* expression and the timing of DD plasticity *51*
Discussion *56*
A conserved role for heterochronic genes in circuit development *56*
The role of UNC-55 COUP-TF in circuit development *57*
What role does HBL-1 play in synaptic remodeling? *58*
microRNA control of circuit refinement *59*
HBL-1 mediates the effects of activity on circuit refinement *59*
Methods *61*
Acknowledgements *64*

Chapter 3: Identification of synapse remodeling factors regulated by UNC-55 COUP-TF ***65***
Introduction *66*
Results *69*
Expression profiling of *unc-55* mutants *69*
RNAi screen of top microarray hits for roles in remodeling *77*
RNAi screen for suppressors of *unc-55* VD remodeling *78*

A potential role for Neuroblast clock homologs *80*
VD/AS cell division is not drastically delayed in *unc-55* mutants *81*
Analysis of the p38 MAPK *pmk-1* *82*
Analysis of the nuclear co-repressor *gei-8* *84*
Analysis of the pantothenate kinase *pnk-4* *86*
Discussion *87*
Many genes regulated by UNC-55 COUP-TF *87*
RNAi screens suggest additional transcriptional regulators of remodeling *89*
A role for cell cycle and cell division machinery? *91*
Methods *93*

Chapter 4: Discussion and Concluding Remarks ***98***
Transcriptional regulation of remodeling *99*
UNC-55 is a general repressor of remodeling *100*
From transcription factors to remodeling machinery *102*
Cell fate vs. remodeling *104*
Remodeling in different systems *106*

Appendix 1: Determining the neuronal activity regulating remodeling ***108***
Introduction *108*
Neuropeptides *109*
Activation of sensory neurons *112*

Appendix 2: The DAF-16 FOXO transcription factor regulates DD remodeling ***114***
Introduction *114*
Rationale *115*
Results *116*
Future Directions *121*

Appendix 3: Other regulators of remodeling ***122***

Appendix 4: Expression Profiling of *mir-1* and *mef-2* mutants ***124***
Overview *124*
Methods *125*

References ***129***

List of Figures and Tables

Chapter 1 Introduction

Fig 1.1. DD neurons remodel neuromuscular synapses between the first and second larval stages. *18*

Chapter 2 HBL-1 patterns synapse remodeling in *C. elegans*

Fig. 2.1. Imaging ectopic VD remodeling in *unc-55* mutants. *27*
Fig. 2.2. Electrophysiological evidence for ectopic VD remodeling in *unc-55* mutants. *29*
Fig. 2.3. Ventral VD synaptogenesis in *unc-55* mutants prior to remodeling. *30*
Fig 2.4. Predicted UNC-55 binding sites in the *hbl-1* promoter and in the promoters of *hbl-1* orthologs in other nematode species. *31*
Fig 2.5. UNC-55 COUP-TF represses *hbl-1* expression in VD neurons. *33*
Fig 2.6. HBL-1 transcriptional reporter *HgfpC* expression in VD neurons increases in *unc-55* mutants. *34*
Fig 2.7. Imaging demonstrates that ectopic VD remodeling in *unc-55* mutants requires HBL-1. *36*
Fig 2.8. Electrophysiology demonstrates that ectopic VD remodeling in *unc-55* mutants requires HBL-1. *38*
Fig 2.9. Cholinergic transmission was not affected by the *hbl-1* mutation. *39*
Fig 2.10. D neuron expression of *hbl-1* did not rescue non-neuronal phenotypes. *40*
Fig. 2.11. Behavior demonstrates that ectopic VD remodeling in *unc-55* mutants requires HBL-1. *41*
Fig 2.12. Expression of *hbl-1* in VD neurons did not cause ectopic remodeling of VD synapses. *42*
Fig 2.13. DD remodeling is patterned spatially and temporally. *43*
Fig 2.14. *hbl-1* is expressed in DD neurons during remodeling. *44*
Fig 2.15. DD remodeling is delayed in *hbl-1* mutants. *45*
Fig 2.16. L1-to-L2 development was not generally delayed in *hbl-1* mutants. *46*
Fig 2.17. The microRNA miR-84 regulates *hbl-1* expression. *48*
Fig 2.18. The microRNA miR-84 regulates the timing of remodeling by regulating *hbl-1*. *49*
Fig 2.19. The *mir-84* mutation did not cause a general change in the timing of L1-to-L2 development. *50*
Fig 2.20. DD remodeling proceeds normally in mutants lacking GABAergic synaptic transmission. *51*
Fig 2.21. Circuit activity regulates HBL-1 expression. *52*
Fig 2.22. Circuit activity determines the timing of DD neuron plasticity by regulating HBL-1. *54*
Fig 2.23. Increased activity mutations did not cause general changes in the timing of L1-to-L2 development. *55*

Chapter 3 Identification of synapse remodeling factors regulated by UNC-55 COUP-TF

Fig 3.1. Classes of UNC-55 targets in VD neurons. *66*
Fig 3.2. *unc-55* domain structure and mutant alleles. *69*
Fig 3.3. Volcano plot of gene expression changes in *unc-55(e1170)* mutants. *71*
Fig 3.4. Multiple microarray analysis methods identify *unc-55*-sensitive changes in gene expression. *71*
Table 3.1. Genes upregulated in *unc-55(e1170)* microarray relative to WT. *72*
Table 3.2. Genes downregulated in *unc-55(e1170)* microarray relative to WT. *74*
Fig 3.5. qPCR validation of microarray results. *76*
Table 3.3. Novel genes hit by RNAi screen for remodeling phenotypes. *77*
Table 3.4. Novel genes hit by 2-generation RNAi screen for *unc-55* suppressors. *78*
Table 3.5. Novel genes hit by 1-generation RNAi screen for *unc-55* suppressors. *79*
Table 3.6. Suppression of *unc-55* ectopic VD remodeling by neuroblast clock homologs. *81*
Fig 3.6. VD/AS terminal division is not delayed in *unc-55(e1170)* mutants. *82*
Fig 3.7. *pmk-1* mutants may have very subtle precocious DD remodeling at 11 hours post-hatching. *83*
Fig 3.8. *pmk-1* slightly suppresses *unc-55* mutant VD remodeling. *84*
Fig 3.9. *gei-8* suppresses *unc-55* mutant VD remodeling. *85*
Fig 3.10. *pnk-4* strongly suppresses *unc-55* mutant VD remodeling. *86*
Table 3.7. "Top hits" genes screened by RNAi for remodeling phenotypes. *96*

Appendix 1 Determining the neuronal activity regulating remodeling

Fig A.1. Precocious remodeling in *slo-1* mutants is suppressed by *hbl-1* mutation. *108*
Fig A.2. *egl-21 carboxypeptidase E* mutation does not suppress precocious remodeling in *slo-1 BK channel* mutants. *111*

Appendix 2 The DAF-16 FOXO transcription factor regulates DD remodeling

Fig B.1. DD remodeling is delayed in *daf-16 FOXO* mutants. *117*
Fig B.2. Delayed remodeling in *daf-2 InsR* mutants at restrictive temperatures. *118*
Fig B.3. *daf-2 InsR* mutation partially suppresses precocious remodeling of *tom-1* mutants. *119*
Fig B.4. Remodeling eventually completed in *daf-2 InsR* and *daf-16 FOXO* mutants. *120*
Fig B.5. *daf-2 InsR* and *daf-16 FOXO* do not suppress *unc-55* ectopic VD remodeling. *121*

Appendix 4 Expression Profiling of *mir-1* and *mef-2* mutants

Fig D.1. Volcano plot of genes differentially expressed in *mir-1* versus N2. *126*
Fig D.2. Signal intensity from *mir-1* and *mir-1;mef-2* microarrays. *127*
Fig D.3. Volcano plot of genes differentially expressed between *mir-1;mef-2* and *mir-1*. *128*

ACKNOWLEDGEMENTS

I would like to start off by thanking Josh Kaplan. He has been a phenomenal advisor for my graduate career. His enthusiasm for science is what originally attracted me to the lab, and it has never flagged. I can only hope to emulate his intellectual rigor and attention to detail. He gave me the space to fix my own mistakes, motivation when I needed it, encouragement when I was anxious, and unwavering support. He was thinking about my future plans well before I was, and helping me prepare for it all. His assistance with everything from the big picture message down to the smallest detail has been both instructive and tireless. He has been everything I knew I needed in a mentor and so many things I didn't know I needed. I have never wished that I had joined any other lab or had any other advisor.

I also owe a deep debt of gratitude to my remodeling buddy, Jihong Bai. Jihong has been my scientific partner since I joined the lab. I was contemplating projects, and Jihong had this super cool remodeling project up and running. From the moment I expressed interest, he has been nothing but enthusiastic and open. I have been so lucky to have such an amazing scientist and friend as a partner throughout graduate school. I can only hope to be as productive and innovative as he is. He was always generous with his time, always willing to take a look at a slide or help trouble-shoot an experiment. No matter where he is, though, Jihong never stops being my role model and colleague.

The Kaplan lab has been through multiple incarnations during my tenure, and I have enjoyed each one. When coming into lab means you get to see your friends, it is fun to be

there even when your experiments aren't going as planned. I learned about worms from my rotation advisor, Jeremy Dittman. Jeremy explains everything so well and so thoroughly that it is only later that you realize how much information he has packed into your brain. I found myself repeating the lessons he taught me when working with newer students, trying to pass on half as much information. His relaxed attitude and thoughtful approach made me immediately comfortable.

When I joined the Kaplan lab, there was an awesome group of graduate students in the lab. Jason McEwen, once you get to know him, is irreverent and sarcastic and thoroughly entertaining. Denise Chun is approachable and has an unexpected sense of humor. Amy Vashlishan Murray is kind and warm and generous. Dave Simon is provoking and opinionated and great fun. Sabrina Hom is a wonderful listener, gives great hugs, and is always up for a good discussion of audiobooks. As predecessors, they could not have set a better path to follow. I would also like to thank the former Kaplan post-docs Jon Madison, Derek Sieburth, QueeLim Ch'ng, Shilpa Vashist, and Susanne Hausselt for their encouragement. I would especially like to thank Kavita Babu, whose enthusiasm for the things she loves is truly impressive.

The current iteration of the Kaplan lab is wonderful as well. I'd like to thank Monica Feliu-Mojer and Seungwon Choi, for their camaraderie in graduate school. I know that they both will do amazing things, and I can't wait to see what. My long-standing bay mate, Ed Pym, has been fantastic. Whether as lab DJ, lunchtime and teatime enforcer, or random outlet for venting, I have appreciated his presence at my back. Zhitao Hu was kind enough to do some electrophysiological recordings for me, and I admire his inhuman productivity. Yingsong Hao is fabulous, especially at odd hours of the night. I am grateful that Dorian

Anderson is crazy enough to want to work on remodeling as well, and am in awe of his energy. Tambu Kudze and XiaJing Tong are excellent newer additions to the lab, and will leave their mark on it as well.

I would like to acknowledge the rotation students with whom I have had the pleasure of working. Monica Thanawala, Peter Wang, and Mike Sussman were all intelligent scientists, and fantastic to work with.

I would be remiss not to acknowledge the contributions of the other worm labs on the Simches 7th floor. I have repeatedly pestered members of the Ruvkun and Ausubel labs, and have received generous guidance in response.

I appreciate the advice of my Dissertation Advisory Committee members. Gary Ruvkun, Mike Greenberg, and Lisa Goodrich have all helped to improve the quality of my research, to clarify my scientific presentations, and to offer advice on for my career and future. I would also like to thank the other professors that allowed me to rotate with them during my first year, Tom Schwarz and Adrian Salic.

Before starting graduate school, I had the wonderful opportunity to work with Alex Kolodkin at Johns Hopkins. Working in Alex's lab set the bar for what working in a lab should be like, so that I knew what I wanted in a graduate lab: everyone was helpful, fun, and insightful, the science was inventive and rigorous, and Alex's mentoring was adapted to each person's needs. Alex has continued to be an invaluable mentor for me throughout my graduate career, and I appreciate his encouragement.

I would like to thank the funding agencies that supported my research. In addition to grants awarded to Josh, I have been supported by the National Science Foundation Graduate Research Fellowship and the Albert J Ryan Foundation Fellowship.

Finally, I deeply and sincerely thank my friends and family for all the many joys they have brought to my life, both big and small. I adored getting to know my brother, Jeff, better during the years we both lived in Boston, and while he may have moved away, I cherish the way that living near each other has changed our relationship. Thank you to my mother and father and stepmother for their continuous love and support. Thank you to my in-laws, I look forward to another opportunity to get trekking again. Lastly, thank you to my wife Sarah, who is the best partner I could have asked for, and who is the reason for my success in so many ways.

Chapter 1

Introduction

Overview of introductory remarks

The correct assembly of neurons into circuits is required for the development of a functional nervous system. After an axon or dendrite is targeted by guidance cues to the proper target area, many factors play essential roles in regulating synaptic specificity to organize neurons into functional circuits (reviewed in (Sanes and Yamagata, 2009)). Even with all of these systems in place, developing neurons often initially make synaptic connections to inappropriate targets or make more synaptic connections than the adult circuit requires. Thus, in addition to specificity during synaptogenesis, synapse elimination is also required for proper circuit assembly. Neurons must balance formation and elimination of synaptic connections during development, to ensure that they have the proper number of connections at the end of developmental plasticity. The coordinated process of adding and removing synapses is called synapse remodeling or refinement.

The experiments in this dissertation investigate the regulation of synapse remodeling, using the nematode *C. elegans*, to better understand how neuronal circuits form during development. In this introduction, I first consider synapse formation, then synapse elimination. I review examples of developmental synaptic remodeling, which coordinates these two processes. I then describe mechanisms regulating developmental time in other tissues. Finally, I introduce an example of synapse remodeling observed in *C. elegans*, which becomes the system we exploit to dissect synapse remodeling.

A brief introduction to synaptogenesis

Mechanisms of synapse formation vary depending on pre-synaptic neuron type and the post-synaptic target (Waites et al., 2005). After guidance of the axon or dendrite to a general region, many redundant signaling mechanisms, both pre-synaptically and post-synaptically located, ensure synaptic specificity in partner selection (Sanes and Yamagata, 2009). For example, pre- and post-synaptic partners may express recognition molecules, as in the retina, where mutual expression of Sidekick or DSCAM homophilic adhesion proteins cause pre- and post-synaptic neurites expressing the same protein to project to the same sublaminal layer (Yamagata and Sanes, 2008). Conversely, inappropriate partners may express repellant molecules, or intermediate targets may guide synaptogenesis. For example, *C. elegans* vulval epithelial cells act as synaptic guideposts to direct HSNL neurons to form synapses with adjacent neurons and muscles, via interactions between the immunoglobulin superfamily protein SYG-1 in the HSNL neuron and SYG-2 in the epithelial cells (Shen and Bargmann, 2003; Shen et al., 2004).

Synaptogenesis follows target selection, and involves trans-synaptic signaling between the axon and the target cell. In some systems, signaling mechanisms within the neuron dictate where synapses are formed, while in other systems signaling from the target cell, such as a dendritic shaft, seem to be instructive (Garner et al., 2006). There is an extensive literature on synaptogenesis at the neuromuscular junction and within the central nervous system, which suggests some common factors but also many divergent pathways that determine the number and localization of synapses. In both the CNS and PNS, activity plays an important role in regulating the number of synapses, through a

variety of mechanisms including activity-dependent expression of transcription factors (Lin et al., 2008).

In the pre-synaptic neuron, the electron-dense presynaptic density must form, synaptic vesicles must aggregate, and the active zone must be assembled (Ziv and Garner, 2004). Synaptogenesis involves the localization of voltage-gated calcium channels, synaptic vesicle fusion machinery such as the SNARE proteins Syntaxin, Synaptobrevin, and SNAP25, and other trafficking machinery such as Synaptotagmin, Rim, Munc13, and Munc18. Endocytic machinery, such as Synaptojanin, Endophilin, dynamin, and AP180 must also be localized to the synapse for SV recycling. Active zones may be separated from non-synaptic regions by periactive zones, defined by proteins like RPM-1 Highwire. The liprin-alpha SYD-2 is important for organizing the presynaptic structure.

Synaptic components are delivered to the axon from the cell body in different packets (Ziv and Garner, 2004). The identities of these packets are not comprehensively described. Some of the components are delivered to the synapse in transport packets, such as the presynaptic scaffolding proteins *bassoon*, *piccolo*, and *Rim*, while others are delivered in association with synaptic vesicles. In cultures of hippocampal neurons during synapse formation, some active zone components have been observed to localize prior to exocytic machinery, suggesting that perhaps active zones assemble first (Ahmari et al., 2000; Shapira et al., 2003). Synaptic vesicles are trafficked from the cell body by the UNC-104 Kinesin KIF1A, along with associated cargo (Hall and Hedgecock, 1991).

In the central nervous system of mammals and *Drosophila*, dendritic filopodia play an early role in synaptogenesis. Filopodial projections from dendritic shafts can be highly motile or relatively stable, depending on the neuron type and developmental time. In

primary cultures of dissociated neurons, dendritic filopodia have been shown to induce the formation of pre-synaptic structures at sites of contact with nearby axons (Ziv and Garner, 2004). Axons are also capable of extending protrusions that might contact dendrites nearby and induce synapse formation.

What molecules are responsible for translating contact into synapse formation? Neurotrophins such as BDNF and NT3, and Wnt ligands can promote synapse formation. Cell adhesion molecules, such as N-CAM, L1, cadherins and protocadherins, neurexins and neuroligins, and syndecans, are important for the adhesion and development of different synapses. For example, N-cadherin is a member of the calcium-dependent family of cell adhesion molecules (CAMs; (Arikkath and Reichardt, 2008)). N-cadherin spans the synaptic cleft to connect the presynaptic active zone and the post-synaptic density, and intracellularly associates with the actin cytoskeleton via alpha- and beta-catenin. Experiments with dominant-negative N-cadherin that has only the intracellular domain decreased the number of presynaptic boutons formed with dendritic protrusions. CAMs are thought to promote synapse formation by stabilizing contact between dendritic protrusions and the axon shaft, as well as by initiating intracellular signaling pathways (Garner et al., 2006).

In mammals, neurons innervate their targets, so the target cell must form a post-synaptic density where neurotransmitter receptors assemble and aggregate. At the mammalian neuromuscular junction, prepatterning of cholinergic receptor clusters in the muscle, involving the muscle specific kinase MuSK, occurs before motor neuron growth cone arrival (Sanes and Lichtman, 2001). Upon arrival at the muscle, motor neurons secrete the proteoglycan agrin to induce further clustering of acetylcholine receptors via

the muscle MuSK receptor and the effector protein rapsyn. Nerve terminals also secrete neuregulin, which increases acetylcholine receptor transcription and maturation of postsynaptic structures, via ErbB tyrosine kinases. In turn, muscle cells, via retrograde signaling, induce maturation of the presynaptic active zone.

At GABAergic synapses, the post-synaptic scaffolding protein gephyrin is important for clustering $GABA_A$ receptors (Kneussel et al., 1999). Dytrophin also seems to play a role in GABAA receptor clustering (Fritschy et al., 2012). $GABA_A$ receptors are pentameric, and different $GABA_A$ receptor subunit composition may contribute to a diversity of responses to GABA. In hippocampal pyramidal neurons and cerebellar granule cells, different subunits preferentially localize to different subcellular domains (Moss and Smart, 2001). GABA synapses also change from excitatory early in development to inhibitory later, due to the late expression of a chloride exporter (Ben-Ari, 2002).

Post-synapse formation at the neuromuscular junction is not a passive process. In *Drosophila*, myoblasts extend actin-rich structures called myopodia (Ritzenthaler et al., 2000). Myopodia, initially even spaced across the muscle, cluster at the time of neuronal innervation, in a manner dependent on local cell adhesion molecule signaling (Ritzenthaler and Chiba, 2003; Kohsaka and Nose, 2009). In *C. elegans*, muscles first send out protrusions, called muscle arms, to contact the *en passant* synapses in the ventral nerve cord before forming post-synaptic densities. Muscle arms are formed both embryonically and post-embryonically. Embryonically formed muscle arms are thought to arise from attachments between the myoblast and the axon prior to myoblast migration, but post-embryonic muscle arm development is regulated by active cytoskeletal rearrangements (Dixon and Roy, 2005). In the absence of functional synaptic signaling in *unc-104* mutants,

muscle arm extension is compromised, suggesting that neurons release an unidentified attractant (Hall and Hedgecock, 1991).

Little is known about the development of post-synaptic structures opposite cholinergic motor neurons in *C. elegans.* Innervation of the muscle by GABAergic neurons is required for clustering and maintenance of $GABA_A$ UNC-49 receptors in *C. elegans* (Gally and Bessereau, 2003). Three splice isoforms of the $GABA_A$ receptor are generated from the UNC-49 locus (Bamber et al., 1999; 2005). Receptor clustering in the muscle only occurs after innervation and the accumulation of synaptic vesicle markers in the neuron. However, animals defective for GABA synthesis, neurotransmitter secretion, or neuropeptide secretion cluster $GABA_A$ receptors normally, so GABA signaling itself is not inducing receptor accumulation (Gally and Bessereau, 2003; Rowland et al., 2006).

Topics in synapse elimination

Synapse elimination is less well understood on a molecular level than synapse formation, nevertheless it plays an equally important role in circuit assembly. Presynaptic, postsynaptic, and non-neuronal signals can direct a synapse for elimination.

Activity plays an important role in regulating which synapses are eliminated. The role of activity, and specifically competition, in regulating synapse elimination has been beautifully described at the mammalian neuromuscular junction (Walsh and Lichtman, 2003). Muscles are initially innervated by multiple motor neurons (Purves and Lichtman, 1980). Competition between neurons results in the expansion of one neuron to occupy the

entire target area, and the elimination of inputs from other neurons (Sanes and Lichtman, 1999).

In the mammalian central nervous system, GABA transmission is implicated in the regulation of synapse elimination during inhibitory circuit development (Huang and Scheiffele, 2008). Live imaging of cortical neurons in mice with blocked GABA release from basket interneurons demonstrated that GABA can regulate synapse elimination and axon pruning (Wu et al., 2012). In these mice, blocking GABA signaling resulted in cell-autonomous bouton stabilization, increased filopodial density, increased axon branch extension, and decreased axon branch retraction (Wu et al., 2012).

In the *Drosophila* neuromuscular junction, disrupting cytoskeletal stability in the presynaptic neuron can cause synapse elimination. Mutations in the spectrin/ankyrin cytoskeleton induce synapse elimination (Koch et al., 2008; Pielage et al., 2008; 2011). In some cases, synapse elimination is the first step towards more severe pruning of neurites, though in other cases synapse elimination occurs in the absence of pruning (reviewed in (Luo and O'Leary, 2005)).

Ubiquitin and the proteasome have been described to play important roles in synapse elimination and pruning (Watts et al., 2003; Kuo et al., 2005; 2006). For example, the E3 ubiquitin ligase complex of SKR-1 and SEL-10 are locally activated in HSN neurons in *C. elegans*, and are responsible for local synapse elimination (Ding et al., 2007). The synapse adhesion molecule SYG-1 protects nearby synapses from elimination by binding SKR-1 and inhibiting complex assembly. Thus, local activation of ubiquitin-mediated protein degradation is important for selective synapse elimination.

Synapse elimination involves not only the pre-synaptic neuron and the post-synaptic target, but other cells as well. Glial cells are important for the process of synapse elimination. Glial cells engulf debris following neurite pruning, and also engulf synapses to drive synapse elimination (Watts et al., 2004; Chung and Barres, 2011). Signaling from non-neuronal cells can induce synapse elimination. Recent work has highlighted the role of immune molecules in signaling for synapse elimination (reviewed in (Schafer and Stevens, 2010)). Immature astrocytes cause postnatal neurons to express C1q, the initiating protein in the complement cascade (Stevens et al., 2007). C1q is localized to synapses. Mice lacking C1q or downstream factors failed to refine retinogeniculate connections. They failed to eliminate excess retinal innervation by lateral geniculate neurons. This suggests that synapses are targeted for elimination by the complement cascade. Similar functions have been described for the MHC1 class of molecules in activity-dependent remodeling in the retinogeniculate circuit and ocular dominance plasticity (Huh et al., 2000).

Remodeling coordinates synapse formation and elimination

Developing neurons need to form new synapses with new targets and eliminate other synapses in a coordinated manner, so that the final number of synapses is neither too many nor too few. The coordinated process of adding and removing synapses is called synapse refinement or remodeling. Remodeling has been studied in a number of mammalian systems. We briefly review four of these systems below, and use one study in each system to highlight a general feature of remodeling.

The retinogeniculate synapse

Visual information is received by the retina, transmitted by retinal ganglion cells to the dorsal lateral geniculate nucleus, specifically to thalamic relay neurons. These relay neurons project to the primary visual cortex for information processing. The retinogeniculate synapse undergoes remodeling in at least three stages (Hong and Chen, 2011). In the first stage up to postnatal day 8, retinal ganglion cell axons project into the lateral geniculate nucleus, and form initial contacts. While inputs from the eyes initially overlap, they segregate into eye-specific zones when some synapses are eliminated while others are retained. This eye-specific segregation phase of remodeling is experience-independent, as it occurs before birth in cats and monkeys or before eye opening in mice and ferrets.

During a second phase, between postnatal day 8 and 16, with eye opening occurring around day 12-14, some retinogeniculate synapses are eliminated while others are strengthened. Spontaneous retinal activity, including retinal waves driven by glutamatergic transmission and the spiking of individual retinal ganglion cells, though not vision itself, drives this phase of remodeling.

During the final phase of remodeling between postnatal day 16 and 32, refinement continues, albeit at a reduced rate. Strong synaptic connections are maintained or strengthened. The transcription factor MeCP2 plays a role in this experience-dependent third phase of retinogeniculate remodeling, but not in the earlier second phase of remodeling (Noutel et al., 2011). Mice lacking MeCP2 form, strengthen, and eliminate synapses normally during the spontaneous activity-driven second phase. During the final phase (after postnatal day 21), mice lacking MeCP2 exhibit disrupted synaptic plasticity in

response to visual deprivation, and retinal inputs fail to strengthen properly. After pruning of a given relay neuron during the second phase or remodeling, MeCP2 mutant mice actually increase the RGC innervation during the third phase, which is the opposite of normal. At a gross anatomical level, defect in eye-specific segregation are observed after postnatal day 34. Dark rearing mice during this final phase usually results in stereotypical changes in retinal input strength; these changes are diminished in MeCP2 mutants.

Together, the retinogeniculate synapse example demonstrates that remodeling can be a multi-step process, with distinct stages for large- and small-scale changes in synaptic connections. These different stages occur at precise times in development. Though activity plays a role in many stages, the nature of the driving activity (spontaneous versus experience-dependent in this case) varies and is interpreted differently. How does the relay neuron know whether the input it receives from the retina is spontaneous or experience-dependent? One potential explanation is that there are different regulators for different stages in the process, so that input results in different cellular responses.

Purkinje neuron & climbing fiber synapses

Synaptic connections between climbing fibers and Purkinje neurons in the cerebellum undergo activity-dependent plasticity (reviewed in (Bosman and Konnerth, 2009)). Climbing fibers from the inferior olive of the brainstem enter the cerebellum, and form synapses onto the only output neurons from the cerebellar cortex, the GABAergic Purkinje neurons. Between postnatal day 3 and 5, an average of five climbing fibers form synapses onto each Purkinje neuron. In an activity-dependent process, one of these is

strengthened and grows, while the others are weakened and eventually disappear. In the adult, a single climbing fiber contacts each Purkinje neuron.

The transition from many to one climbing fiber connecting to the Purkinje neuron is the result of multiple events. Climbing fibers engage in mutual competition with the other neurons presynaptic to the Purkinje neurons, the parallel fibers, to restrict the target field of each input. Additionally, not all climbing fibers are created equal: size and strength differences exist from almost the beginning, and the same Purkinje neuron activity that strengthens already strong inputs also weakens already weak inputs. It has been proposed that stronger climbing fibers contact mainly the dendrites of Purkinje neurons, while the weaker climbing fibers contact mainly the Purkinje cell body, and that this may contribute to their differences.

We can conclude that neuronal activity, and in this case competition between neurons of the same type and between neurons of different types, regulates remodeling. How might competition regulate remodeling? The Purkinje neurons could decide which synapses to retain or eliminate, and then weaker inputs could receive less neurotrophic support or punishment signals. Retrograde signaling pathways initiated by the Purkinje neurons could signal to climbing fibers to retract. The complex calculations performed by target cell to determine which synapses are retained or eliminated are not yet understood.

Eye-specific segregation in the primary visual cortex

The primary visual cortex is one of the most well described systems for the examination of experience-dependent remodeling (reviewed in (Hensch, 2005; Sugiyama et al., 2009)). Inputs from each eye initially converge on the same binocular zone of the

visual cortex. Competitive interactions eventually determine which eye dominates the cortical cells. Imbalances in visual activity during specific critical periods of development, due to monocular deprivation or other experimental manipulations, result in the strengthening of one eye's input at the expense of the other. The neurotransmitter GABA plays a key role in this process, as mice lacking the ability to synthesize GABA fail to strengthen one input or weaken the other (Hensch et al., 1998; Chattopadhyaya et al., 2007). Additionally, the brain-derived neurotrophic factor BDNF plays an important role in the regulation of ocular dominance (Huang et al., 1999). Transgenic mice with early expression of BDNF have precocious maturation of GABAergic innervation, development of visual acuity, and termination of the ocular dominance critical period. Experience-dependent expression of microRNAs also play a role in restricting ocular dominance formation, although the target genes regulated by these microRNAs have yet to be identified (Mellios et al., 2011; Tognini et al., 2011).

Recent work described the role of the homeodomain protein Otx2, which is expressed in bipolar and photoreceptor cells in the retina and the interneurons in the lateral geniculate nucleus (Sugiyama et al., 2008). Otx2 seems to move trans-synaptically to the parvalbumin-positive neurons in the visual cortex in an experience-dependent manner, where it regulates PV-cell maturation and ocular dominance remodeling potential. The maturation of PV-cells is coincident with the initiation of remodeling potential. It would be interesting to know what aspects of PV-cell maturation are responsive to Otx2 delivery, and how the delivery of Otx2 is so tightly controlled by vision.

More generally, we see that transcription factors can mediate experience-dependent remodeling, in this case through non-cell autonomous mechanisms. These transcription

factors regulate the timing of remodeling by promoting the maturation of the neurons, in this case the PV-cells. Non-autonomous delivery of Otx2 to only some cells provides a mechanism to explain how cells that are initially similar acquire distinct features.

Pyramidal neurons in the neocortex

Pyramidal neurons in the neocortex are perhaps the most amenable to long-term live imaging of neuronal structure, through windows in the skull or thinned skull segments (Xu et al., 2007). Dendritic spines and filopodia can be imaged using two-photon microscopy over extended periods of time. Alterations in spine density were originally observed by Ramon y Cajal, who noted that pyramidal neuron spine density was higher during early postnatal development than in adults (Hua and Smith, 2004). Spines undergo developmental activity-dependent remodeling, stabilization, and pruning (Grutzendler et al., 2002; Trachtenberg et al., 2002; Holtmaat et al., 2005). Similar spine changes are observed during learning or following alterations in the sensory environment (Holtmaat and Svoboda, 2009; Yang et al., 2009; Lai et al., 2012). Spine growth precedes synapse formation, although certainly not all spines result in synapses (Knott et al., 2006). Recent work has suggested that local glutamate increases are capable of inducing spine formation from an adjacent dendritic shaft (Kwon and Sabatini, 2011). Exactly how glutamate signals for spine formation during this period in development, but not at other points, is not yet understood.

Pyramidal neurons retain some ability to remodel their synapses in the adult, although different studies describe different levels of plasticity, and it is certainly at a reduced level than during development (Grutzendler et al., 2002; Trachtenberg et al., 2002;

Holtmaat et al., 2005; Pan and Gan, 2008). This ability to remodel in the adult seems to be cell-type specific (reviewed in (Holtmaat and Svoboda, 2009)). As an example, layer 2/3 pyramidal cell apical dendrites turn over spines less than layer 5 pyramidal cells (Holtmaat et al., 2005).

In this example, as in others, the capacity for remodeling is often different between different cell types. Selective expression of factors responsive to activity, that initiate remodeling programs, could be responsible for this feature.

Regulation of developmental time

In order to better understand how the timing of remodeling is regulated, it is helpful to think about how the timing of development is regulated in other tissues. The coordination of developmental events across tissues is an important general question for developmental biologists (reviewed in (Frasch, 2008)). We discuss three examples to illustrate general principles of how developmental time is regulated.

In *C. elegans*, genes that control the timing of developmental events are called heterochronic genes (Ambros and Horvitz, 1984). When these genes are mutated, developmental events such as cell division or differentiation are precocious or delayed. Heterochronic genes are often either transcription factors or the microRNAs that regulate the expression of those transcription factors (Pasquinelli and Ruvkun, 2002; Moss, 2007). *lin-14* was one of the first heterochronic genes identified, and is one of the best described. The heterochronic transcription factor *lin-14* is responsible for defining developmental events during the first larval stage of *C. elegans*. Mutants lacking *lin-14* skip L1

developmental events. LIN-14 is expressed at high levels during this stage. The expression of LIN-14 is shut off by the expression of the microRNA LIN-4, which is turned on at the end of the L1 stage. Mutants lacking *lin-4* express LIN-14 at high levels throughout development, and reiterate L1 events at later stages in development. In general, heterochronic genes in *C. elegans* are responsible for temporal identity (Frasch, 2008).

In the *Drosophila* nervous system, the sequence of transcription factors known as the neuroblast clock plays an important role in defining the temporal identity of daughter cells as they divide from the neuroblast (Grosskortenhaus et al., 2005). The transcription factors generally promote the expression of the next gene, and repress the expression of the next+1 gene. In general, the transition from the expression of one gene to the next is tied to mitotic division (Cleary and Doe, 2006).

While heterochronic genes and neuroblast clock transcription factors act mostly cell-autonomously, non-autonomous mechanisms can coordinate development between tissues. In *Drosophila*, pulses of the steroid hormone ecdysone are responsible for defining the boundaries between different stages in development (Thummel, 2001; Frasch, 2008). Ecdysone acts through activation of the ecdysone receptor (EcR) and RXR homolog Ultraspiracle (Usp) heterodimeric receptor complex. Different isoforms of these receptor subunits, expressed at different stages of development and in different tissues, partially account for the variety of responses to a single hormone. Ecdysone complexed with EcR/Usp binds the regulatory sequences of primary response genes, like the zinc finger transcription factor *Broad Complex (Br-C)* and the ETS domain transcription factor *E74*. These primary response genes then activate or repress expression of secondary effector

genes that direct specific developmental events in different tissues. Signaling by the EcR regulates pruning of neurons during development (Lee et al., 2000; Marin et al., 2005).

From all of these examples, we can see that transcription factors play an important role in the regulation of developmental time, both in defining temporal identity and defining temporal boundaries. Hormone or microRNA regulation restricts transcription factor activity, either by regulating TF expression or by regulating TF activity.

Synapse Remodeling in *C. elegans*

While insights into synaptogenesis have arisen from work in *C. elegans*, fewer studies have examined other aspects of circuit assembly, such as synapse remodeling. Combining genetic analysis with a stereotyped nervous system presents specific advantages to study the process of remodeling.

The nervous system of *C. elegans* consists of 302 neurons with defined lineages, locations in the animal, and synaptic partners (White et al., 1986). Synapses in *C. elegans* are *en passant*, meaning that synaptic boutons form along the neurite shaft with muscle arms reaching into the nerve cord to form synapses (White et al., 1976). In *C. elegans* adults, two neurotransmitters, acetylcholine and GABA, regulate body muscle contraction. GABAergic signaling from D-type motor neurons inhibits muscle contraction. There are two types of GABAergic neurons: 13 VD neurons that form synapses onto the ventral muscle, and 6 DD neurons that form synapses onto the dorsal muscle. By contrast, cholinergic motor neurons, which can be categorized as ventral VA and VB neurons and dorsal DA and DB neurons, cause muscle contraction. The DA, DB, and DD neurons are

born embryonically, while the VA, VB, and VD neurons are born post-embryonically, during the late L1 period(Sulston, 1976).

What regulates ventral muscle contraction in animals during the first larval stage (L1) right after hatching? Electron microscopy demonstrated that DD neurons in L1 animals form neuromuscular junctions with the ventral muscle, and receive input dorsally from DA and DB neurons (Fig. 1.1, left) (White et al., 1978). Between the first and second larval stages, the connectivity of DD neurons reverses, so that they form neuromuscular junctions with the dorsal muscle (Fig 1.1, right). This highly stereotyped example of synapse remodeling has been observed using EM, GFP-tagged synaptic proteins expressed in neurons, GFP-tagged $GABA_A$ UNC-49 receptors, and the localization of muscle arms (White et al., 1978; Hallam and Jin, 1998; Gally and Bessereau, 2003; Dixon and Roy, 2005).

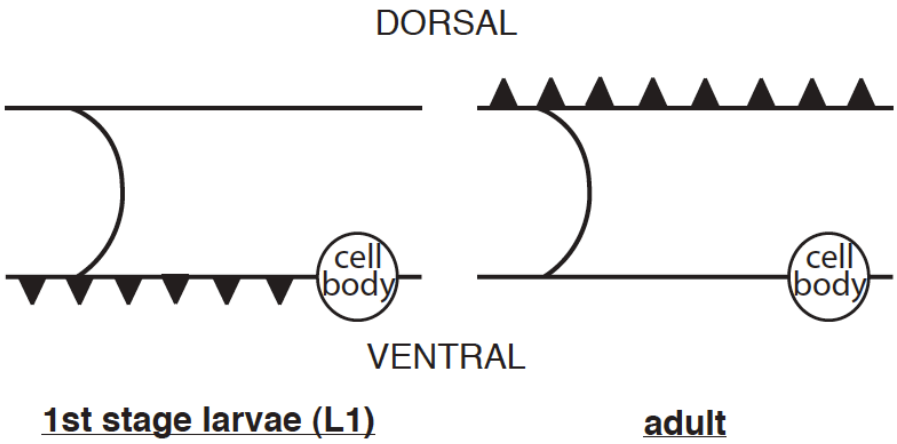

Fig 1.1. DD neurons remodel neuromuscular synapses between the first and second larval stages. During the first larval stage (L1, left), DD neurons form NMJs (triangles) with ventral muscle. After remodeling, in the second larval stage through adulthood (right), DD neurons form NMJs with dorsal muscle. DD cell bodies (circles) are located in the ventral nerve cord. Neurites in the ventral and dorsal nerve cords are connected by a commissure.

The timing of DD neuron remodeling is regulated by the heterochronic transcription factor *lin-14* (Hallam and Jin, 1998). Without *lin-14* expression, DD remodeling occurs precociously. *lin-14* acts as a general determinant of L1-stage events (Pasquinelli and Ruvkun, 2002). *lin-14* mutants skip L1 developmental events in many tissues, and later developmental events occur precociously (Ambros and Horvitz, 1987). Genetic screens for mutants that caused precocious DD remodeling similar to *lin-14* mutations identified many proteins essential for determining where synaptogenesis occurs, such as *syd-1,* and *syd-2 liprin-alpha*, but not other regulators of remodeling (Zhen and Jin, 1999; Hallam et al., 2002).

VD and DD neurons are quite similar. They function in the adult motor circuit in complimentary fashions, each receiving input on one side of the animal and responsible for relaxing the muscle on the opposite side of the animal. There are 13 VDs to 6 DD neurons, and they send out projections that occupy distinct but adjacent positions within the nerve cord (White et al., 1986). Yet, even though they are born at different times and arise from different lineages, they express an almost identical set of genes. In both neuron types, the transcription factor UNC-30 specifies expression of genes required for GABA synthesis and signaling (Jin et al., 1994).

The most notable difference between VD and DD neurons is the ability of DD neurons to remodel, while VD neurons do not remodel their synapses. The comparison between DD neurons that can remodel with VD neurons that cannot remodel forms the basis for much of our work. As will be discussed in Chapters 2 and 3, the VD neurons cannot remodel because they express the transcription factor UNC-55 COUP-TF, which acts

as a repressor of remodeling. We have used the search for genes repressed by UNC-55 COUP-TF as a way to identify genes important for promoting remodeling.

Dissertation Overview

In Chapter 2, I provide evidence that the heterochronic transcription factor Hunchback-like-1 (HBL-1) is an important target of UNC-55 COUP-TF repression in VD neurons, and that this in part accounts for the ectopic VD neuron remodeling in *unc-55 COUP-TF* mutants. Furthermore, HBL-1 plays an important role coordinating developmental cues with circuit activity to determine the timing of DD neuron remodeling. In Chapter 3, I more thoroughly introduce what is known about the mammalian homologs of *unc-55*, COUP-TFI and II. I discuss experiments to identify and characterize other genes that play an important role in synapse remodeling by looking at genes whose expression is regulated by the remodeling repressor UNC-55. Expression profiling experiments using microarrays were followed by RNAi screening for remodeling defects, and further characterization of some of the hits. Finally, in Chapter 4, I discuss the wider implications of this work, and possible connections to remodeling in other systems. I discuss preliminary experiments for future directions in the appendices, including attempts to isolate the neuronal activity that regulates remodeling (Appendix 1), a role for FOXO transcription factors in regulating remodeling (Appendix 2), and RNAi knockdown of other genes, including heterochronic genes, that perturbs remodeling (Appendix 3).

Chapter 2

HBL-1 patterns synaptic remodeling in *C. elegans*

This chapter contains work published as Thompson-Peer KL, Bai J, Hu Z, & Kaplan JM. (2012) HBL-1 patterns synaptic remodeling in *C. elegans*. *Neuron*. Volume 73, Issue 3, 453-465, 9 February 2012.

Katherine Thompson-Peer and Jihong Bai contributed equally to this work. Jihong generated the synaptically localized GFP strain used to image D neuron synapses, and first noticed the *hbl-1* remodeling defect. He also performed most of the cloning and subcloning, imaged the dorsal cord of adult animals, and generated a few of the strains. Katherine performed all of the other imaging experiments, the locomotion and quantitative PCR experiments, some of the subcloning, and generated most of the strains. Zhitao Hu performed all of the electrophysiological recordings. Katherine and Joshua Kaplan assembled the manuscript, with input from Jihong.

ABSTRACT

During development, circuits are refined by the dynamic addition and removal of synapses; however, little is known about the molecular mechanisms that dictate where and when synaptic refinement occurs. Here we describe transcriptional mechanisms that pattern remodeling of *C. elegans* neuromuscular junctions (NMJs). The embryonic GABAergic DD motor neurons remodel their synapses, while the later born VD neurons do not. This specificity is mediated by differential expression of a transcription factor (HBL-1), which is expressed in DD neurons but is repressed in VDs by UNC-55/COUP-TF. DD remodeling is delayed in *hbl-1* mutants whereas precocious remodeling is observed in mutants lacking the microRNA *mir-84*, which inhibits *hbl-1* expression. Mutations increasing and decreasing circuit activity cause corresponding changes in *hbl-1* expression, and corresponding shifts in the timing of DD plasticity. Thus, convergent regulation of *hbl-1* expression defines a genetic mechanism that patterns activity-dependent synaptic remodeling across cell types and across developmental time.

INTRODUCTION

A hallmark of all nervous systems is the dynamic addition and removal of synaptic connections. Despite its universality, synaptic remodeling has primarily been studied in vertebrates. In mammals, synaptic remodeling occurs in many, and perhaps all circuits. For example, at the neuromuscular junction (NMJ), each muscle is initially innervated by multiple axons, and the mature pattern of mono-innervation emerges following a period of synaptic elimination (Purves and Lichtman, 1980; Goda and Davis, 2003; Luo and O'Leary, 2005). Similarly, in the cerebellum, Purkinje cells eliminate exuberant climbing fibers inputs (Bosman and Konnerth, 2009). Live imaging studies in the mouse cortex also suggest that dendrites continuously extend and retract spines during development (Grutzendler et al., 2002; Trachtenberg et al., 2002; Holtmaat et al., 2005). From these and other studies, a great deal has been learned about how changes in axonal and dendritic structures are patterned during development.

Much less is known about the molecular mechanisms that pattern synaptic refinement in vertebrates. In particular, several important questions remain unanswered. Although remodeling occurs throughout the life of an animal, there is a general trend for increased plasticity earlier in development. For each circuit, plasticity often occurs during brief time intervals, which are termed critical periods (Hensch, 2004). While remodeling occurs in most, and perhaps all circuits, different cell types within a circuit exhibit the capacity for plasticity at distinct times. For example, in the visual cortex, plasticity in layer 4 ends prior to plasticity in more superficial layers (Oray et al., 2004; Jiang et al., 2007). How is plasticity restricted to specific cell types and specific developmental times? In all known cases, vertebrate synaptic refinement is highly

dependent on circuit activity, which implies that plasticity is dictated by competition between cells in these circuits. A few activity-induced genes have been implicated in synaptic refinement. For example, ocular dominance plasticity is correlated with activity-induced changes in the expression of CREB and BDNF (Hensch, 2004). However, activity induces CREB and BDNF expression in many (perhaps all) neurons, including dissociated neurons in culture (Lonze and Ginty, 2002; Cohen and Greenberg, 2008). How does altered expression of general activity induced genes confer cell and temporal specificity on circuit refinement? Because circuit refinement plays a pivotal role in shaping cognitive development, there is great interest in defining the molecular and genetic mechanisms that determine how refinement is patterned.

To address these questions, we exploited an example of genetically programmed synaptic remodeling in *C. elegans*. During the first larval stage (L1), the DD GABAergic motor neurons undergo a dramatic remodeling whereby synapses formed with ventral body muscles in the embryo are eliminated and replaced by synapses with dorsal muscles (White et al., 1978; Hallam and Jin, 1998; Park et al., 2011). DD remodeling occurs without retraction or extension of neurite processes. Instead, the DD ventral process switches from an axonal to a dendritic fate (and vice versa for the dorsal process).

Many aspects of *C. elegans* larval development are controlled by cell intrinsic developmental timing genes, which are generically termed heterochronic genes (Moss, 2007). In particular, the heterochronic gene *lin-14* controls the timing of hypodermal development, whereby L2 hypodermal cell fates are expressed precociously during the L1 in *lin-14* mutants (Ambros and Horvitz, 1984). Similarly, *lin-14* is expressed in DD neurons, and DD remodeling occurs earlier in *lin-14* mutants, initiating during embryogenesis (Hallam and Jin, 1998). Thus,

LIN-14 dictates when DD remodeling is initiated. This was the first study to show that heterochronic genes play a role in post-mitotic neurons to pattern synaptic plasticity. Because *lin-14* orthologs are not found in other organisms, it remains unclear if control of synaptic plasticity by heterochronic genes represents a conserved mechanism. DD plasticity (like other forms of invertebrate plasticity) is generally considered to be genetically hard wired, i.e. dictated by specific cell intrinsic genetic pathways. Thus, it also remains unclear if activity-induced refinement of vertebrate circuits and DD plasticity represent fundamentally distinct processes, which are mediated by distinct molecular mechanisms.

Here we show that a second heterochronic gene, *hbl-1*, regulates several aspects of DD plasticity. The *hbl-1* gene encodes the transcription factor HBL-1 (Hunchback like-1) (Fay et al., 1999). We show that convergent pathways regulate *hbl-1* expression in D neurons, conferring cell and temporal specificity and activity dependence on D neuron plasticity. Thus, our results define a cell intrinsic genetic pathway that dictates a form of activity dependent synaptic refinement.

RESULTS

VD neurons undergo ectopic synaptic remodeling in *unc-55* mutants

The DD motor neurons are born during embryogenesis, and remodel their synapses during the L1. A second class of GABAergic motor neurons, the VD neurons, is born during the late L1 stage but does not undergo remodeling. VD neurons share many other characteristics with DD neurons, including similar cell body positions, similar axon morphologies, similar roles in controlling locomotion, and similar expression profiles (Jorgensen, 2005). Like DDs, VD neurons initially form ventral synapses; however, unlike the DDs, VD neurons retain these ventral synapses in the adult. VD and DD neurons also differ in that a transcriptional repressor (UNC-55) is expressed in the VD but not in the DD neurons, and this difference has been proposed to explain the disparity in their ability to undergo synaptic remodeling (Walthall, 1990; Walthall and Plunkett, 1995; Zhou and Walthall, 1998; Shan et al., 2005).

Prior studies suggested that VD neurons undergo ectopic remodeling in *unc-55* mutants (Walthall and Plunkett, 1995; Zhou and Walthall, 1998; Shan et al., 2005). These studies showed that adult *unc-55* mutant VD neurons lacked ventral axonal varicosities and ventral GFP-tagged synaptobrevin (SNB-1) puncta, consistent with the idea that ventral VD synapses in *unc-55* had been eliminated due to ectopic expression of the DD neuron remodeling program (Walthall and Plunkett, 1995; Zhou and Walthall, 1998; Shan et al., 2005) (Fig. 2.1a). To confirm these results, we analyzed VD synapses in adult *unc-55* mutants by both imaging and electrophysiology. To image these synapses, we expressed two GFP-tagged pre-synaptic proteins (UNC-57 endophilin and SNB-1 synaptobrevin) in the D neurons (using the *unc-25*

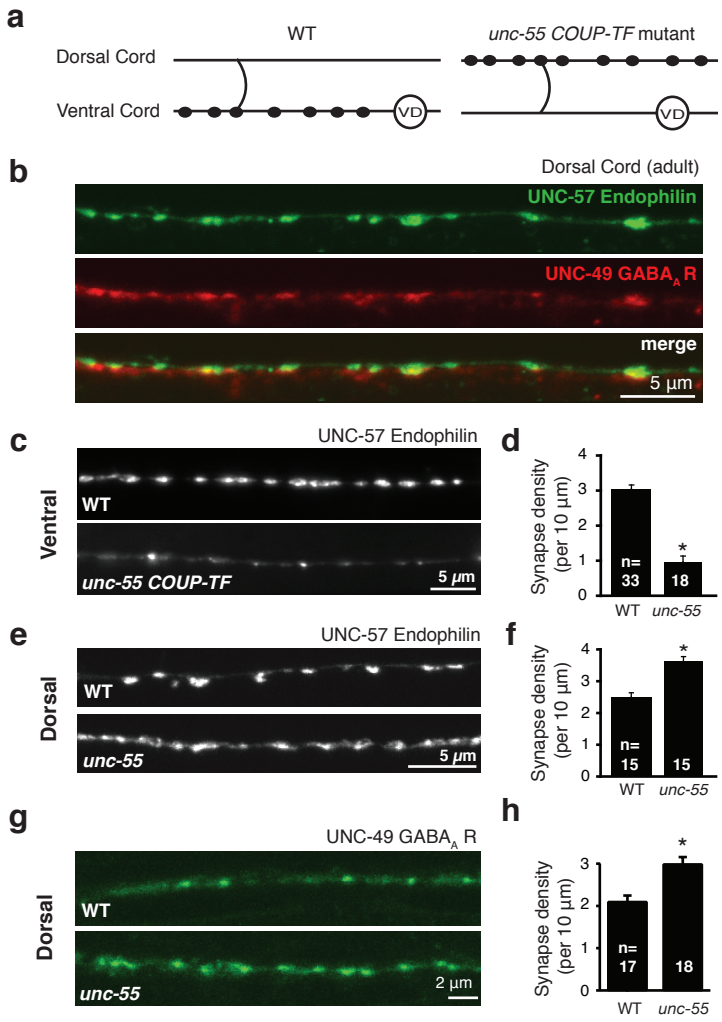

Fig 2.1. Imaging ectopic VD remodeling in *unc-55* mutants. **(a)** Schematic illustrations of VD neuron NMJs (filled ovals) in wild type and *unc-55* adults. Dorsal is up and posterior is to the right in both illustrations; open circles are cell bodies. In wild type adults VD neurons retain ventral NMJs, whereas in *unc-55* mutants ventral NMJs are eliminated and replaced with dorsal synapses. **(b)** Dorsal cord GABAergic synapses are visualized using pre- (Endophilin UNC-57::GFP, *unc-25* promoter) and post-synaptic ($GABA_A$ receptor UNC-49::mCherry, *myo-3* promoter) markers in the adult. **(c-h)** Imaging of adult GABAergic NMJs using the pre-synaptic UNC-57::GFP marker (c-f) and the post-synaptic $GABA_A$ receptor UNC-49 marker (g-h). Representative images and summary data for ventral (c,d) and dorsal (e-h) GABAergic NMJs. Error bars indicate SEM, * $p< 0.001$ by student's t test.

GAD promoter). In wild type adults, both UNC-57 and SNB-1 were expressed in a punctate pattern in the nerve cords, and these puncta were closely apposed to post-synaptic sites in body muscles (labeled with mCherry-tagged UNC-49 $GABA_A$ receptors) (Fig. 2.1b and data not shown). These ventral cord puncta likely correspond to VD NMJs, since the VDs are the only neurons that form ventral GABAergic synapses in adults (White et al., 1986). In *unc-55* adults, the density of UNC-57 puncta in the ventral cord was significantly reduced compared to wild type controls (Fig. 2.1c-d). By contrast, pre-synaptic (UNC-57) and post-synaptic (UNC-49 $GABA_A$) puncta densities were significantly increased in the dorsal cord of *unc-55* adults (Fig. 2.1e-h).

To assay the function of GABAergic synapses, we recorded inhibitory post-synaptic currents (IPSCs) from adult ventral and dorsal body muscles. In *unc-55* mutants, ventral IPSC rates were significantly reduced (33 Hz wild type, 0.1 Hz *unc-55*, $p < 0.0001$), whereas dorsal IPSC rates were significantly increased (33 Hz wild type, 65 Hz *unc-55*, $p < 0.0001$ Student's t test) (Fig. 2.2a-d). Thus, inactivation of *unc-55* shifts GABAergic NMJs from ventral to dorsal muscles, as assessed by both imaging and electrophysiology. The rates and amplitudes of excitatory post-synaptic currents (EPSCs) were indistinguishable in wild type and *unc-55* ventral body muscles (Fig. 2.2e-g), suggesting that cholinergic transmission was unaltered. Consequently, the loss of ventral synapses in *unc-55* mutants was specific for GABAergic (i.e. VD) synapses.

The absence of ventral GABAergic NMJs in *unc-55* adults could result from decreased formation or decreased retention of ventral NMJs. To assay ventral synapse formation, we imaged ventral GABAergic synapses in L2 larvae. We observed similar patterns of closely apposed pre-synaptic (UNC-57) and post-synaptic (UNC-49 $GABA_A$ receptor) puncta in the

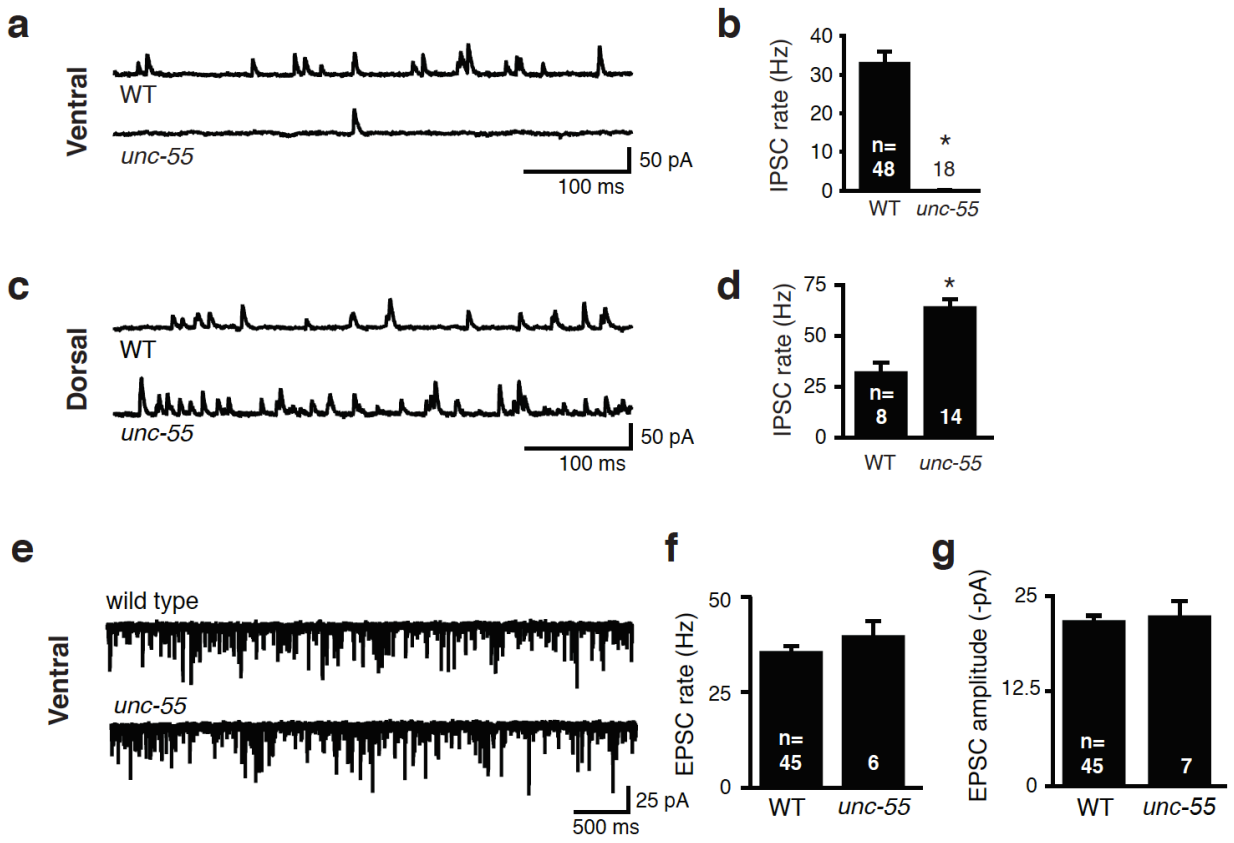

Fig 2.2. Electrophysiological evidence for ectopic VD remodeling in *unc-55* mutants. **(a-d)** Representative traces and summary data for endogenous IPSCs recorded from adult ventral (a,b) and dorsal (c,d) muscles. Summary data for IPSC amplitudes are shown in Fig. 2.8e-f. **(e-g)** Representative traces and summary data for endogenous EPSCs recorded from adult ventral muscles. No significant differences in EPSC rate or amplitude were observed in *unc-55* mutants.

ventral cord of *unc-55* and wild type L2 larvae, indicating that inactivation of *unc-55* did not disrupt ventral synapse formation by VD neurons (Fig. 2.3). These ventral NMJs in L2 animals were detected using transgenes driving UNC-57::GFP expression in both DDs and VDs (using the *unc-25* promoter; Fig. 2.3a-b), and those driving expression in VD and AS neurons (using the *unc-55* promoter; Fig. 2.3c-d). The AS neurons are cholinergic neurons that form dorsal NMJs (White et al., 1986); consequently, the ventral puncta labeled by both transgenes likely

correspond to ventral VD synapses. Collectively, these results suggest that VD neurons initially form ventral synapses in *unc-55* mutants but that these ventral synapses are subsequently removed by ectopic expression of the DD remodeling pathway, as proposed in the prior studies (Walthall and Plunkett, 1995; Zhou and Walthall, 1998; Shan et al., 2005).

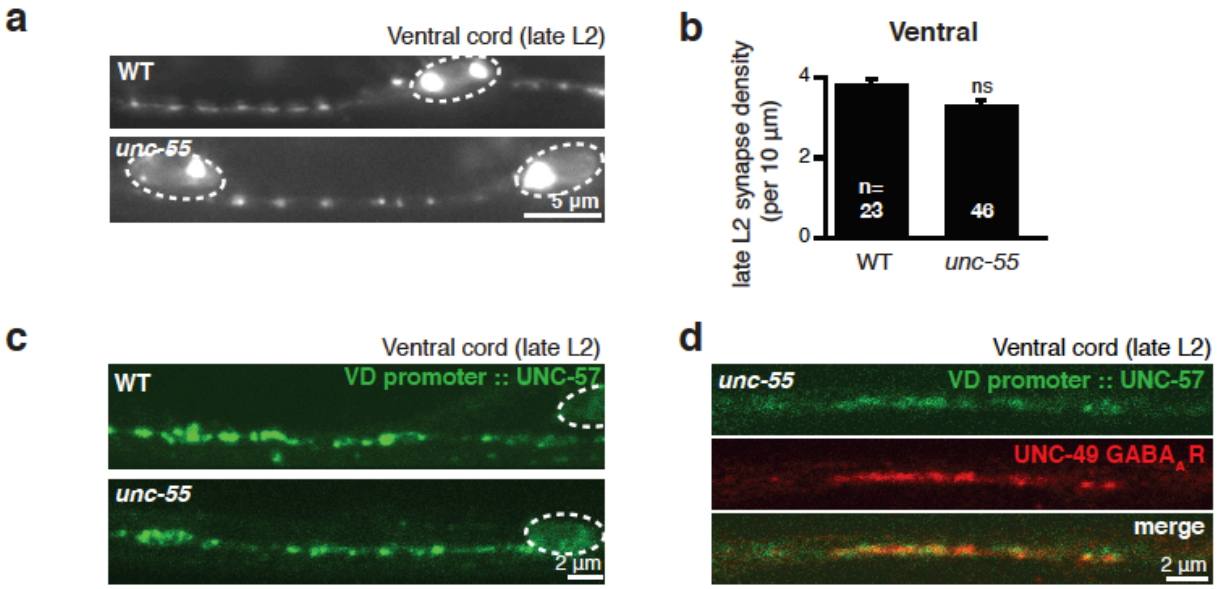

Fig 2.3. Ventral VD synaptogenesis in *unc-55* mutants prior to remodeling. Ventral VD synapses were labeled with UNC-57::GFP expressed in D neurons (*unc-25* promoter) (a,b) or in VD and AS neurons (*unc-55* promoter) (c,d). No significant differences (ns) were observed in the density of ventral VD synaptic puncta in wild type and *unc-55* mutant L2 larvae (b). Ventral UNC-57 pre-synaptic puncta in L2 larvae were apposed to UNC-49 $GABA_A$ receptor puncta, expressed in body muscles (d). Dashed lines circle the D neuron cell bodies.

The *unc-55* gene encodes an orphan nuclear hormone receptor that is expressed in the VD but not the DD motor neurons (Zhou and Walthall, 1998). Several results suggest that UNC-55 acts as a transcriptional repressor. In VD neurons, UNC-55 represses expression of the proneuropeptide gene *flp-13* (Melkman and Sengupta, 2005; Shan et al., 2005). Furthermore, UNC-55 orthologs in mammals (COUP-TF) and *Drosophila* (Sevenup) both function as

transcriptional repressors (Zelhof et al., 1995; Tsai and Tsai, 1997; Pereira et al., 2000). These results lead to the hypothesis that UNC-55 inhibits remodeling of VD synapses by repressing expression of target genes required for remodeling (Zhou and Walthall, 1998).

UNC-55 inhibits *hbl-1* expression in VD neurons

In *Drosophila*, Sevenup represses expression of the C2H2-type Zinc finger transcription factor *hunchback* (Kanai et al., 2005; Mettler et al., 2006). Prompted by the *Sevenup* data, we considered the possibility that the *C. elegans* hunchback ortholog (*hbl-1*) is an UNC-55 target (Fay et al., 1999). Consistent with this idea, the *hbl-1* promoter contains four predicted UNC-55 binding sites, and similar binding sites were found in promoters of *hbl-1* orthologs in *C. remanei, C. briggsae, C. brenneri*, and *C. japonica* (Fig. 2.4). Furthermore, we found that expression of the *hbl-1* mRNA (as assessed by qPCR) was increased in whole worm lysates isolated from *unc-*

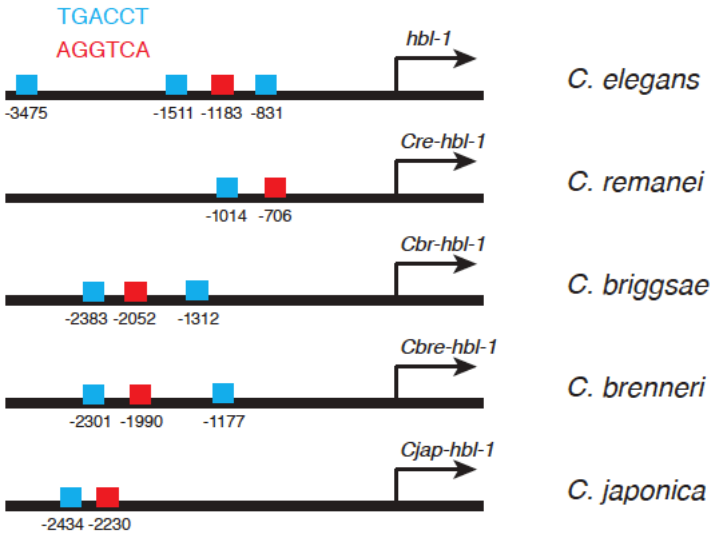

Fig 2.4. Predicted UNC-55 binding sites in the hbl-1 promoter and in the promoters of hbl-1 orthologs in other nematode species. The C. elegans hbl-1 promoter has four predicted UNC-55 binding sites (at -831 bp, -1183 bp, and -1511 bp, and -3475 bp relative to the start site) (Shan et al., 2005).

55 mutants, compared to wild type controls (14±1.7% increase, $p < 0.01$). Based on these initial results, we did several further experiments to test the idea that *hbl-1* is an UNC-55 target.

If *hbl-1* is an UNC-55 target, then *hbl-1* expression in DD neurons should be greater than that found in VDs. To test this idea, we analyzed expression of two GFP reporter constructs containing the *hbl-1* promoter (Fig. 2.5). To distinguish between transcriptional and post-transcriptional regulation of *hbl-1*, the reporter constructs contain 3' UTR sequences derived from either a control (*unc-54* myosin) or the *hbl-1* mRNA (*HgfpC* and *HgfpH*, respectively). VD and DD neurons were identified using a GABA marker (mCherry expressed by the *unc-25* GAD promoter) and were distinguished based on the position and morphology of their cell bodies (detailed in the methods). We compared *hbl-1* reporter expression in VD10 and DD5, which have adjacent cell bodies in the ventral cord. For both reporters, DD5 expression was significantly higher than that observed in VD10 (DD5/VD10 fluorescence ratios: *HgfpC* 6.6±0.8, $p < 0.0001$ paired Student's t test; *HgfpH* 3.6±0.7, $p < 0.05$ paired Student's t test; Fig. 2.5c). Similar results were observed when reporter expression was compared in all DD and VD neurons (DD/VD fluorescence ratios: *HgfpC* 5.6 ±0.5, $p < 0.0001$ paired Student's t test; *HgfpH* 2.6±0.4, $p < 0.005$ paired Student's t test; Fig. 2.5a-b, Fig. 2.6a,c). These results indicate that the *hbl-1* promoter is expressed at significantly higher levels in DD neurons than in VD neurons.

The decreased *hbl-1* reporter expression in VD neurons could result from UNC-55 mediated repression of the *hbl-1* promoter. To test this possibility, we analyzed expression of the *HgfpC* reporter in *unc-55* mutants. *HgfpC* expression in VD neurons was significantly increased in *unc-55* mutants (197% wild type levels, $p<0.001$ Student's t test), indicating increased transcription of the *hbl-1* promoter in *unc-55* mutant VD neurons (Fig. 2.5d, 2.6). The magnitude of the increased *HgfpC* expression differed in individual VD neurons. For VD10,

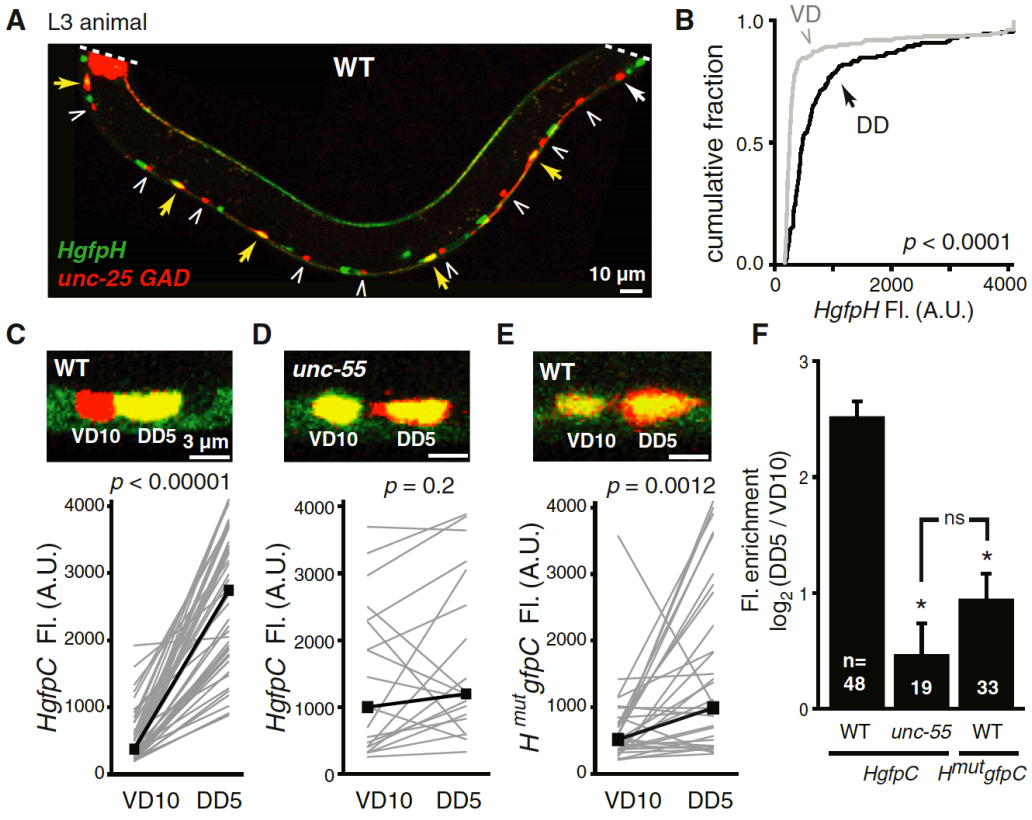

Fig 2.5. UNC-55 COUP-TF represses *hbl-1* expression in VD neurons.

(a-b) A representative image and summary data of *hbl-1* (*HgfpH*, green) and GAD (red) reporter expression in wild type L3 animals. Yellow arrows indicate DD cell bodies expressing both markers, white arrows indicate DD cell bodies lacking *HgfpH* expression, and carrots indicate VD cell bodies. *HgfpH* expression was significantly lower in VD than DD neurons ($p < 10^{-5}$ by Kolmogorov-Smirnov test; 150 DD (black) and 260 VD (gray) cells were analyzed). **(c-f)** *HgfpC* (c,d) or H^{mut}*gfpC* (e) transcriptional reporter expression (green) is compared for adjacent VD10 and DD5 neurons in wild type (c,e) and *unc-55* (d) mutant animals. Gray lines connect VD10 and DD5 cells in the same animal, black lines connect median values (p-values by paired Student's t test). Average $\log_2$ of the ratio of DD5 to VD10 fluorescence for *HgfpC* and H^{mut}*gfpC* was plotted in (f), and n = number of animals analyzed (*, $p<10^{-5}$ difference from WT; ns, p=0.2; by Student's t test). Error bars indicate SEM.

HgfpC expression in *unc-55* mutants rose to the same level observed in DD5 neurons (Fig. 2.5d); however, in most cases, *HgfpC* expression in *unc-55* mutant VD neurons remained significantly lower than that observed in DD neurons (DD/VD fluorescence ratio in *unc-55*: *HgfpC* 2.3±0.4, *p*

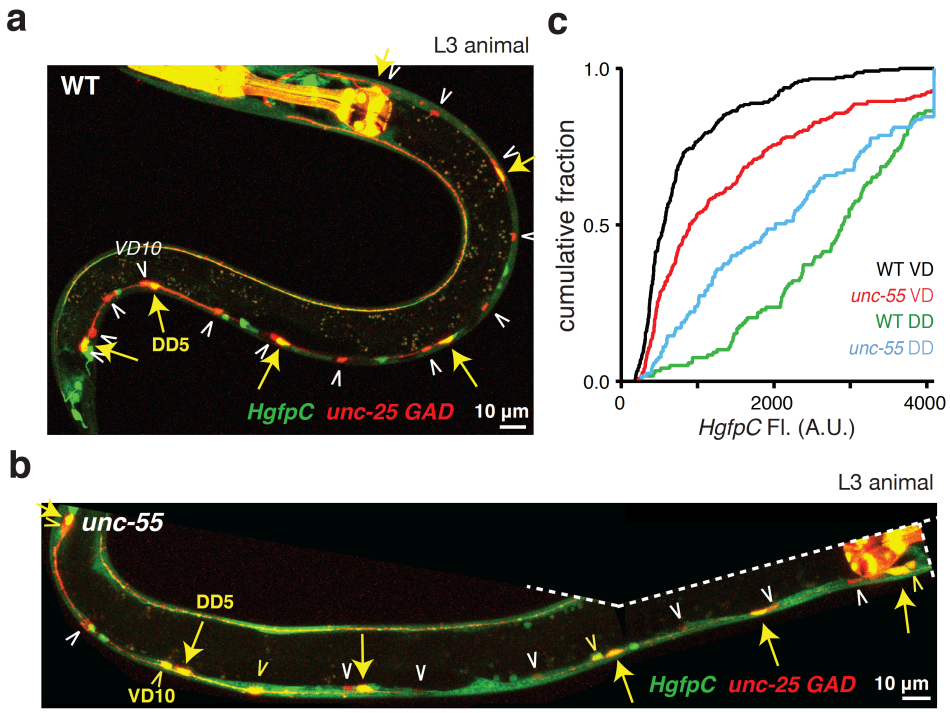

Fig 2.6. HBL-1 transcriptional reporter *HgfpC* expression in VD neurons increases in *unc-55* mutants. Representative images and summary data are shown for *HgfpC* reporter expression (green) in wild type (a) and *unc-55(e1170)* mutant (b) L3 animals. DD and VD neuron cell bodies are identified using the *unc-25* GAD reporter (red). Yellow arrows indicate DD cell bodies expressing both markers, white arrowheads indicate VD cell bodies lacking *HgfpC*, and yellow arrowheads indicate VD cell bodies expressing both markers. VD10 and DD5 are indicated. Cumulative probability distributions for *HgfpC* fluorescence in DD and VD neurons of wild type and unc-55 mutants are shown (c). In wild type, *HgfpC* expression was 5.2-fold enriched in DD neurons (n=188 DD neurons, green line) compared to VD neurons (n=239 VD neurons, black line) ($p < 0.0001$ Kolmogorov-Smirnov test). In *unc-55* mutants, *HgfpC* expression in VD neurons was significantly increased compared to wild-type controls (239 *unc-55* mutant VD neurons (red line), $p < 0.0001$ Kolmogorov-Smirnov test).

< 0.001 Student's t test; Fig. 2.6b-c). By contrast, *HgfpC* expression in DDs did not increase in *unc-55* mutants and instead was modestly decreased (Fig. 2.5d, 2.6c). This is unlikely to be a direct effect of UNC-55 on the *hbl-1* promoter because *unc-55* is not expressed in DD neurons (Zhou and Walthall, 1998). Taken together, these data support the idea that UNC-55 inhibits expression of the *hbl-1* promoter in VD neurons and that *hbl-1* expression in D neurons is likely regulated by additional factors beyond UNC-55.

In *Drosophila*, the UNC-55 ortholog (Sevenup) represses Hunchback (Hb) transcription (Kanai et al., 2005; Mettler et al., 2006). As in *Drosophila*, the *C. elegans hbl-1* promoter contains four predicted UNC-55 binding sites, suggesting the *hbl-1* could be a direct target for UNC-55 repression. To test this idea, we mutated the UNC-55 binding sites in the *hbl-1* promoter, and assayed its expression pattern. The mutant *hbl-1* promoter (H^{mut}*gfpC*) had a significantly reduced DD5/VD10 expression ratio (*HgfpC* 6.6 ±0.8; H^{mut}*gfpC* 2.7 ±0.3, p<0.0001 Student's t test) (Fig. 2.5e), which was not significantly different from the ratio observed for the wild type reporter (*HgfpC*) in *unc-55* mutants (1.8 ±0.3, p = 0.17, Student's t test) (Fig. 2.5f). Thus, the UNC-55 binding sites are required for differential expression of the *hbl-1* promoter in VD and DD neurons.

hbl-1 is required for ectopic remodeling of VD synapses in *unc-55* mutants

If UNC-55 repression of *hbl-1* prevents VD remodeling, we would expect that mutations reducing *hbl-1* activity would diminish ectopic remodeling of VD synapses in *unc-55* mutants. In this scenario, *unc-55; hbl-1* double mutant adults would have significantly more ventral GABAergic synapses and fewer dorsal synapses than *unc-55* single mutants. We did several experiments to test this idea. For these experiments, we utilized the *hbl-1(mg285)* mutation,

which significantly reduces (but does not eliminate) *hbl-1* gene function (Lin et al., 2003). It was not possible to analyze *hbl-1* null mutations as these mutants are not viable (Lin et al., 2003; Roush and Slack, 2009).

We imaged both ventral and dorsal GABAergic synapses with the UNC-57::GFP pre-synaptic marker (expressed in both DD and VD neurons). The *unc-55; hbl-1* double mutant adults had a significant increase in ventral UNC-57 puncta density and a corresponding decrease in dorsal UNC-57 puncta density compared to *unc-55* single mutants (Fig. 2.7). Thus, inactivation of *hbl-1* in *unc-55* mutants shifts GABAergic NMJs from dorsal to ventral muscles.

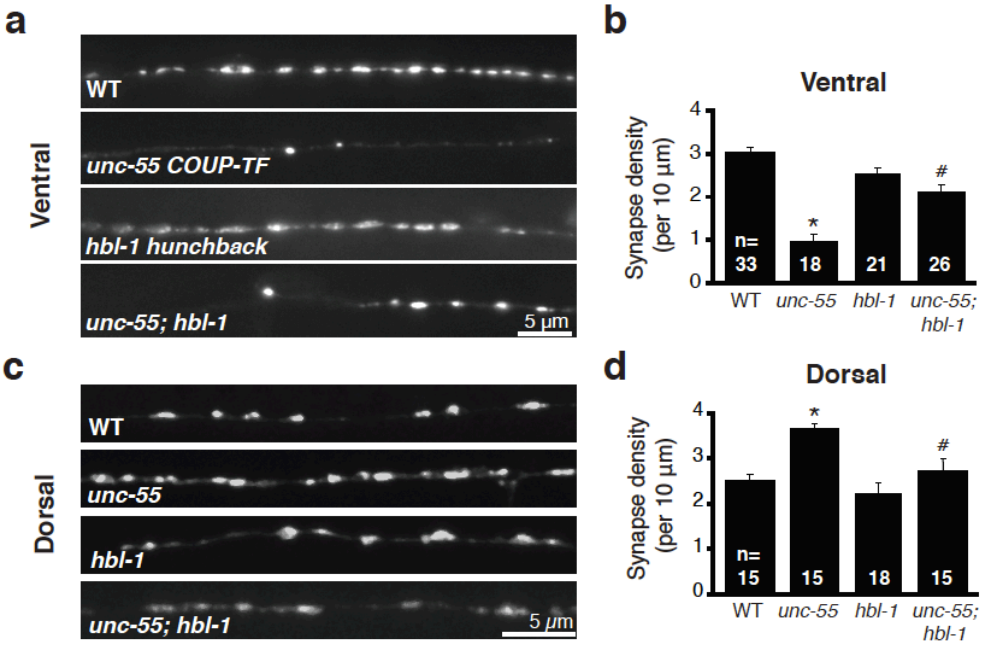

Fig 2.7. Imaging demonstrates that ectopic VD remodeling in *unc-55* mutants requires HBL-1. Imaging of GABAergic NMJs (using the UNC-57::GFP marker). Representative images and summary data for ventral (a,b) and dorsal (c,d) GABAergic NMJs. Error bars indicate SEM. Significant differences ($p < 0.01$) are indicated as follows: *, significantly different from WT; #, significantly different from *unc-55* single mutants. The number of animals analyzed is indicated for each genotype.

This shift could be caused by reduced remodeling of either DD or VD synapses in *unc-55; hbl-1* double mutants. We did two experiments to distinguish between these possibilities. First, ventral and dorsal UNC-57 puncta density, and ventral and dorsal IPSC rates were all unaltered in *hbl-1* single mutants, suggesting that DD remodeling was successfully completed in *hbl-1* adults (Fig. 2.7 and 2.8). Second, we selectively labeled DD synapses with UNC-57::GFP (using the *flp-13* promoter). Using this DD specific synaptic marker, we did not detect any ventral synapses in *hbl-1* adults (data not shown). Consequently, defects in DD remodeling are unlikely to explain the dorsal to ventral shift of GABA synapses in *unc-55; hbl-1* double mutants. Instead, these results support the idea that *hbl-1* mutations decreased ectopic VD remodeling in *unc-55; hbl-1* double mutants.

To assay the function of the ventral VD synapses, we recorded IPSCs from ventral and dorsal body muscles. We found that, compared to *unc-55* single mutants, *unc-55; hbl-1* double mutants had a significantly higher ventral IPSC rate and a significantly lower dorsal IPSC rate (Fig. 2.8a-d), both indicating decreased VD remodeling in double mutants. In both dorsal and ventral recordings, *unc-55* IPSC defects were only partially suppressed in *unc-55; hbl-1* double mutants. The dorsal IPSC rate observed in *unc-55; hbl-1* double mutants remained significantly higher than that observed in *hbl-1* single mutants (Fig. 2.8c-d). By contrast, the rates and amplitudes of excitatory post-synaptic currents (EPSCs) in ventral body muscles (Fig. 2.9) were unaltered in both *hbl-1* single mutants and *hbl-1; unc-55* double mutants, suggesting that cholinergic transmission was unaffected. The restoration of ventral IPSCs in double mutants was partially penetrant, i.e. the increased ventral IPSC rate was only observed in a subset of the double mutant animals (14 out of 43 recordings). Double mutant recordings fell into either of two categories, having ventral IPSC rates similar to *unc-55* or to wild type, while none had

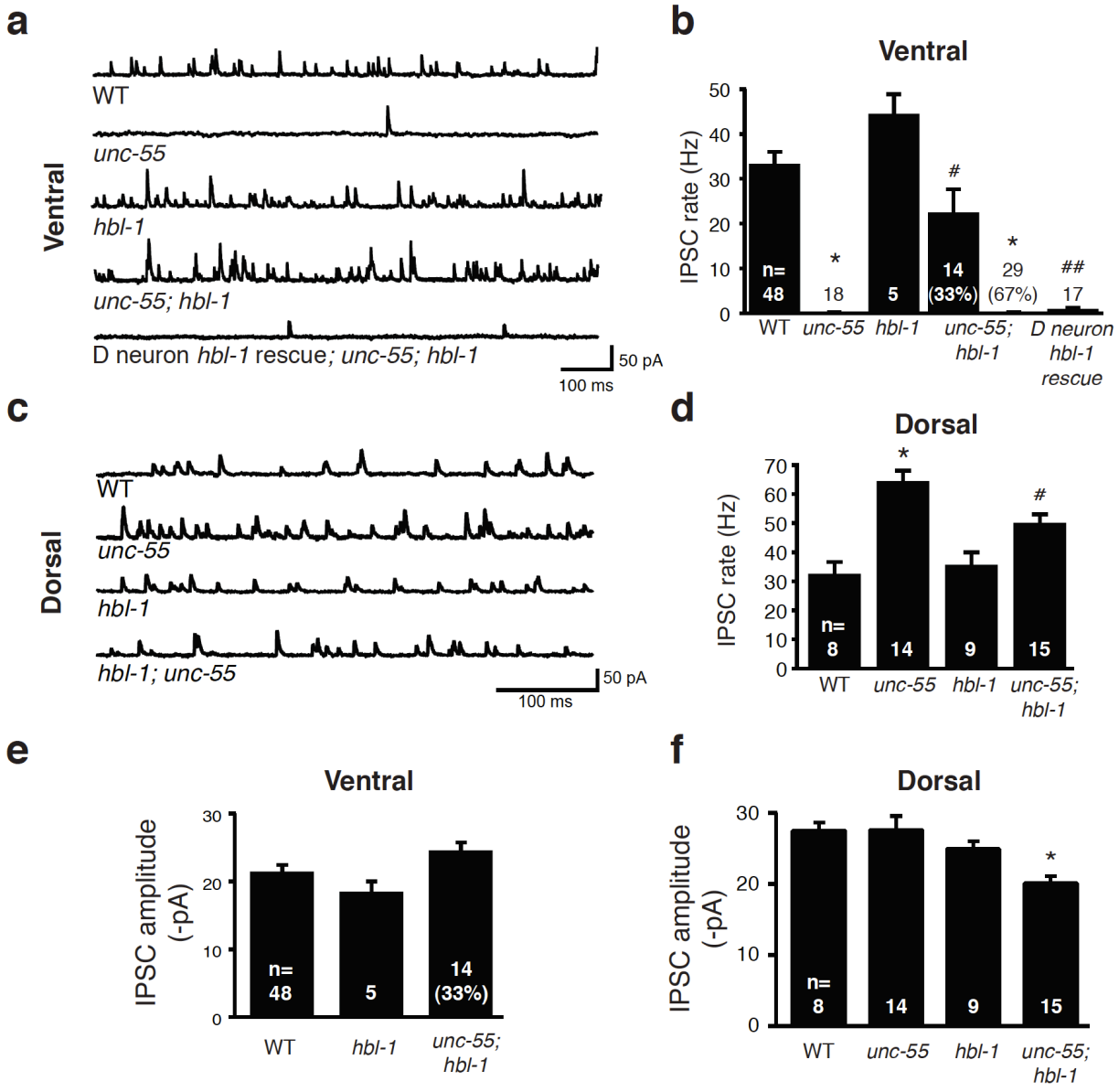

Fig 2.8. Electrophysiology demonstrates that ectopic VD remodeling in *unc-55* mutants requires HBL-1. Representative traces and summary data for endogenous IPSCs recorded from adult ventral (a,b,e) and dorsal (c,d,f) muscles are shown for the indicated genotypes. Error bars indicate SEM. Significant differences ($p < 0.01$) are indicated as follows: *, significantly different from WT; #, significantly different from *unc-55* single mutants; ##, significantly different from *unc-55; hbl-1* double mutants. The number of animals analyzed is indicated for each genotype.

intermediate values (Fig. 2.8a-b). Incomplete penetrance of ventral remodeling in double mutants was also observed by imaging. In *unc-55; hbl-1* double mutants, we observed patches of the ventral nerve cord that contained an approximately normal number of synapses, while other regions totally lacked synapses (data not shown). A transgene expressing *hbl-1* in the VD and DD neurons of *unc-55; hbl-1* double mutants (using the *unc-25* promoter) decreased the ventral IPSC rate to that observed in *unc-55* single mutants (Fig. 2.8a-b) but did not rescue the non-neuronal *hbl-1* defects (Fig. 2.10). These results suggest that HBL-1 acts in VD neurons to promote ectopic remodeling.

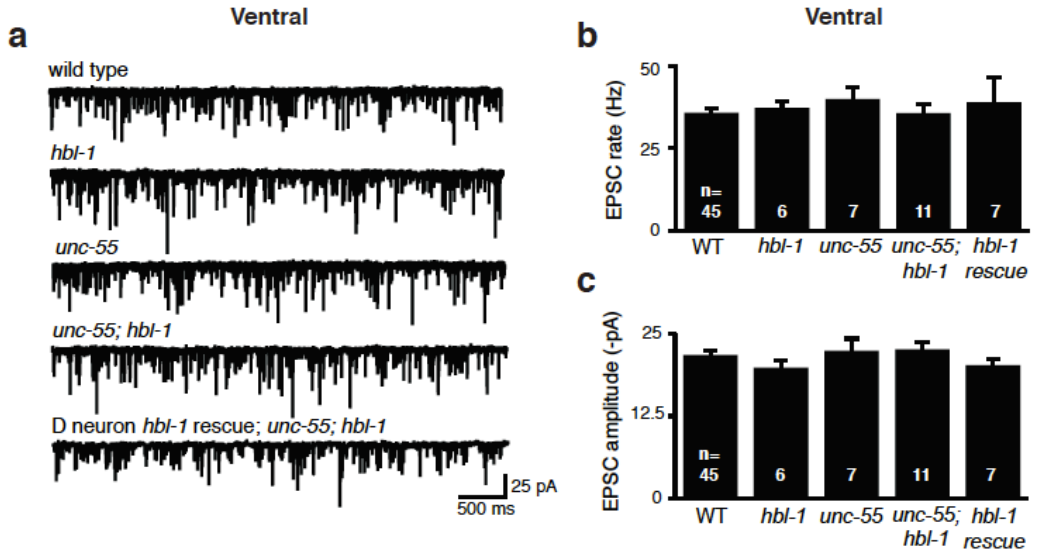

Fig 2.9. Cholinergic transmission was not affected by the *hbl-1* mutation. Representative traces (a) and summary data are shown for endogenous EPSCs recorded from ventral body muscles of adult animals of the indicated genotypes. No significant differences in EPSC rate (b) or amplitude (c) were observed.

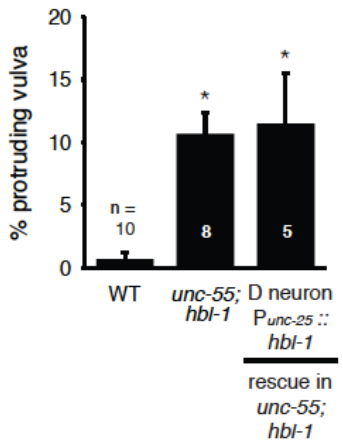

Fig 2.10. D neuron expression of *hbl-1* did not rescue non-neuronal phenotypes. Expression of *hbl-1* in D neurons using the *unc-25* promoter did not rescue the protruding vulva phenotype of hbl-1 mutants, consistent with expression of this transgene in D neurons but not in the vulva. Error bars indicate SEM. The number of replicate assays (30-50 animals/assay) is indicated. * $p < 0.001$ compared to WT by Student's t test.

To further document the functional integrity of the ventral VD synapses, we analyzed the locomotion behavior of *unc-55; hbl-1* double mutants. A prior study showed that ectopic remodeling of VD synapses in *unc-55* mutants was accompanied by a locomotion defect (Zhou and Walthall, 1998). During backward movement, *unc-55* mutants assume a ventrally coiled body posture, presumably due to the absence of inhibitory input to the ventral body muscles (Fig. 2.11a). This *unc-55* coiling defect was significantly reduced (but not eliminated) in *unc-55; hbl-1* double mutants (Fig. 2.11b). The coiling defect was restored by transgenes driving *hbl-1* expression in the D neurons (using either the *unc-25* GAD or the *unc-30* promoter) in *unc-55; hbl-1* double mutants (Fig. 2.11b), as would be predicted if HBL-1 acts in VD neurons to promote remodeling. Thus, the imaging, electrophysiology, and behavioral assays all support the idea that *hbl-1* is a functionally important UNC-55 target whose expression promotes ectopic remodeling of VD synapses in *unc-55* mutants.

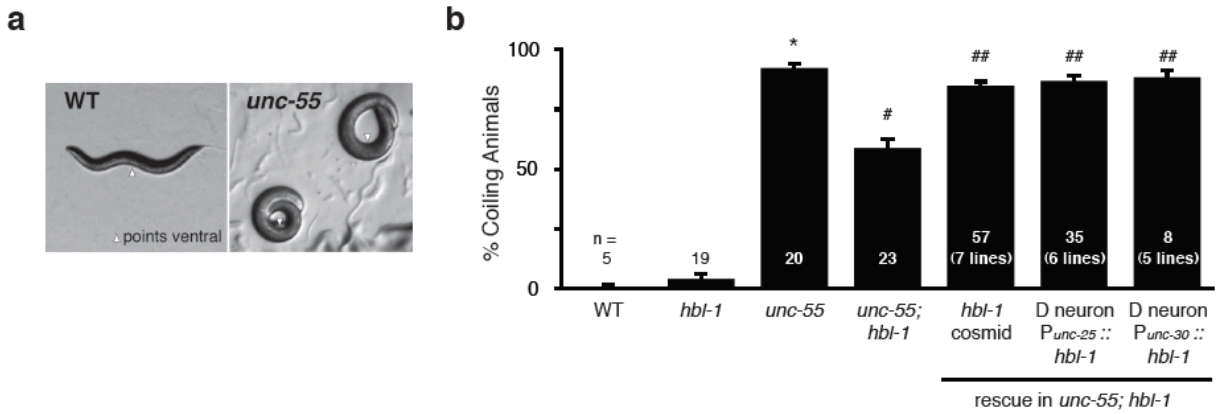

Fig 2.11. Behavior demonstrates that ectopic VD remodeling in *unc-55* mutants requires HBL-1. The ventral coiling phenotype of *unc-55* mutant adults during backward locomotion defect was partially suppressed by an *hbl-1* mutation and was restored by transgenes containing either the *hbl-1* cosmid and by *hbl-1* transgenes expressed in D-neurons by a GABA promoter (using either the unc-25 or unc-30 promoters). Rescue was observed using the indicated number of independent transgenic lines for each construct: *hbl-1* cosmid (7 lines), *unc-25* GAD promoter (6 lines), and *unc-30* promoter (5 lines). The number of replicate behavioral assays (20 animals/assay) is indicated for each genotype. Error bars indicate SEM. Significant differences (p <0.01) are indicated as follows: *, significantly different from WT; #, significantly different from *unc-55* single mutants; ##, significantly different from *unc-55; hbl-1* double mutants.

The partial suppression and incomplete penetrance observed in the *unc-55; hbl-1* double mutants indicate that the *hbl-1(mg285)* mutation did not completely abolish remodeling of VD synapses. The persistent VD remodeling observed in double mutants could reflect residual *hbl-1* activity in *hbl-1(mg285)* mutants, or the activity of other UNC-55 target genes (Lin et al., 2003). Consistent with the latter idea, transgenic expression of *hbl-1* in DD and VD neurons (with the *unc-25* promoter) was not sufficient to cause ectopic remodeling of VD synapses (Fig. 2.12). Thus, *hbl-1* is unlikely to be the only UNC-55 target involved in D neuron remodeling.

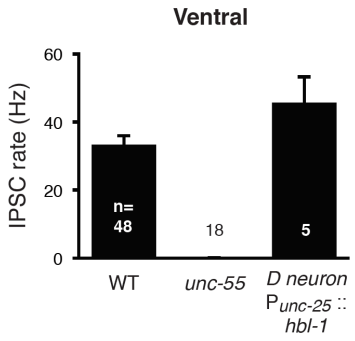

Fig 2.12. Expression of *hbl-1* in VD neurons did not cause ectopic remodeling of VD synapses. Summary data is shown for ventral IPSC rate recorded from adult animals of the indicated genotypes. The number of animals analyzed is indicated for each genotype.

DD remodeling occurs during a precise time window and is patterned spatially

Thus far, our results show that *hbl-1* promotes ectopic remodeling of *unc-55* mutant VD neurons but that *hbl-1* expression alone is not sufficient to cause VD remodeling. We next analyzed DD remodeling, which occurs in wild type animals (White et al., 1978; Walthall, 1990). Prior to hatching, DD neurons form ventral NMJs, which can be identified as ventral UNC-57::GFP puncta. During the L1 stage, these ventral DD synapses are eliminated and new dorsal synapses are formed (visualized as dorsal UNC-57 or RAB-3 puncta; Fig. 2.13a and 2.15c). The UNC-57::GFP transgene is expressed in both DD and VD neurons; consequently, we were unable to analyze loss of ventral DD synapses, due to the confounding signal of the nascent ventral VD synapses. For this reason, we restricted our analysis to formation of new UNC-57 puncta in dorsal cord DD axons during the L1. Using this assay, we followed the time course of DD remodeling. The entire DD remodeling process occurred in a discrete time window during the late L1 and early L2 stage (from 12-19 hours post-hatching; Fig. 2.13b), consistent with prior studies (Hallam and Jin, 1998; Park et al., 2011). The newly formed dorsal DD synapses occur in a stereotyped spatial pattern, where dorsal cord UNC-57 puncta adjacent to the commissures

form first, while puncta in more distal axon segments form later (Fig. 2.13a). These results suggest that formation of dorsal DD synapses during remodeling occurs in a proximal-to-distal spatial pattern.

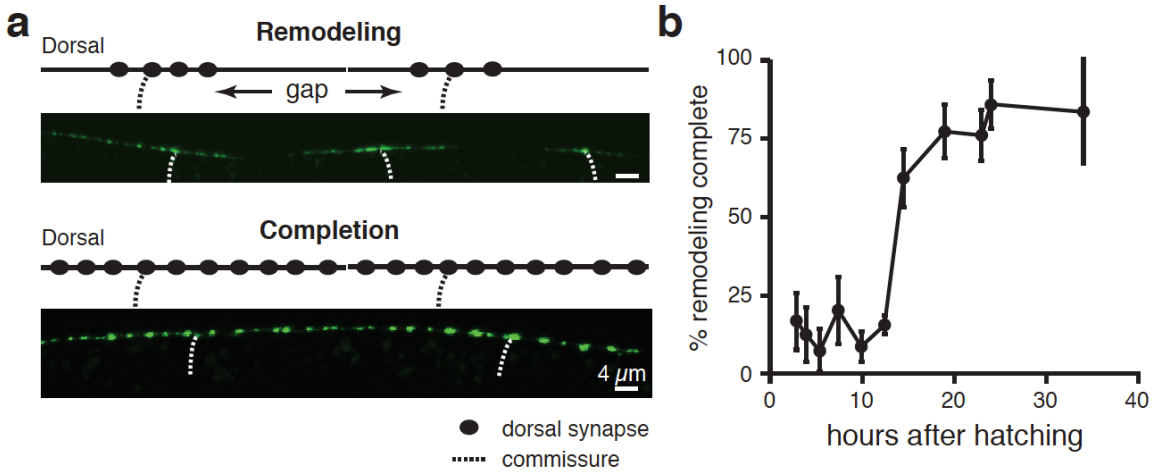

Fig 2.13. DD remodeling is patterned spatially and temporally. (a) DD remodeling was visualized by dorsal synapse formation with the UNC-57::GFP marker. Representative images of the dorsal cord during remodeling (above) and after completion (below) are shown. During remodeling, DD neurons form en passant synapses with the dorsal muscle. DD neuron commissures are indicated by dotted lines. **(b)** Summary data illustrating the time course of DD neuron remodeling is shown. 15-30 animals were analyzed for all time points except 12 hrs (where n= 160 animals).

DD remodeling is delayed in *hbl-1* mutants

Our analysis of *unc-55* mutants suggests that *hbl-1* expression promotes ectopic VD remodeling. Given these results, we wondered whether *hbl-1* also plays a role in DD remodeling. Consistent with this idea, the *HgfpH* and *HgfpC* reporters were expressed in six GABAergic DD neurons of wild type L1 larvae, before the VD neurons are born (Fig. 2.14, and data not shown). Thus, *hbl-1* is likely to be expressed in the DD neurons during the remodeling period.

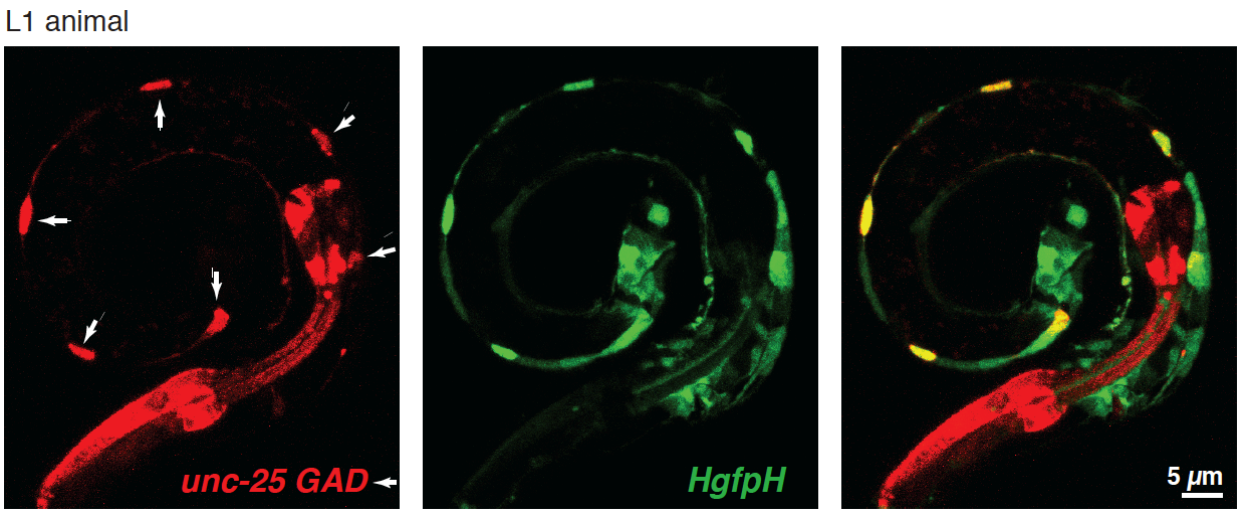

Fig 2.14. *hbl-1* is expressed in DD neurons during remodeling. The *HgfpH* reporter (green) is expressed in DD neurons (identified with the GAD reporter, red) during the L1 when remodeling is occurring. A representative image of a wild type L1 larva is shown. Arrows indicate the six DD cell bodies.

We next asked if HBL-1 is required for DD remodeling. At 12 hours post-hatching, DD remodeling had been initiated in both wild type and *hbl-1* mutants (data not shown), implying that onset of remodeling had not been altered. By contrast, at 23 hours post-hatching, nearly all wild type animals (81 ±5%) had completed remodeling, whereas significantly fewer *hbl-1* mutants (14 ±5%, $p<0.0001$ Student's t test) had completed this process (Fig. 2.15). Similar delays were observed in strains containing two independent *hbl-1* alleles (*mg285* and *ve18*), both of which reduce but do not eliminate *hbl-1* gene activity (Abrahante et al., 2003; Lin et al., 2003; Roush and Slack, 2009). The *hbl-1* delayed remodeling defect was rescued by a transgene containing the F13D11 cosmid (which spans the *hbl-1* gene; Fig. 2.15b). The effect of *hbl-1* was not specific to the UNC-57::GFP marker because similar delays in DD remodeling were detected using a second synaptic marker (mCherry::RAB-3; Fig. 2.15d). Although remodeling was delayed, *hbl-1* mutants eventually completed DD remodeling, as *hbl-1* adults had normal dorsal

and ventral NMJs as assessed by both imaging and electrophysiology (Fig. 2.7 and 2.8). This persistent remodeling activity could reflect residual gene activity in *hbl-1(mg285)* mutants or residual expression of other remodeling factors.

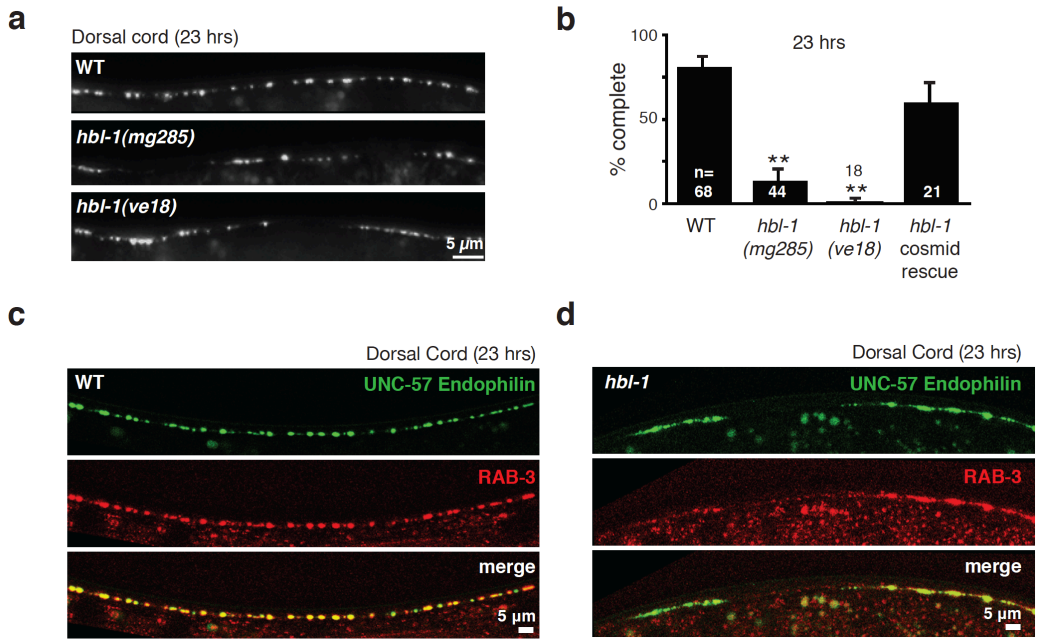

Fig 2.15. DD remodeling is delayed in *hbl-1* mutants. Representative images of dorsal DD NMJs (a), and summary data (b) for completion of DD remodeling are shown at 23 hours posthatching. The majority of wild-type animals have completed DD remodeling, whereas significantly fewer *hbl-1* mutants have finished this process (**, $p < 0.0001$ Chi square test). This delay was rescued by a transgene containing the *hbl-1* cosmid. Error bars indicate SEM. **(c-d)** The *hbl-1* DD remodeling defect was observed using two presynaptic markers. Endophilin UNC-57::GFP (green) and mCherry::RAB-3 (red) are shown in D neuron dorsal cord axons of wild type (c) and *hbl-1* mutants (d).

Because *hbl-1* is a heterochronic gene, the delayed DD remodeling in *hbl-1* mutants could be caused by a generalized delay in larval development. This seems unlikely because inactivating *hbl-1* causes several aspects of hypodermal development to occur earlier (including seam cell fusions, alae formation, and division of vulva precursor cells), whereas DD remodeling

is delayed (Reinhart et al., 2000; Abrahante et al., 2003; Lin et al., 2003; Grosshans et al., 2005; Nolde et al., 2007). These *hbl-1* hypodermal defects occur later in development, during the L2. Therefore, we did several additional experiments to control for changes in the timing of L1 development in *hbl-1* mutants. We used two developmental landmarks during the L1: the onset of expression of the *mlt-10* gene (which occurs at 11-14 hours post-hatching), and the Pn.ap neuroblast (hereafter referred to as the AS/VD neuroblast) cell division (which occurs at 12.5-14 hours post-hatching) (Sulston, 1976; Frand et al., 2005). The AS/VD cell division was monitored with a GFP reporter expressed in its daughter cells (the VD and AS neurons) using the *unc-55* promoter. Although completion of DD remodeling was delayed by at least 20 hours in *hbl-1* mutants, corresponding delays were not observed for the onset of *mlt-10* expression or for the timing of the AS/VD cell division (Fig. 2.16). Thus, a generalized delay in the timing of L1 development is unlikely to explain the *hbl-1* mutant delay in DD remodeling.

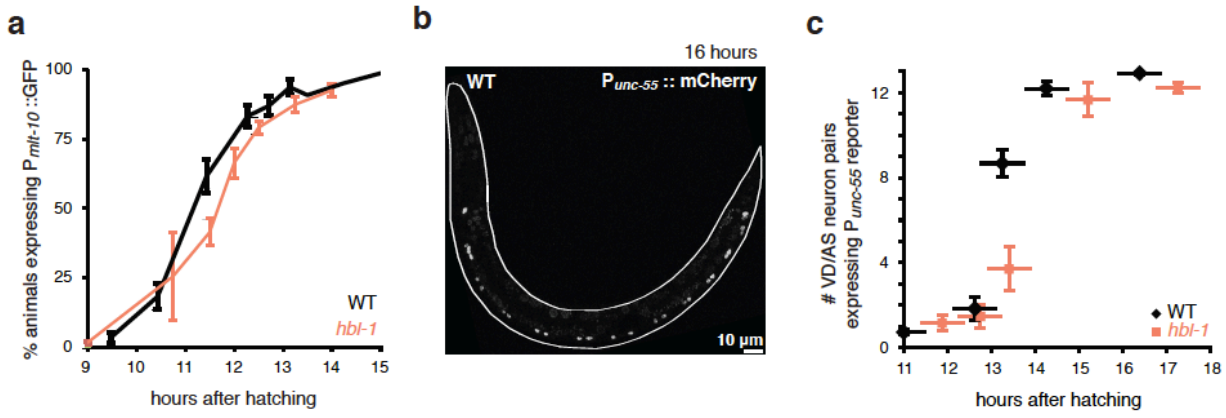

Fig 2.16. L1-to-L2 development was not generally delayed in *hbl-1* mutants. Timing of mlt-10 reporter expression (a) and of the appearance of sister VD/AS cell pairs in the ventral cord (b-c) during the L1-to-L2 development was compared in wild type and *hbl-1* mutants; no delay was observed. Onset of *mlt-10* reporter expression occurs with a characteristic timing, just prior to the L1 molt (Frand et al., 2005). GFP was expressed in AS and VD neurons using the *unc-55* promoter. Vertical error bars indicate SEM, while horizontal bars indicate the 1 hr time range for each measurement.

DD remodeling occurs earlier in *mir-84* mutants

In the hypodermis, *hbl-1* expression is negatively regulated by the *let-7* family of microRNAs (Abrahante et al., 2003; Lin et al., 2003; Abbott et al., 2005; Nolde et al., 2007; Roush and Slack, 2008). The 3' UTR of the *hbl-1* mRNA contains binding sites for three *let-7* paralogs (*let-7*, *mir-48*, and *mir-84*) (Roush and Slack, 2008). Prior studies showed that mature miR-84 is expressed in the early L1, suggesting that *let-7* microRNAs could regulate *hbl-1* expression in DD neurons during the remodeling process (Abbott et al., 2005; Esquela-Kerscher et al., 2005). To test this idea, we analyzed expression of the *HgfpH* reporter in *mir-84* mutants (Fig. 2.17a-b). In the L1, *HgfpH* expression was significantly increased in *mir-84* mutant DD neurons compared to wild type controls (7.5 fold increase in median, $p < 0.0001$ Kolmogorov-Smirnov test; Fig. 2.17a-b). By contrast, the *mir-84* mutation did not significantly change expression of the *HgfpC* reporter, which lacks the *hbl-1* 3'UTR (Fig. 2.17c). These results suggest that miR-84 regulates *hbl-1* expression in DD neurons when remodeling is occurring.

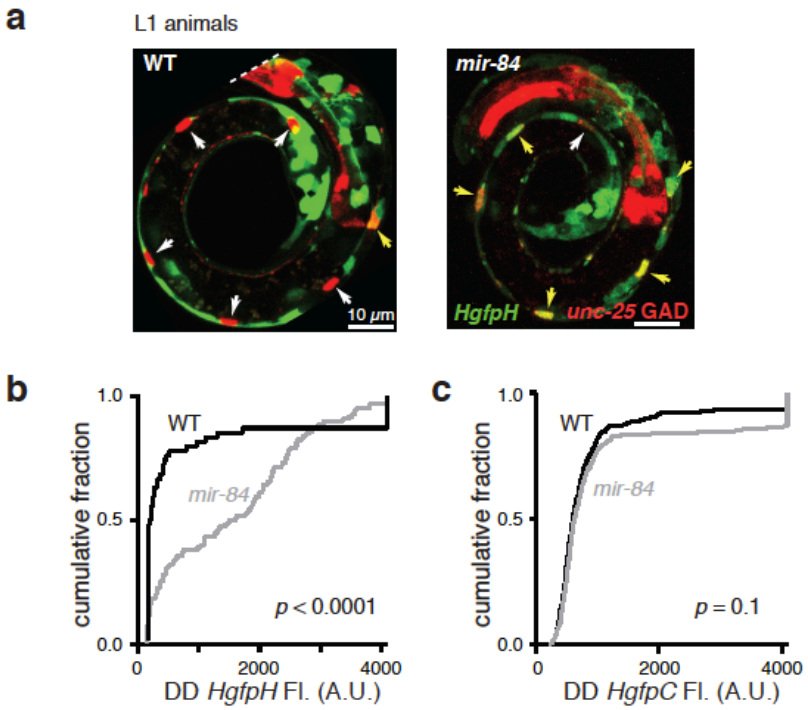

Fig 2.17. The microRNA miR-84 regulates *hbl-1* expression. Representative images (a) and summary data (b) are shown for *HgfpH* expression (green) in DD neurons (labeled with the GAD reporter, red, and indicated by arrows) of L1 larvae. In *mir-84* mutants, *HgfpH* expression was significantly increased (** p <0.0001 by Kolmogorov-Smirnov test). **(c)** Summary data are shown comparing the fluorescent intensity of the *HgfpC* reporter in DD neurons of wild type and *mir-84(tm1304)* mutants; no significant difference was observed (p=0.1 Kolmogorov-Smirnov test). 54 wild-type and 118 mir-84 DD neurons were analyzed for median *HgfpH* expression (b); and 233 wild-type and 379 *mir-84* DD neurons were analyzed for *HgfpC* expression (c).

If miR-84 inhibits *hbl-1* expression in DD neurons during the remodeling period, we would expect that the timing of remodeling would be altered in *mir-84* mutants. Indeed, at 11 hours after hatching, a significantly larger fraction of *mir-84* mutants had completed remodeling than was observed in wild type controls (Fig. 2.18a-b). These results suggest that completion of DD remodeling occurs precociously in *mir-84* mutants. Corresponding changes in the timing of *mlt-10* expression and of the AS/VD cell division were not observed in *mir-84* mutants (Fig.

2.19), suggesting that global changes in the timing of L1 development are unlikely to explain the *mir-84* remodeling defect. The earlier remodeling in *mir-84* mutants could be caused by increased *hbl-1* expression in DD neurons. Consistent with this idea, the effect of the *mir-84* mutation on remodeling was eliminated in *hbl-1; mir-84* double mutants (Fig. 2.18c-d). These results suggest that mutations increasing and decreasing HBL-1 activity (*mir-84* and *hbl-1*, respectively) produce opposite shifts in the timing of DD plasticity.

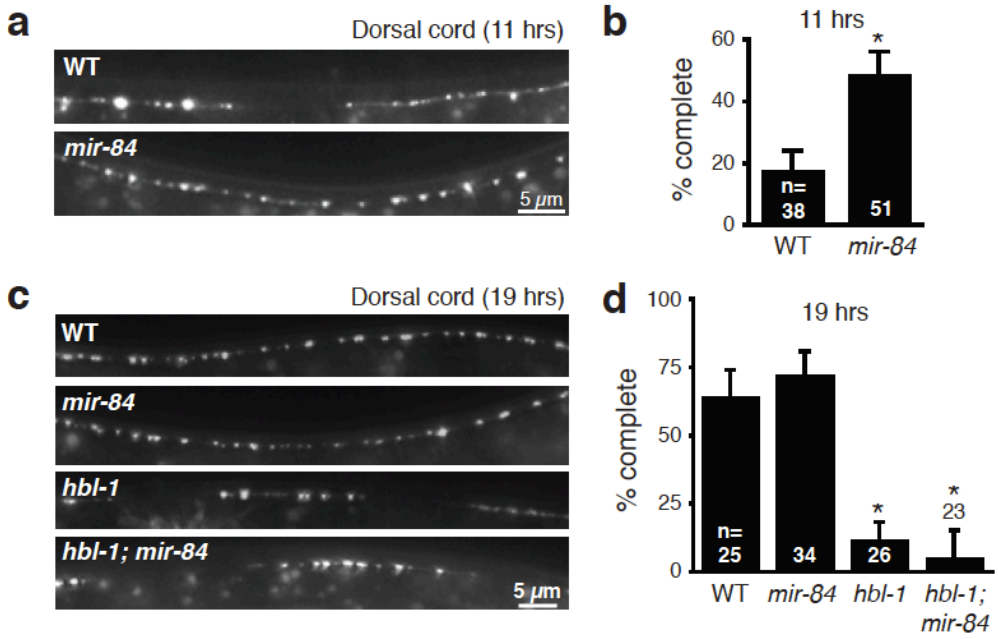

Fig 2.18. The microRNA miR-84 regulates the timing of remodeling by regulating *hbl-1*. (a-b) DD remodeling occurs earlier in mir-84 mutants. Representative images (a) and summary data (b) are shown for dorsal DD NMJs at 11 hours post-hatching. Remodeling was completed significantly earlier in *mir-84* mutants (*, $p < 0.01$ Chi square test). **(c-d)** The impact of *mir-84* on remodeling was eliminated in *hbl-1; mir-84* double mutants. Representative images (c) and summary data (d) are shown for dorsal DD NMJs at 19 hours post-hatching. The extent of remodeling in *hbl-1* single mutants and *hbl-1; mir-84* double mutants were not significantly different.

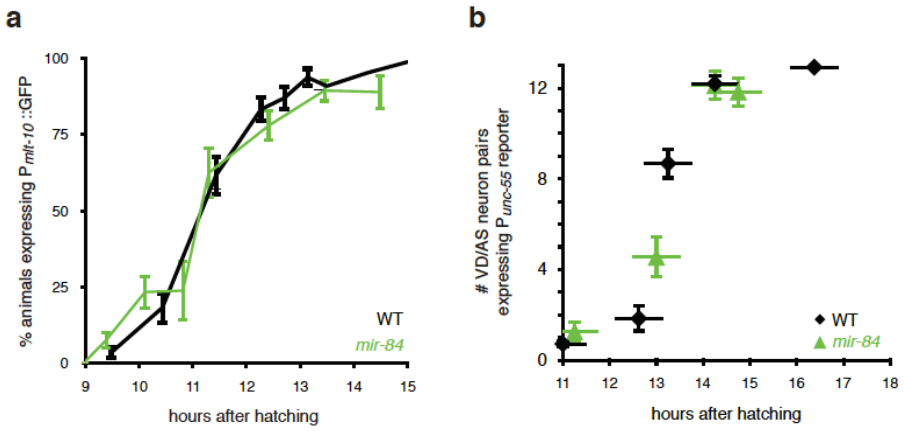

Fig 2.19. The *mir-84* mutation did not cause a general change in the timing of L1-to-L2 development. Timing of *mlt-10* reporter expression (a) and VD/AS cell pair appearance (b) in the ventral cord are compared for wild type and *mir-84* mutants; no delay was observed. Vertical error bars indicate SEM. Horizontal bars indicate the 1hr time range for each measurement.

Changes in GABA release do not alter the timing of DD plasticity

In mammals, changes in GABA transmission regulates ocular dominance plasticity as well as other aspects of synapse development (Hensch, 2004; Chattopadhyaya et al., 2007). However, GABA release is unlikely to be required for DD plasticity, as a prior study showed that DD remodeling was unaltered in *unc-25* mutant adults (which lack the GABA biosynthetic enzyme GAD) (Jin et al., 1999). To confirm these results, we analyzed *unc-47* mutants (which lack the vesicular GABA transporter VGAT) and *unc-25* GAD mutants for DD remodeling defects in L1 and L2 larvae. We observed normal or slight changes in the timing of DD remodeling in either GABA defective mutant (Fig. 2.20), indicating that GABA transmission does not play an important role in the timing of DD remodeling.

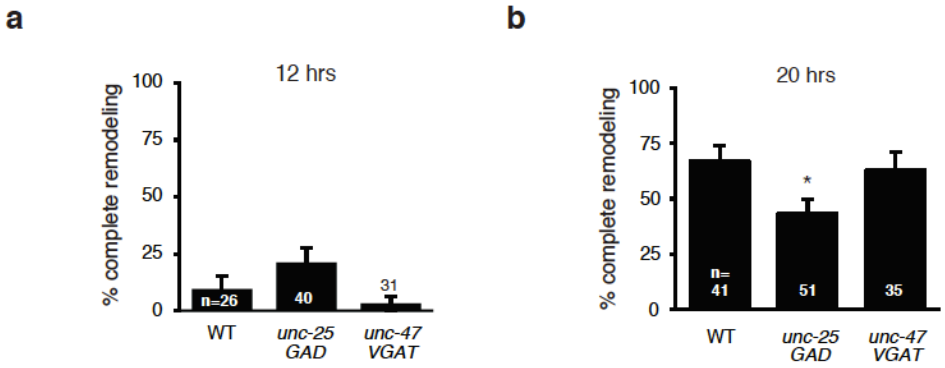

Fig 2.20. DD remodeling proceeds normally in mutants lacking GABAergic synaptic transmission. (a-b) DD remodeling time course is shown for *unc-25* GAD or *unc-47* VGLUT mutants, 12 hours (a) or 20 hours (b) after hatching. Error bars indicate SEM. The subtle remodeling delay in *unc-25* GAD mutants at 20 hours (WT 67% versus *unc-25* 43% complete, * $p < 0.005$ Chi square test) is likely due to the slight developmental delay observed in these animals (data not shown).

Circuit activity regulates *hbl-1* expression and the timing of DD plasticity

Since synaptic refinement is often regulated by circuit activity, we wondered if changes in activity would also alter the timing of DD remodeling (Sanes and Lichtman, 1999; Hua and Smith, 2004). To test this idea, we analyzed mutants that have altered circuit activity. For this analysis, we used mutations that either block or exaggerate synaptic transmission. Mutants lacking UNC-13 and UNC-18 have profound defects in synaptic vesicle docking and priming, which result in dramatically reduced rates of synaptic transmission (3% and 10% of wild type rates, respectively) (Richmond et al., 1999; Weimer et al., 2003; McEwen et al., 2006). By contrast, mutations inactivating *tom-1* Tomosyn and *slo-1* BK channels exaggerate synaptic transmission. In *tom-1* mutants, the pool of fusion competent (i.e. primed) synaptic vesicles is increased (Gracheva et al., 2006; McEwen et al., 2006). In *slo-1* mutants, repolarization of nerve terminals is delayed, leading to prolonged neurotransmitter release (Wang et al., 2001).

First, we compared expression of the *hbl-1* promoter in these activity mutants. Expression of the *HgfpC* reporter in DD neurons was significantly decreased in *unc-13* mutants (Fig. 2.21a-b), whereas increased *HgfpC* expression was observed in *tom-1* mutants (Fig. 2.21c-

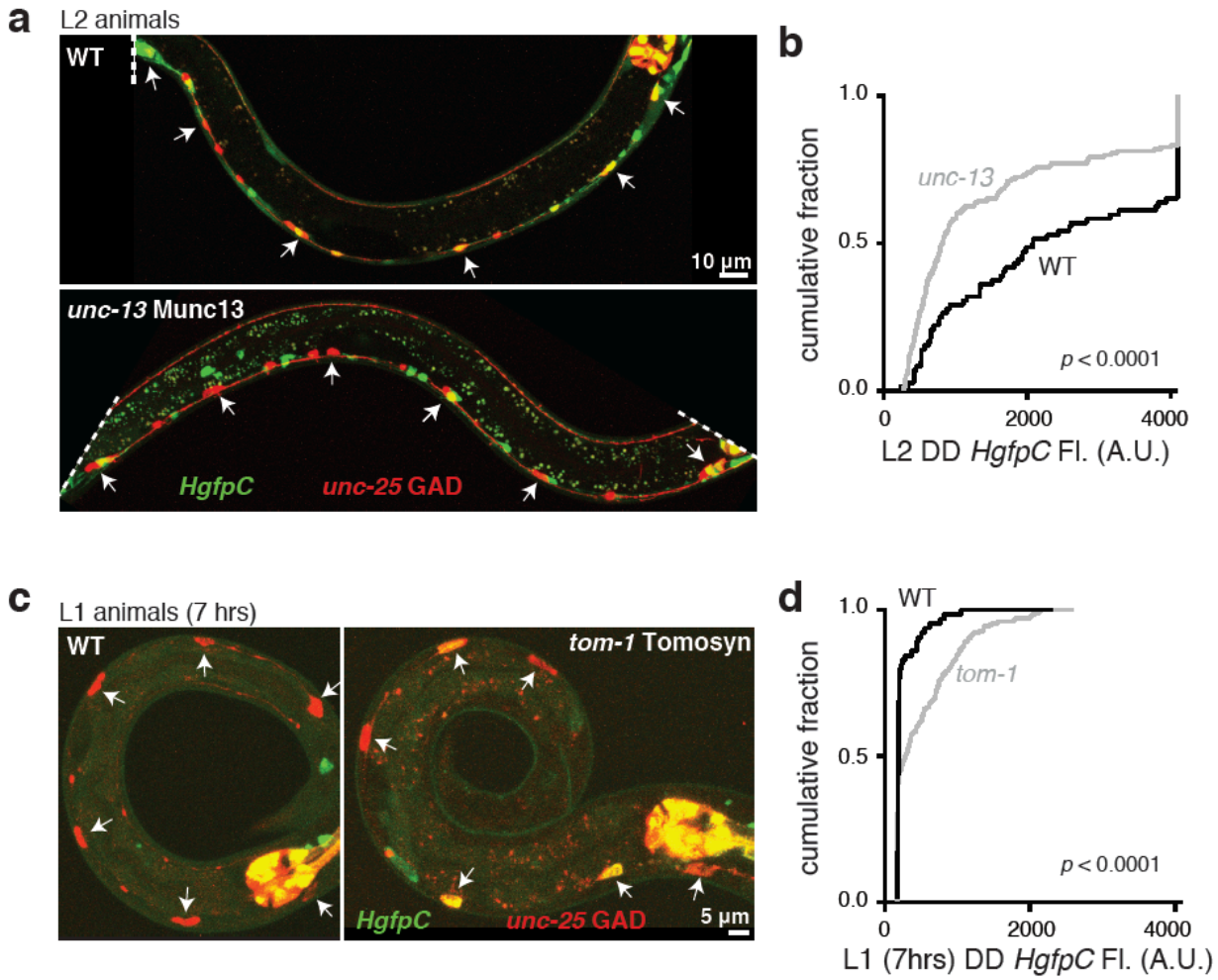

Fig 2.21. Circuit activity regulates HBL-1 expression. Representative images (a,c) and summary data (b,d) are shown for *hbl-1* expression (*HgfpC*, green) in DD neurons (labeled with the GAD reporter, red, indicated by arrows). *HgfpC* expression significantly decreased in *unc-13* mutants (a-b) and increased in *tom-1* mutants (c-d; ** p <0.0001 Kolmogorov-Smirnov test; 72 wild type and 149 *unc-13* L2 DD neurons; 64 wild type and 179 *tom-1* L1 DD neurons). Expression of *HgfpC* in DD neurons was analyzed at different times in *unc-13* and *tom-1* mutants because the remodeling defects observed in these mutants occurred at different times.

d). Thus, decreased and increased circuit activity were accompanied by corresponding changes in *hbl-1* promoter expression in DD neurons.

We next asked if circuit activity alters the timing of DD plasticity. The overall rate of larval development was significantly delayed in both *unc-13* and *unc-18* mutants, presumably due to decreased feeding. To control for this general developmental delay, we synchronized animals at a specific stage of L3 development, defined by the dorsal turn of the gonad arms. In these late L3 larvae, *unc-13* and *unc-18* mutants had significantly delayed DD remodeling compared to wild type L3 larvae (Fig. 2.22a-b). By contrast, remodeling occurred significantly earlier in *tom-1* and *slo-1* mutants than in wild type controls (Fig. 2.22c-d). This earlier remodeling phenotype cannot be explained by a general shift in developmental timing, as neither the *tom-1* nor *slo-1* mutants had corresponding changes in the timing of other L1-to-L2 developmental events (Fig. 2.23). Thus, decreased and increased synaptic activity were accompanied by corresponding changes in *hbl-1* promoter expression in DD neurons, and corresponding shifts in the timing of DD plasticity. The earlier remodeling phenotypes observed in *tom-1* and *slo-1* single mutants were eliminated in double mutants lacking *hbl-1* (Fig. 2.22e), suggesting that changes in *hbl-1* activity are required for the activity-induced shifts in the timing of DD plasticity.

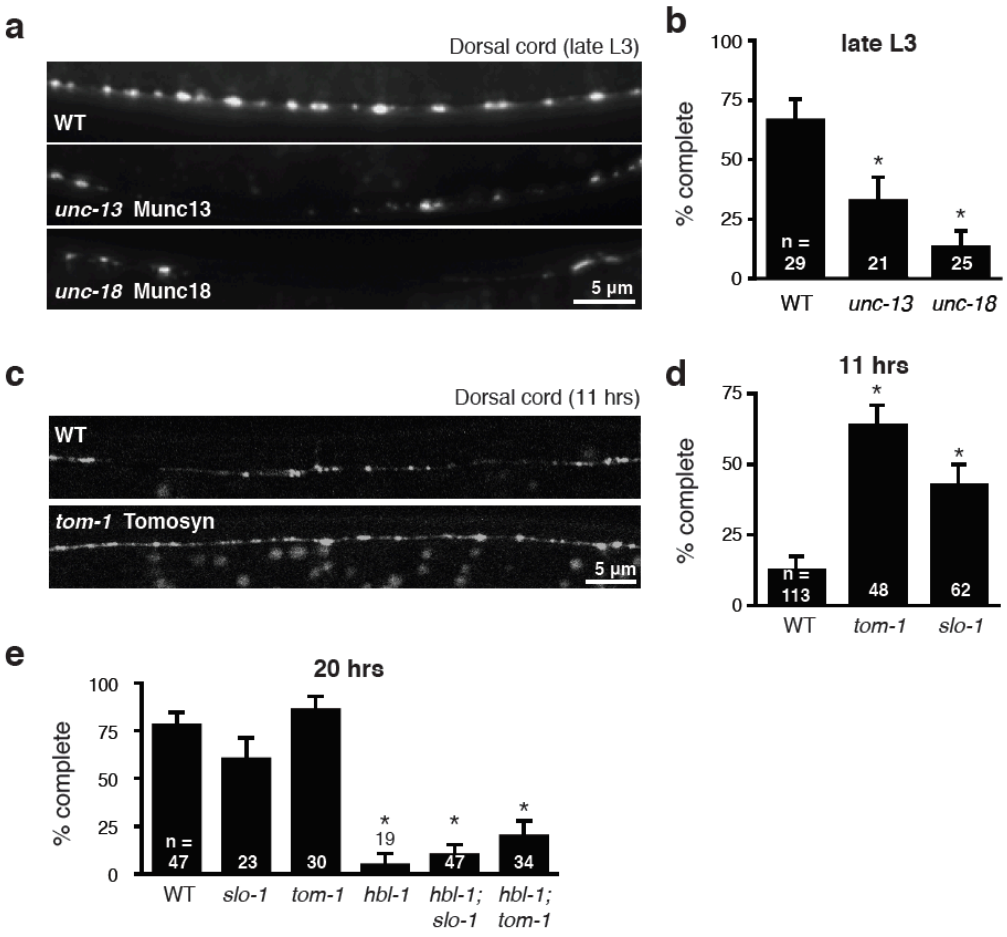

Fig 2.22. Circuit activity determines the timing of DD neuron plasticity by regulating HBL-1. (a-d) Completion of DD remodeling shown for dorsal GABAergic NMJs in *unc-13* and *unc-18* mutants in late L3 animals (a-b) or in *tom-1* and *slo-1 mutants* at 11 hours post-hatching (c-d). **(e)** Summary data for completion of DD remodeling at 20 hours after hatching shows that the impact of *slo-1* and *tom-1* on remodeling was eliminated in double mutants with *hbl-1*. (* : significantly different than wild-type, $p < 0.001$, Chi squared test). Error bars indicate SEM, numbers indicate number of animals analyzed.

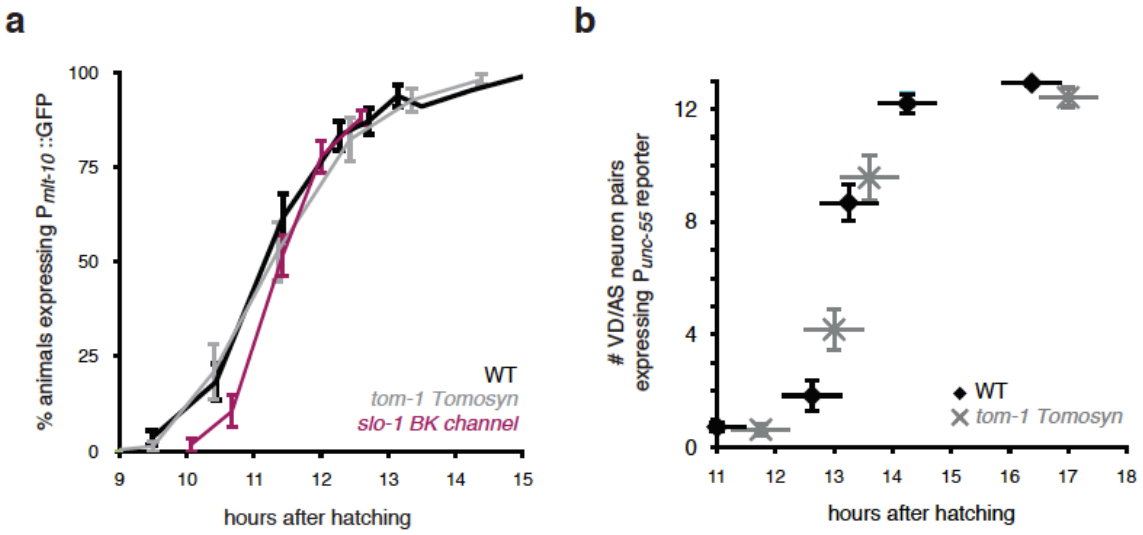

Fig 2.23. Increased activity mutations did not cause general changes in the timing of L1-to-L2 development. (a) Time course of *mlt-10* reporter expression during the L1-to-L2 development is compared in wild type and *tom-1* and *slo-1* mutants; no delay was observed. **(b)** The timing of VD/AS cell pair appearance in the ventral cord is compared for wild type and *tom-1* mutants. Vertical error bars indicate SEM. Horizontal bars indicate the 1 hr time range for each measurement.

DISCUSSION

To investigate the genetic mechanisms that pattern synaptic plasticity, we analyzed the developmentally programmed remodeling of D-type motor neuron synapses in *C. elegans*. Our results, together with prior studies, show that DD plasticity is extensively regulated. First, DD synapses are remodeled during a precise time window (12-19 hours post-hatching). Second, circuit activity governs the timing of remodeling. Third, plasticity is restricted to a specific cell type: the earlier born DD neurons undergo this plasticity while the later born VD neurons do not. And fourth, remodeling is patterned spatially, with new DD synapses forming in a proximal to distal order. Thus, DD plasticity shares many features with other examples of developmental plasticity (including critical period plasticity in mammals). Given these similarities, characterizing the molecular mechanisms that pattern DD remodeling may provide insights into the mechanisms underlying circuit refinement elsewhere.

A conserved role for heterochronic genes in circuit development

In both worms and flies, the timing of many aspects of development is controlled by transcriptional cascades that confer temporal cell fates. In worms, these cascades are generically referred to as heterochronic pathways. A prior study showed that LIN-14, a heterochronic transcription factor, acts cell autonomously in DD neurons, where it determines when remodeling is initiated (Hallam and Jin, 1998). Here we show that a second heterochronic gene (*hbl-1*) also acts cell autonomously to pattern remodeling. Several aspects of these results are significant. First, unlike *lin-14*, *hbl-1* orthologs are found in other organisms and *Drosophila* Hunchback plays an analogous role in regulating temporal cell fates in neuroblast lineages (Kanai et al., 2005; Mettler et al., 2006). Thus, our results strongly suggest that heterochronic

genes represent a conserved mechanism for patterning the timing of circuit development. Second, different heterochronic genes control different aspects of plasticity. LIN-14 determines when DD remodeling is initiated while HBL-1 determines when remodeling is completed. Third, a heterochronic gene can have opposite effects on developmental timing in different tissues. Inactivating *hbl-1* caused delayed DD plasticity whereas hypodermal fates occurred precociously (Abrahante et al., 2003; Lin et al., 2003). By contrast, inactivating *lin-14* caused precocious expression of both DD plasticity and hypodermal development (Ambros and Horvitz, 1987; Hallam and Jin, 1998). Fourth, increased and decreased HBL-1 expression produce opposite shifts in the timing of DD plasticity. Identifying genes that mutate to opposite phenotypes has historically been utilized in developmental genetics as a criterion to identify the key regulatory elements in a process. Thus, our results identify HBL-1 as a critical genetic determinant patterning DD plasticity.

The role of UNC-55 COUP-TF in circuit development

During development, maturing circuits are modified by the addition of newly born neurons, and by refinement of connectivity. We propose that the UNC-55/COUP-TF family of transcriptional repressors plays an important role in both of these aspects of circuit development. In *C. elegans*, synaptic remodeling is restricted to the earlier born DD neurons because UNC-55 COUP-TF represses *hbl-1* expression in the later born VD neurons. Inactivating UNC-55 orthologs in other organisms alters the timing of other aspects of neural development. In *Drosophila*, Sevenup repression of Hunchback allows neuroblast daughters to adopt later cell fates (Kanai et al., 2005; Mettler et al., 2006). Similarly, knocking down both mouse UNC-55 orthologs (COUP-TF1 and COUP-TFII) prolongs the generation of early-born neurons at the

expense of later cell types (Naka et al., 2008). Collectively, these results suggest that UNC-55 orchestrates how newly born neurons are integrated into circuits, and the capacity of developing circuits to undergo plasticity. In this respect, it is intriguing that a mouse UNC-55 ortholog (COUP-TFII) is expressed in several classes of GABAergic cortical interneurons (Tripodi et al., 2004; Armentano et al., 2007; Kanatani et al., 2008). Like UNC-55, COUP-TFII is selectively expressed in a sub-population of interneurons that have later birth dates (Zhou et al., 2001b). We speculate that COUP-TFII expressing interneurons (like the VDs) will have a more limited capacity to undergo synaptic refinement compared to interneurons that are born earlier.

What role does HBL-1 play in synaptic remodeling?

HBL-1 expression could reprogram VD neurons to adopt the DD cell fate, thereby causing ectopic expression of the remodeling program. This scenario seems unlikely because bidirectional changes in *hbl-1* expression produce corresponding shifts in the timing of DD plasticity. If HBL-1 were inducing the DD cell fate, we would not expect HBL-1 expression to bidirectionally alter the timing of DD remodeling. HBL-1 activity could accelerate DD remodeling by regulating expression of factors that directly mediate synapse elimination and formation. Finally, HBL-1 could be part of a timing mechanism that dictates when remodeling occurs. The effects of UNC-55 orthologs (COUP-TFs and Sevenup) and an HBL-1 ortholog (Hb) on developmental timing in flies and mice provide support for HBL-1 function as part of a conserved timing mechanism. Ultimately, identifying the relevant HBL-1 transcriptional targets will be required to distinguish between these models.

microRNA control of circuit refinement

Many aspects of early neuronal development are regulated by microRNAs (e.g. neuronal fate determination, neural tube closure, and mitotic exit) (Fiore et al., 2008; Fineberg et al., 2009). microRNAs have also been implicated in the functional plasticity of mature circuits (Fiore et al., 2008; Simon et al., 2008; Fineberg et al., 2009). Our results show that microRNAs play an important role in restricting when plasticity occurs during development. In particular, we show that miR-84 regulates the timing of DD plasticity, and that it does so by regulating *hbl-1*. The *Drosophila* microRNA Let-7 plays a similar role in dictating the timing of NMJ growth during larval development (Caygill and Johnston, 2008; Sokol et al., 2008). It is interesting that Let-7 and miR-84 are paralogs that bind to related seed sequences in target mRNAs. Thus, Let-7 microRNAs (and their targets) represent an ancient mechanism for determining the timing of circuit development.

HBL-1 mediates the effects of activity on circuit refinement

Perhaps the most surprising aspect of our results is that the timing of DD plasticity is regulated by activity. Mutations increasing and decreasing circuit activity had opposite effects on the timing of DD plasticity. These results are significant because they suggest that DD plasticity (and other forms of genetically programmed plasticity) and activity-dependent circuit refinement are not necessarily distinct processes, and may utilize similar genetic pathways. In this context, it is noteworthy that all of the genetic factors we identify (UNC-55/COUP-TF, HBL-1, and miR-84) are conserved in vertebrates, and vertebrate orthologs are all expressed in the CNS. It will be interesting to see if these molecules also play a role in refining vertebrate circuits. Several forms of plasticity are triggered by changes in the activity of the post-synaptic targets. Post-synaptic

activity is unlikely to play a role in this case as mutations blocking GABA transmission had no effect on the timing DD plasticity.

Our results also identify HBL-1 as a molecular mediator of activity's effects on DD plasticity. HBL-1 expression is restricted to a specific set of neuronal cell types, and thus could confer activity dependence in a cell and circuit specific manner. By contrast, it is unclear how the general activity-induced genes that are implicated in ocular dominance plasticity (e.g. CREB and BDNF) could mediate refinement in a cell and temporally specified manner. This result also demonstrates that the effect of *hbl-1* on developmental timing is regulated by the nervous system. It will be interesting to see if the nervous system also controls other heterochronic pathways.

In summary, we show that patterning of DD plasticity is achieved by the convergence of multiple regulatory pathways on *hbl-1*. Convergent regulation of *hbl-1* defines a cell intrinsic pathway that confers cell and temporal specificity and activity-dependence on this form of circuit refinement.

METHODS

Strains were maintained at 20°C using standard protocols, on lawns of OP50 for imaging and behavior, and on HB101 for electrophysiology. Strains are listed in the supplementary material.

qPCR

Whole worm lysates of synchronized L3 animals were prepared by Trizol extraction (Invitrogen). Three biological replicates of wild type and *unc-55(e1170)* samples were collected on different days. cDNA library construction, primer validation, and quantitative RT-PCR were carried out according to standard protocols. Changes in *hbl-1* mRNA levels, were normalized relative to *rpl-32* levels.

HBL-1 Reporters

The *hbl-1* reporters are similar to those used previously (Fay et al., 1999). These constructs contain 7.7 kb, including 6.4 kb upstream and 1.3 kb of exons 1-4. These constructs encode a protein containing the first 133 amino acids of *hbl-1* fused to GFP-PEST, along with 1kb of the *hbl-1* 3'UTR (*HgfpH*) or the control *unc-54* 3'UTR (*HgfpC*). In $H^{mut}gfpC$, the four 6bp UNC-55 binding sites in the *hbl-1* promoter were replaced with BamHI sites. Images were collected on a laser-scanning Olympus FV1000 confocal microscope. To quantify GFP fluorescence, areas of interest were drawn around DD or VD neuron cell bodies (identified by the *unc-25* GAD mCherry signal) in a single plane through the center of the cell bodies, and median GFP fluorescence was determined for that plane. DD neurons were distinguished from VD neurons based on anterior-posterior position in the ventral nerve cord, cell body size, and

morphology (White et al., 1986). The ratio of GFP signal in DD5 to VD10 was determined in each animal, $\log_2$ transformed, then averaged for all animals of a genotype. To enhance our ability to detect increases in *hbl-1* expression in *mir-84* and *tom-1* mutants, we used an *HgfpH* transgene (*nuIs427*) that has a low baseline expression level.

Electrophysiology

Electrophysiology was done on ventral and dorsal body muscles of dissected *C. elegans* adults as described, using 1 mM Ca^{2+} in the external saline solution (Richmond and Jorgensen, 1999; McEwen et al., 2006; Simon et al., 2008; Vashlishan et al., 2008). Ventral IPSC rates in *unc-55; hbl-1* could not be analyzed by Student's t test because many recordings totally lacked IPSCs; consequently, chi-squared tests were used to compare the number of recordings with and without IPSCs for *unc-55* single and double mutants.

Coiling Behavior

Young adult animals were assayed for the reverse coiling behavioral phenotype as described (Walthall and Plunkett, 1995). Animals were scored as either fully coiling or not, with partial coiling or failed coiling attempts scored as not coiling.

***in vivo* Fluorescence Microscopy and Image Analysis**

Dorsal and ventral nerve cord synapses were imaged in animals expressing GFP-tagged UNC-57/Endophilin or mCherry-tagged RAB-3 (nuIs279) using either a Zeiss Axioskop widefield epifluorescence microscope (using an Olympus PlanAPO 100x 1.4 NA objective) or an Olympus FV1000 confocal microscope (using an Olympus PlanAPO 60x 1.45 NA). Pre-

synaptic markers were expressed in GABAergic neurons using the *unc-25* promoter (all figures except Fig. 2.3c-d), or in the VD and AS neurons using the *unc-55* promoter (Fig. 2.3c-d). Animals were immobilized with 30mg/mL 2,3-butanedione monoxime (Sigma). Image stacks were captured, and maximum intensity projections were obtained using Metamorph 7.1 software (Molecular Devices). Line scans of ventral or dorsal cord fluorescence were analyzed in Igor Pro (WaveMetrics) using custom designed software as described (Burbea et al., 2002; Dittman and Kaplan, 2006).

DD Remodeling

The timing of DD remodeling was analyzed in synchronized animals. Briefly, plates containing isolated embryos were incubated at 20°C for 30 minutes and newly hatched L1 larvae were picked to fresh plates. DD remodeling was analyzed in resulting cohorts at defined times after hatching. Each time point comprises 1 hour of development (due to the time required for sample preparation and image acquisition). The extent of remodeling was quantified by counting the number of asynaptic gaps in the dorsal cord, using the GFP-tagged synaptic marker UNC-57 Endophilin expressed in the D neurons by the *unc-25 GAD* promoter, unless noted otherwise. Each animal can have 0 to 5 asynaptic gaps (between the 6 DD neurons). Wild type adults often have one gap (opposite the vulva opening); consequently, animals with zero or one gap were scored as completely remodeled. Images were scored in random order by an investigator unaware of the animal's genotype.

ACKNOWLEDGEMENTS

We thank members of the Kaplan lab for helpful discussions and comments; the *Caenorhabditis* Genetics Center (which is funded by the NIH National Center for Research Resources (NCRR)), G. Hayes, and S. Russell for strains; and the Wellcome Trust Sanger Institute for the *hbl-1* cosmid. This work was supported by a graduate research fellowship from National Science Foundation (K.T.-P.), a postdoctoral fellowship from the Jane Coffin Childs Memorial Fund for Medical Research (J.B.), and grants from the National Institutes of Health (NIH) to J.M.K. (NS32196) and J.B. (K99MH085039). K.T.-P. is an Albert J. Ryan Foundation fellow.

Chapter 3

Identification of synapse remodeling factors regulated by UNC-55 COUP-TF

Two researchers scored each RNAi screen described in this chapter: Jihong Bai and the author for the top hits screen; Monica Thanawala, a rotation student, and the author for the *unc-55* suppression screen. In addition, rotation students performed some of the follow-up work on genes identified in these screens. Their contributions are noted in the text.

INTRODUCTION

As demonstrated by our work and that of other labs, and discussed at length in the previous chapter, UNC-55 COUP-TF acts a general repressor of remodeling in VD neurons. We hypothesized that it functions by repressing the expression of remodeling-promoting genes like *hbl-1*, and by promoting the expression of remodeling-repressing genes (Fig. 3.1). Regulation of *hbl-1* expression accounts for some of this effect, but not all. Specifically, the incomplete suppression of *unc-55* mutant remodeling phenotype by *hbl-1* mutation (Figs. 2.7, 2.8, and 2.11) and the insufficiency of ectopic HBL-1 expression to force VD remodeling (Fig. 2.12) both suggest that other UNC-55 targets are also important. The hypomorphic nature of the *hbl-1(mg285)* allele could explain this first observation. However, the insufficiency of HBL-1 to force remodeling still suggests that other factors are important for remodeling.

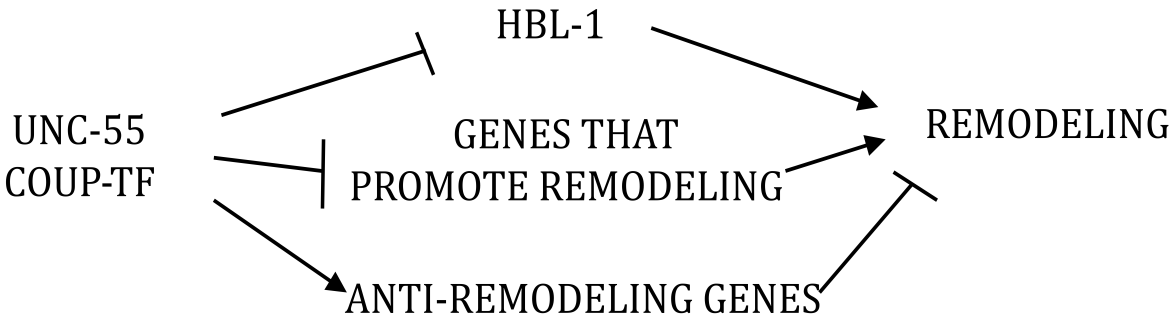

Fig 3.1. Classes of UNC-55 targets in VD neurons. UNC-55 COUP-TF represses the expression of pro-remodeling genes, and enhances the expression of anti-remodeling genes.

unc-55 and its mammalian homologs COUP-TF1 and COUP-TF2 are orphan receptors of the steroid/thyroid hormone receptor superfamily (Tang et al., 2010). COUP-

TFI and COUP-TFII, also known as Nr2f1 and Nr2f2, play important roles in a variety of biological processes (Lin et al., 2011). COUP-TFs can either inhibit or activate transcription of target genes, depending on cofactor binding (Pereira et al., 2000; Lin et al., 2011). COUP-TFs bind to a variety of DNA domains, often as homodimers to direct repeats spaced by a variable number of bases, but also inverted and everted repeats. Additionally, they can form heterodimers with RXR, a common half of many nuclear receptor heterodimers. Similarly, in *Drosophila*, the COUP-TF homolog *sevenup* (*svp)* forms heterodimers with the RXR homolog *Ultraspiracle (Usp*). RXR/*Usp* plays an important role in retinoid and thyroid hormone signaling in mammals, and ecdysone signaling in flies. By binding to RXR/*Usp*, COUP-TF/*svp* represses expression of genes normally activates by these hormones.

COUP-TFI and II regulate many aspects of early neuronal development. During eye development, COUP-TFI and II regulate the fate of progenitor cells (Tang et al., 2010). Single loss-of-function experiments suggest that the loss of one transcription factor is compensated by the presence of the other. In double eye-specific knockout experiments, retinal progenitor cells fail to differentiate properly, and dorsalization of the eye is compromised. COUP-TFs regulate multiple genes important for optic vesicle development, including *Pax6* and *Otx2*. COUP-TFs also regulate later stages of retinal development, where they suppress expression of subtypes of opsin photopigment genes in cone cells of the dorsal retina (Satoh et al., 2009).

In the cerebellum, COUP-TFI and II regulate proliferation of precursor cells. In COUP-TFII conditional knockout mice, the cerebellum size is reduced, and Purkinje cells

have fewer dendrite branches (Kim et al., 2009a). COUP-TFII specifically regulates the decision of granule cell precursors to proliferate or undergo apoptosis.

In the cortex, COUP-TFI regulates multiple aspects of cortical development, including neurogenesis, differentiation, proliferation, cell death, arborization, axon myelination, and cortex patterning (Lin et al., 2011). Animals lacking COUP-TF1 in the cortex display defects in differentiation of layer IV neurons, inappropriate connections between the cortex and thalamus, failure of thalamocortical neurons to send proper projections, delayed differentiation of oligodendrocytes, and severe defects in the specification of the caudoventral region of the cortex. COUP-TFI represses a corticospinal motor neuron differentiation program in the somatosensory cortex to regulate timing of birth and specification of this area (Tomassy et al., 2010).

In the peripheral nervous system, COUP-TFI mutants also have defects in axon guidance and arborization, specifically in the IX cranial ganglion, the oculomotor nerve, and the trigeminal nerve (Lin et al., 2011).

In this chapter, we identify targets of UNC-55 regulation, and begin to determine which genes play a role in remodeling. We use microarrays to identify genes whose expression changes in *unc-55* mutant animals. We then use RNAi knockdown in two independent screens to test for the function of these genes in remodeling. We follow up with genetic mutants for a few of these genes. We also perform a third small-scale RNAi screen to test for a role of a temporal sequence of transcription factors in the regulation of remodeling. These experiments provide a framework for further investigation of UNC-55-regulated genes.

RESULTS

Expression profiling of *unc-55* mutants

The *C. elegans* COUP-TF, *unc-55*, is expressed in the 13 VD and, presumably, the 11 AS motor neurons (Fig. 2.16b and (Zhou and Walthall, 1998)). VD and AS motor neurons terminally divide from each other at the end of the L1 stage (Sulston, 1976). *unc-55* does not seem to be expressed at high levels in any other tissue, based on transcriptional reporters. Therefore, we reasoned that changes in gene expression in *unc-55* mutants should be specific to changes in the VD and AS motor neurons.

We obtained two recessive *unc-55* mutants, *e402* and *e1170*. Because the nature of these mutations was not known and neither allele had a significantly stronger plate phenotype, we sequenced both alleles. *unc-55(e402)* is an EMS-induced C→T point mutation at position 682, which forms an early stop codon within the *unc-55* hormone binding domain (Fig. 3.2)(Brenner, 1974). *unc-55(e1170)* is an ICR191-induced C insertion at position 145, which causes a frameshift and an early stop shortly thereafter, upstream of both the zinc finger and ligand binding domains (Barnes and Hekimi, 1996; Zhou and Walthall, 1997). We chose to use the *unc-55(e1170)* allele for our experiments, because it

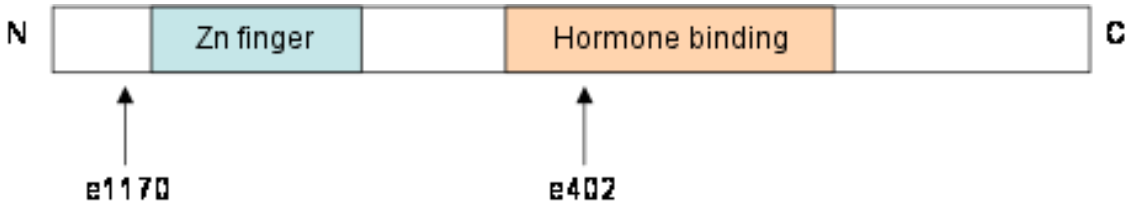

Fig 3.2. *unc-55* domain structure and mutant alleles. The nuclear hormone receptor *unc-55* is composed of a C4 zinc finger domain and a ligand-binding domain. The *e1170* allele adds a cytosine to a string of four Cs, causing a frameshift and early stop. The *e402* allele is a point mutation that generates a stop codon.

is more likely to be a true null allele.

Whole animal RNA was purified from L3 stage animals, during the period when VD neurons are undergoing ectopic remodeling. We used Affymetrix GeneChip *C. elegans* microarrays to determine gene expression changes. We analyzed the microarrays for changes in gene expression using three algorithms, RMA+LIMMA, GCRMA+LIMMA, and Rosetta Resolver (see Methods section for further discussion). Genes were categorized as significantly differentially expressed if they changed expression with $p < 0.01$, regardless of the magnitude of the change.

Relatively few genes were detected as differentially expressed, and with small fold change. As *unc-55* is only expressed in VD and AS motor neurons, subtle transcriptional effects would not be detected in a whole-worm lysate. Volcano plots of the magnitude of fold change versus statistical significance show few genes that change expression with $p < 0.01$ (Fig. 3.3 shows GCRMA+LIMMA). RMA detected the fewest genes changed, and Resolver detected the most, however most genes detected by Resolver were not detected by the other programs (Fig. 3.4; Tables 3.1 and 3.2).

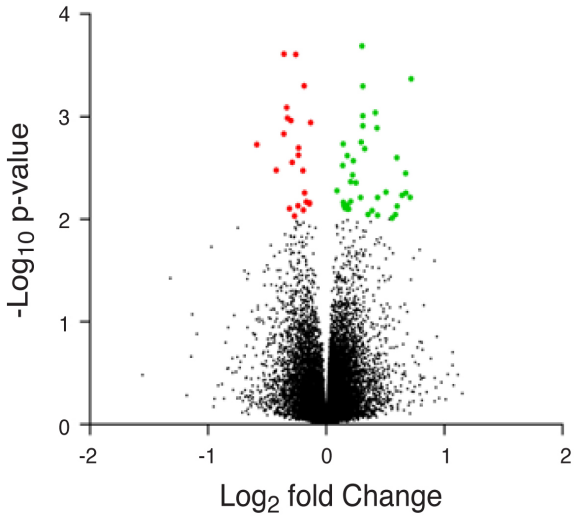

Fig 3.3. Volcano plot of gene expression changes in *unc-55(e1170)* mutants. GCMRA+LIMMA analysis of gene expression in wild type versus *unc-55(e1170)* L3-stage whole animal lysates. For each probeset, the $\log_2$ fold change in gene expression is plotted against the statistical significance of the fold change. Probesets with significantly ($p < 0.01$) higher expression in *unc-55* over WT appear in green; higher expression in WT over *unc-55* in red; no significant difference in expression in black.

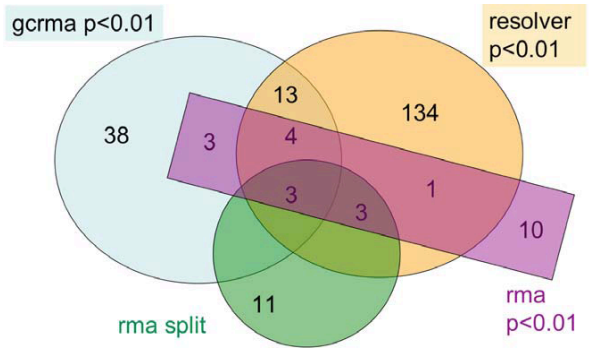

Fig 3.4. Multiple microarray analysis methods identify *unc-55*-sensitive changes in gene expression. Using three different microarray analysis algorithms ("rma", "gcrma", "resolver"), we identified genes differentially expressed between *unc-55* and N2 using a p-value cutoff of 0.01. Additionally, we also paired each control sample to the *unc-55* mutant sample collected on the same day for RMA analysis ("rma split").

Gene Name	Sequence name	rma +LIMMA p<0.01	gcrma +LIMMA p<0.01	resolver ratiobuild p<0.01	rma split	UNC-55 binding sites	avg FC	avg p-value	annotation
nspb-4	F38A5.10	■		■	■		1.97	0.00266	nematode-specific peptide
nspb-3	F38A5.5	■		■	■		2.37	0.00278	nematode-specific peptide
	F39C12.1			■			1.20	0.00000	
	F25G6.7		■	■		■	1.74	0.00101	transporter
daf-15	C10C5.6		■	■			1.33	0.00170	RAPTOR
	H22K11.2		■	■			1.69	0.00463	glycosyl hydrolase
spn-4	ZC404.8		■	■		■	2.59	0.00567	RNA-binding domain
	K01A2.4			■		■	2.76	0.00003	
	F45D11.3			■		■	1.44	0.00004	
	F47G4.4			■			1.65	0.00004	mei-2 paralog
hmit-1.1	Y51A2D.4			■			2.36	0.00008	myo-inositol transporter
	Y51A2D.9			■		■	1.19	0.00013	transthyretin-like
	K07B1.8		■				2.28	0.00025	
	K05F1.6		■				1.81	0.00025	organic cation transporter
cdk-1	T05G5.3			■			1.22	0.00029	cyclin-dependent kinase
	C06A8.5		■				1.54	0.00050	myosin
	K02B9.1			■		■	1.95	0.00058	
frm-7	C51F7.1			■			1.12	0.00059	FERM domain
srw-39	F19B2.3			■			1.91	0.00059	7TM receptor
	C17B7.5				■	■	1.57	0.00070	
sre-28	T07C12.6			■		■	1.94	0.00073	GPCR
eps-8	Y57G11C.24			■		■	1.10	0.00077	EGFR kinase substrate 8
inx-3	F22F4.2			■		■	1.47	0.00078	innexin
gei-8	C14B9.6			■			1.16	0.00080	Q/N-rich domain
snf-1	W03G9.1			■		■	1.15	0.00085	sodium/neurotransmitter symporter
	K04G2.10			■			1.88	0.00098	
rad-50	T04H1.4		■				2.14	0.00104	DNA repair
	F42A9.6				■	■	1.42	0.00105	
tag-324	C27C12.5			■			1.41	0.00109	ion channel
dyc-1	C33G3.1		■				1.99	0.00109	CAPON homolog, functions with dystrophin
	C06A5.5			■			1.41	0.00114	alternative splicing
	EEED8.3		■			■	1.36	0.00115	Fatty acid binding protein
nhx-2	B0495.4			■			1.11	0.00115	sodium/proton exchanger
	T20D4.12			■			1.41	0.00122	
	T23F4.3			■		■	2.87	0.00124	
hbl-1	F13D11.2			■			1.18	0.00146	zinc finger domains
eea-1	T10G3.5			■			1.18	0.00152	endocytosis
	F37A4.2			■			1.18	0.00183	
	C13B9.1			■		■	1.23	0.00184	S/T kinase ?
mpz-1	C52A11.4		■			■	1.72	0.00202	multiple PDZ domains
egl-30	M01D7.7			■		■	1.22	0.00227	G alpha q
	F36H5.8			■			2.56	0.00228	F-box domain
	Y54G2A.10		■			■	1.72	0.00238	
	K09A9.6			■		■	1.09	0.00239	aspartyl beta hydroxylase
	F17B5.1				■		1.44	0.00248	
zen-4	M03D4.1		■				1.94	0.00280	kinesin
apb-3	R11A5.1			■			1.14	0.00300	AP-3 adaptin
cln-3.3	ZC190.1			■			1.52	0.00303	CLN3 homolog
uaf-1	Y92C3B.2			■		■	1.20	0.00306	U2AF
pkc-1	F57F5.5			■		■	1.26	0.00317	S/T kinase
	Y39A1A.9			■		■	1.28	0.00366	
	R06F6.8			■		■	1.22	0.00375	WD40 repeats
	F31D4.4			■		■	1.20	0.00380	C-type lectin
unc-105	C41C4.5			■			1.27	0.00384	muscle degenerin mechanosensory channel

Table 3.1. Genes upregulated in *unc-55(e1170)* microarray relative to WT. If probesets were differentially expressed by multiple algorithms, averaged fold changes (FC) and p-values are shown. Fold changes ≥ 1.4 are highlighted in green.

Gene Name	Sequence name	rma p<0.01	gcrma p<0.01	resolver ratiobuild p<0.01	rma split	UNC-55 binding sites	avg FC	avg p-value	annotation
	ZK682.2			■		■	1.31	0.00444	sodium/phosphate transporter
	Y46B2A.1			■		■	2.86	0.00464	F-box domain
ttm-1	Y39E4A.2			■		■	1.25	0.00469	Zn2+ transporter
clec-60	ZK666.6	■					3.51	0.00505	C-type lectin
unc-61	Y50E8A.4			■		■	1.26	0.00523	septin
	F43G9.10			■		■	1.29	0.00534	microfibrillar-associated
	ZK1240.6			■		■	1.96	0.00550	zinc finger, E3 Ub ligase?
cdl-1	R06F6.1		■			■	1.53	0.00554	HBP/SLBP
	ZK353.1			■			1.14	0.00563	cyclin
	F45D11.2			■		■	1.30	0.00573	
puf-6	F18A11.1			■			1.92	0.00578	RNA binding
sre-37	F15A4.3			■			2.02	0.00590	GPCR
cyd-1	Y38F1A.5	■				■	2.01	0.00592	cyclin D homolog
	C53A5.2			■			1.27	0.00629	
sre-15	Y39C12A.7			■		■	2.14	0.00635	7TM receptor
	C04F12.1			■		■	1.21	0.00643	eIF2C
gsp-1	F29F11.6			■			1.18	0.00652	S/T protein phosphatase
	Y51H4A.24+25			■			1.25	0.00673	
spp-18	F27C8.4		■			■	1.48	0.00678	saposin-like
dpy-22	F47A4.2			■			1.40	0.00679	TRAP230 homolog
	W09C5.7		■				1.39	0.00694	Inositol polyphosphate-5-phosphatase
	B0207.11			■		■	2.27	0.00706	coiled-coil & SH2 domain
	Y119D3B.12		■				1.39	0.00709	cisplatin-resistance associated
mgl-2	F45H11.4			■		■	1.22	0.00730	mGluR
pqn-47	F59B10.1		■			■	1.74	0.00741	N/Q-rich domain
	T19D12.1			■			1.24	0.00754	Mucin-2 precursor homolog
rbd-1	T23F6.4				■		1.33	0.00757	MRD1
sdz-30	T04D3.2			■		■	2.14	0.00778	coiled-coil domain
	T20D4.13			■			2.32	0.00785	
elt-6	F52C12.5		■			■	2.05	0.00789	erythroid-like transcription factor
math-3	C08F1.4			■		■	1.22	0.00790	MATH-domain
hum-7	F56A6.2		■			■	1.56	0.00815	unconv. myosin heavy chain
	F57C9.4			■			1.18	0.00822	zinc finger
pgp-11	DH11.3			■			1.50	0.00830	ATP-binding
	T16G12.8			■			1.67	0.00838	
dig-1	K07E12.1			■		■	1.08	0.00865	cell adhesion
	W06H8.5			■			1.10	0.00870	non-coding transcript
	none			■		?	1.56	0.00871	
	F58B3.9			■		■	3.64	0.00874	transthyretin-like
	C35C5.6			■			1.54	0.00879	
	Y59H11AR.4			■		■	1.34	0.00887	transporter
	Y6G8.2			■		■	1.16	0.00888	F-box domain
	F22A3.6			■			1.12	0.00907	lysozyme
spat-1	F57C2.6			■		■	1.32	0.00910	BORA homolog, polarity
klf-1	F56F11.3			■		■	2.17	0.00921	kruppel-like factor
	F10G7.9	■					1.94	0.00933	
	K01A2.3	■					2.51	0.00938	
	F49E2.5			■			1.15	0.00950	neurofilament heavy polypeptide
pry-1	C37A5.9			■		■	1.44	0.00995	axin homolog
	F45D11.15				■	■	1.43	0.01447	

Table 3.1, cont. Genes upregulated in *unc-55(e1170)* microarray over WT. If probesets were differentially expressed by multiple algorithms, averaged fold changes (FC) and p-values are shown. Fold changes ≥ 1.4 are highlighted in green.

Gene Name	Sequence name	rma p<0.01	gcrma p<0.01	resolver ratiobuild p<0.01	rma split	UNC-55 binding sites	avg FC	avg p-value	annotation
	K11H12.4	■	■	■	■	■	-3.41	0.00028	
lbp-9	Y40B10A.1		■	■		■	-1.63	0.00062	Fatty acid-binding protein
	F02H6.5	■	■	■	■	■	-3.08	0.00233	Sulfide:quinone oxidoreductase
clc-1	C09F12.1	■	■	■			-1.91	0.00313	claudin
cpr-3	T10H4.12	■	■	■	■		-2.27	0.00600	Cysteine proteinase Cathepsin
cpr-3	T10H4.12		■	■			-1.68	0.00020	Cysteine proteinase Cathepsin
	F09B9.1			■	■		-1.67	0.00137	acetyl transferase
atgr-9	T22H9.2	■		■	■	■	-2.91	0.00267	autophagy related
tag-120	F40F9.2	■	■	■			-1.69	0.00279	NMDA receptor-associated protein
tyr-4	C34G6.2	■	■	■		■	-2.04	0.00345	tyrosinase
tsp-2	C02F5.11	■	■	■			-2.56	0.00355	tetraspanin
	W05G11.6			■			-1.18	0.00000	Phosphoenolpyruvate carboxykinase
uvt-3	C42D8.3		■	■			-1.61	0.00116	pantothenate kinase
dhs-30	T25G12.7		■	■		■	-1.67	0.00120	dehydrogenase
efk-1	F42A10.4			■			-1.26	0.00133	calcium/calmodulin-dependent protein kinase
	C31A11.5		■	■		■	-3.12	0.00278	
	F43D2.1			■		■	-1.11	0.00316	cyclin
asna-1	ZK637.5		■	■		■	-1.31	0.00376	membrane transporter
	F54D1.6		■	■		■	-1.26	0.00413	
vha-14	F55H2.2	■	■				-1.92	0.00489	Vacuolar ATP synthase
	C17C3.1		■	■		■	-2.47	0.00496	acetyl-CoA thioesterase
	T15B7.16		■	■			-1.79	0.00649	ligand gated ion channel
srh-11	R09F10.6	■		■			-1.69	0.00661	7TM receptor
	C17C3.1	■	■			■	-3.36	0.00736	acetyl-CoA thioesterase
	R02D5.3			■			-1.18	0.00001	
msp-63	K05F1.7			■			-1.62	0.00002	major sperm protein
	F01D5.1			■			-1.32	0.00008	
	Y56A3A.2			■			-1.34	0.00012	protease
cnc-4	R09B5.9				■	■	-1.59	0.00013	
arl-8	Y57G11C.13			■			-1.14	0.00017	ADP-ribosylation factor
lact-4	M05D6.4				■	■	-1.54	0.00028	esterase
	C18E9.9			■			-1.11	0.00032	
arl-8	Y57G11C.13			■			-1.23	0.00040	ADP-ribosylation factor
efk-1	F42A10.4			■		■	-1.20	0.00045	calcium/calmodulin-dependent protein kinase
	F12A10.1 + .			■			-1.48	0.00050	
	Y119C1B.1			■			-1.79	0.00056	
pmk-1	B0218.3			■		■	-1.19	0.00057	p38 MAPK
	C04G2.1			■			-1.32	0.00060	transthyretin-like
	F59C6.11			■		■	-1.32	0.00065	claudin
	F43G9.3			■		■	-1.25	0.00072	mitochondrial carrier protein
	K02C4.2				■		-1.48	0.00074	
	F15B9.6				■		-1.66	0.00080	
srt-23	Y55F3C.2			■			-2.65	0.00104	7TM receptor
	Y105C5B.15			■			-1.15	0.00124	serine/threonine protein phosphatase
tsp-1	C02F5.8			■			-1.46	0.00132	tetraspanin
stdh-1	C06B3.4			■		■	-1.22	0.00132	estradiol dehydrogenase
clec-41	B0365.6			■			-1.36	0.00149	C-type lectin
	C17H12.8			■		■	-1.08	0.00150	
	K08E4.7			■			-2.18	0.00169	
cyp-34A3	C41G6.1			■			-2.27	0.00172	cytochrime P450
	ZK829.4		■			■	-1.39	0.00185	Glutamate dehydrogenase
	F47B10.9			■			-1.18	0.00200	
	F56C9.10			■			-1.08	0.00211	Breast carcinoma amplified sequence
gly-6	H38K22.5		■			■	-1.51	0.00241	glycosyl transferase
nhr-42	C33G8.6			■			-1.19	0.00242	nuclear hormone receptor
unc-64	F56A8.7			■			-1.11	0.00254	syntaxin
	M60.6		■			■	-1.70	0.00270	

Table 3.2. Genes downregulated in *unc-55(e1170)* microarray relative to WT. If probesets were differentially expressed by multiple algorithms, averaged fold changes (FC) and p-values are shown. Fold changes ≥ -1.4 are highlighted in red. Occasionally multiple probesets are designed to detect a single gene and indicated changes in gene expression; different probesets are listed in different rows.

Gene Name	Sequence name	rma p<0.01	gcrma p<0.01	resolver ratiobuild p<0.01	rma split	UNC-55 binding sites	avg FC	avg p-value	annotation
	K11H3.3			■		■	-1.28	0.00275	Tricarboxylate transporter
cgt-1	T06C12.10			■			-1.24	0.00275	Ceramide glucosyltransferase
	F53A9.9			■		■	-1.23	0.00278	Serine/threonine-protein phosphatase 1 regulatory subunit
spp-22	ZK867.2 + .3			■		■	-1.21	0.00279	Glutamate receptor or 7TM receptor
cyp-35C1	C06B3.3				■		-1.43	0.00295	cytochrime P450
	F54C9.7		■				-1.38	0.00300	
	MTCE.25			■		■	-1.09	0.00334	NADH dehydrogenase
	T02D1.4			■			-2.37	0.00337	
sptl-3	T22G5.5			■		■	-1.29	0.00339	Serine palmitoyltransferase
srv-36	F57G8.8	■				■	-2.39	0.00369	7TM receptor
	C46F11.2		■				-1.67	0.00373	glutathione oxidoreductase
	F21E9.3			■			-1.38	0.00413	
	C49C3.6		■			■	-1.61	0.00432	
pas-5	F25H2.9		■				-1.78	0.00442	20S proteasome zeta chain
	F21C10.10			■			-1.26	0.00444	
pyp-1	C47E12.4			■		■	-1.07	0.00452	inorganic pyrophosphatase
	C49C3.9			■			-1.34	0.00472	
	C30F12.6			■		■	-1.17	0.00479	7TM receptor
	Y38C1AA.8			■			-1.41	0.00489	
	C44B12.5			■		■	-1.39	0.00512	
	K04A8.1			■			-1.12	0.00518	
	Y110A7A.6			■			-1.13	0.00526	phosphofructokinase
col-70	H17B01.2		■			■	-1.23	0.00529	collagen
	R02D3.1			■			-1.15	0.00533	dehydrogenase
	Y39A1A.1		■			■	-3.20	0.00546	WD40 repeat
	B0218.2			■		■	-1.21	0.00584	amidase
	R102.6		■				-4.38	0.00586	
tag-38	B0222.4		■				-5.13	0.00613	glutamate decarboxylase
cdk-7	Y39G10AL.3		■				-2.71	0.00615	cyclin-dependent kinase
ooc-3	B0334.11		■			■	-1.95	0.00615	embryonic polarity
	C17B7.12			■			-2.10	0.00644	
	C53D6.5			■			-2.20	0.00672	
	Y19D10B.6		■			■	-1.61	0.00673	neprilysin
snb-1	T10H9.4		■			■	-1.39	0.00686	synaptobrevin
	D1054.1			■			-1.15	0.00697	palatin-like phospholipase
act-4	M03F4.2			■			-1.08	0.00703	actin
	C01A2.5			■		■	-1.17	0.00704	
srt-17	F48G7.6			■			-2.26	0.00711	7TM receptor
	C52B9.4		■			■	-1.51	0.00728	transmembrane
	ZK1307.2		■				-1.41	0.00738	
	Y37A1A.2		■			■	-3.98	0.00749	
	C40H5.8			■			-1.81	0.00768	
	F32A5.8			■			-1.20	0.00782	WW domain-containing oxidoreductase
gmd-2	F56H6.5				■	■	-1.50	0.00783	GDP-mannose dehydratases
	C35B1.5		■				-1.51	0.00796	thioredoxin
	R31.2		■				-1.55	0.00797	
	Y45F3A.9	■					-2.31	0.00808	RNA Methylase
	Y92H12BR.2			■		■	-1.34	0.00820	
sri-71	D2062.3	■				■	-2.05	0.00823	7TM receptor
gst-22	F21H7.1		■			■	-2.44	0.00827	glutathione s transferase
nhr-155	C14C6.4	■				■	-2.49	0.00848	nuclear hormone receptor
cdh-8	F18F11.3	■				■	-1.94	0.00873	cadherin
rpl-1	Y71F9AL.13			■			-1.05	0.00896	arge ribosomal subunit protein
	C46E10.5			■			-2.25	0.00900	F-box domain
	M05B5.2			■			-1.17	0.00917	
	F21H7.2	■					-1.95	0.00928	neurofilament heavy protein
	B0432.1			■			-2.04	0.00952	
	C50F4.8			■		■	-1.19	0.00964	

Table 3.2, cont. Genes downregulated in *unc-55(e1170)* microarray versus WT. If probesets were differentially expressed by multiple algorithms, averaged fold changes (FC) and p-values are shown. Fold changes ≥ -1.4 are highlighted in red. Occasionally multiple probesets are designed to detect a single gene and indicated changes in gene expression; different probesets are listed in different rows.

UNC-55 binding sites have been proposed based on similarity to the binding sites of COUP-TFs, the *unc-55* mammalian homologs (Shan et al., 2005). In addition, UNC-55 has been shown to repress expression of *hbl-1* and the neuropeptide *flp-13* in VD neurons, dependent on a half UNC-55 binding site in the promoter. *unc-55* mutants inappropriately express *hbl-1* and *flp-13* reporters in the VDs, and reporters lacking the UNC-55 binding site are expressed in VD neurons regardless of *unc-55* expression. We found UNC-55 half binding sites in 49% of the promoters for genes differentially expressed by microarray (promoters were uniformly designated as the 3kb upstream of the TSS; Tables 3.1 and 3.2).

We validated the directions of a few of our gene expression changes by quantitative PCR. Using qPCR, we confirmed the subtle changes in expression predicted by the microarray for four of the five genes (three samples per genotype, two technical replicates; Fig. 3.5).

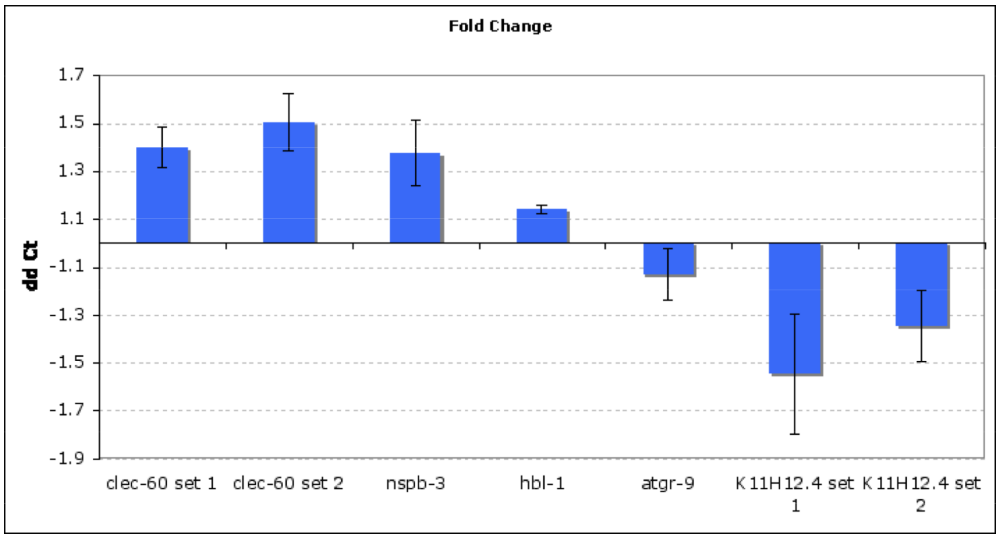

Fig 3.5. qPCR validation of microarray results. Of five genes picked from *unc-55* microarray hits for validation, four behave as expected by qPCR: *clec-60, hbl-1*, and *nspb-3* increased in the microarray and by qPCR, while K11H12.4 decreased. *atgr-9* decreased in the microarray, but was unchanged by qPCR. Average fold change ± SEM. Shown here one of two representative technical replicates.

RNAi screen of microarray 'top hits' for roles in remodeling

We used feeding RNAi knockdown to test the 71 most convincing microarray hits for roles in remodeling. Although we had high false positive and negative rates, we convincingly hit 19 novel genes, of which 7 have mutant alleles available ($p<0.05$, Chi^2 test; Table 3.3). We primarily identified genes whose absence causes precocious DD remodeling similar to *mir-84*, or genes that act like *unc-55 COUP-TF* to repress VD remodeling.

gene		hit rate	phenotype	Mutant alleles?
efk-1	calcium/calmodulin-dependent protein kinase	3 of 4	L1: early dorsal fluorescence.	Yes
F39C12.1	futsch homolog (MT binding)	3 of 4	L1: early dorsal fluorescence. adult: VNC disorganized.	Yes
gei-8	putative nuclear co-repressor	4 of 4 (v. strong)	L1: early dorsal fluorescence. adult: VNC/DNC dim, disorganized	Yes
lgc-54	ligand-gated ion channel GABA receptor beta-2	3 of 4	L1: early dorsal puncta.	Yes
pmk-1	p38 MAPK	5 of 6	L1: early dorsal puncta. adult: VNC disorganized	Yes
pnk-4/uvt-3	pantothenate kinase	3 of 4 (weak?)	adult: VNC/DNC dim, disorganized	Yes
spdl-1	coiled-coil protein, *spindly* homolog	3 of 4	adult: some VNC sections are dim, disorganized	Yes
Y56A3A.2	metalloprotease	3 of 4	L1: some early dorsal fluorescence.	Yes
dhs-30	dehydrogenase	3 of 4 (weak?)	adult: DNC disorganized	Transposon insertion
F25G6.7	sugar transporter	3 of 4	adult: VNC dim or disorganized	Mos insertion
rbd-1	RNA binding protein	3 of 4	L1: early completion of remodeling.	Mos insertion
F01D5.1	secreted surface protein	4 of 4	adult: VNC puncta small, disorganized	No
F54D1.6	cell-matrix adhesion	3 of 4	adult: VNC disorganized.	No
lbp-6	lipid binding	3 of 4	L1: early dorsal fluorescence. adult: VNC dim	No
msp-63	antagonizes Eph/ephrin signaling	3 of 4	adult: VNC very dim	No
oac-14	o-acyltransferase	3 of 4	adult: VNC dim	No
sre-28	GPCR 7TM receptor	3 of 4	L1: early dorsal fluorescence. adult: VNC diffuse	No
tsp-2	tetraspanin TM	3 of 4	L1: early dorsal fluorescence.	No

Table 3.3. Novel genes hit by RNAi screen for remodeling phenotypes. Precocious remodeling like *lin-14* or improper synapse formation like *syd-2* was detected as early dorsal fluorescence in the L1. Inappropriate VD remodeling like *unc-55* was detected as dim VNC synapses in the adult.

Presumably the high false positive and negative rates for this screen were due to the wide variety of phenotypes being scored, the multiple stages of development being observed, and the reliance on imprecise indicators, like size, to estimate developmental stage.

We chose some of these genes for further study, based on the availability of genetic mutants at the time, in December 2008. We obtained mutant alleles for *pmk-1, pnk-4,* and *gei-8*. Our results with these mutants are discussed below. Since 2008, mutants have become available for more of these genes (Table 3.3).

RNAi screen for suppressors of *unc-55* VD remodeling

We hypothesize that in VD neurons UNC-55 COUP-TF prevents remodeling by repressing the expression of remodeling genes. In *unc-55 COUP-TF* mutants the ectopic VD expression of these remodeling genes promotes remodeling. Therefore, the loss of these genes should suppress the *unc-55 COUP-TF* ectopic remodeling phenotype. We screened through all of the 104 genes repressed by UNC-55 COUP-TF (Table 3.1) for suppression of the *unc-55 COUP-TF* mutant phenotype, using *hbl-1* as a positive control. False positive and negative rates were much improved for this screen. We hit 17 genes with high confidence ($p < 0.03$; Table 3.4).

Table 3.4. Novel genes hit by 2-generation RNAi screen for *unc-55* suppressors.

GENE	ANNOTATION	ALLELES	HIT RATE
apt-6/apb-3	Adaptin, beta-3 subunit of AP-3	one	4/7
cyd-1	cyclin D	six	3/7
clec-264	C-type lectin	transposon insertions	3/7
F57C9.4	C2H2 Zinc finger domains; homolog of *Drosophila glass* (transcription factor essential for photoreceptor differentiation)	two	3/7
gei-8	interacts with GEX-3, two myb-like DNA binding domains, homolog of nuclear co-repressors, HDAC-interacting domain	two	4/8

hbl-1	*Hunchback-like* C2H2 Zinc finger transcription factor	four	positive control (28/28)
klf-1	Kruppel-like transcription factor, C2H2 Zinc finger domains,	two	6/7
K01A2.4	predicted integral membrane protein; paralog of *mps-2*, a single pass TM protein that regulates K channels	two	4/8
mpz-1	multiple PDZ-binding domains, colocalizes with pre-synaptic proteins, binds 5-HT receptor SER-1, may bind NPR-1	two	3/7
pgp-11	ATP binding cassette (ABC) transporter; mutants defective in some feeding RNAi	one	3/7
pkc-1	neuropeptide secretion, positive regulation of locomotion	seven	3/7
pry-1	Axin homolog; antagonizes Wnt pathway in Q neuroblast migration, VPC fate, postdereid formation, male ray formation, HSN migration, seam cell V5 polarity, etc.	three	4/7
spdl-1	kinetochore receptor	one	4/7
T20D4.13	predicted integral membrane protein, worm-specific	two large deletions	3/7
unc-61	septin, required for postembryonic cytokinesis	three	4/7
Y39A1A.9	Uncharacterized. possible homology to SWI/SNF subunit	two	4/7
Y119D3B.12	Splicing factor	no	3/7
ZK1240.6	predicted E3 ubiquitin ligase	two large deletions	4/7

Table 3.4, cont. Novel genes hit by 2-generation RNAi screen for *unc-55* suppressors.

Some RNAi clones produced lethal or arrested phenotypes. These RNAi clones were screened in a 1-generation RNAi screen. This screen had a 0% false positive rate, so we cannot determine the statistical significance of these hits.

GENE	**ANNOTATION**	**ALLELES**	**HIT RATE**
gsp-1	catalytic subunit of serine/threonine specific protein phosphatase PP1	one	3/4
mfap-1	microfibrillar-associated protein, potential role in splicing	one	2/4
zen-4	Kinesin-like member of kinesin-6 subfamily of plus-end-directed microtubule motors. Role in cytokinesis, spindle microtubule formation and/or maintenance. Polarization of epithelial arcade cells in pharynx development.	eight	2/4
cdl-1	homolog of proteins that bind to the hairpin structure in core histone mRNAs to promote histone pre-mRNA processing and translation	six	2/4
cdk-1	cyclin-dependent kinase	ten	2/4

Table 3.5. Novel genes hit by 1-generation RNAi screen for *unc-55* suppressors.

A potential role for Neuroblast clock homologs

The *Drosophila* homologs of *unc-55* (*Sevenup, Svp*) and of *hbl-1* (*hunchback, hb*) are members of a transcriptional cascade known as the Neuroblast clock that controls the temporal identity of progeny neurons and glia during development (Isshiki et al., 2001; Mettler et al., 2006; Urban and Mettler, 2006). In the *unc-55* mutant microarray, we detected increased expression of the *hb* target gene, *Kruppel (Kr)* in *Drosophila* and *klf-1 (Kruppel-like factor)* in *C. elegans* (Table 3.1). This suggests that *klf-1* expression may be repressed by the UNC-55 protein. The statistical significance of this change was not enough to include *klf-1* in the top hits RNAi screen. However, in the *unc-55* suppression RNAi screen, *klf-1* strongly suppressed ectopic VD remodeling (Table 3.4).

We hypothesized that other members of the neuroblast clock cascade of transcription factors might play a role in regulating remodeling. We BLASTed the other components of the neuroblast clock against the *C. elegans* proteome, and picked RNAi clones targeting these genes. We screened these RNAi clones for suppression of *unc-55* ectopic VD remodeling. Remarkably, RNAi clones targeting homologs of many of the genes in this pathway were strong hits, on par with RNAi against *hbl-1* (Table 3.6). Of special note, knockdown of *lin-29*, which has been extensively characterized as a downstream effector of *hbl-1* in the regulation of hypodermal development in the worm, suppressed ectopic VD remodeling (Abrahante et al., 2003; Lin et al., 2003). Again, we had a 0% false positive rate for the 29 times we scored our negative controls, so we cannot determine the statistical significance of these hits. All hits were scored as such multiple times. This suggests that some or all of the components of this transcriptional cascade may be reused in these neurons.

Fly Neuroblast clock genes	**Worm homologs**	**Suppression of *unc-55* ectopic VD remodeling by RNAi ?**
Svp	*unc-55*	
Hb	*hbl-1*	Yes
Kr	*klf-1*	Yes
	klf-2	Yes
	che-1	No
	mel-26	Arrested/lethal
	blmp-1	Yes
	mua-1	Arrested/lethal
	tra-1	No
	mnm-2	Arrested/lethal
	pag-3	Arrested/lethal
Pdm	*ceh-6*	No
	unc-86	Yes
	F41H10.3	Yes
	ceh-18	Yes
Cas	C01G8.6	No
	K05F1.5	Yes
	pgl-1	No
Grh	*grh-1*	Embryonic arrest
Prospero	*ceh-26*	No
Sqz	*lin-29*	Yes

Table 3.6. Suppression of *unc-55* ectopic VD remodeling by neuroblast clock homologs.

VD/AS cell division is not drastically delayed in *unc-55* mutants

Transitioning from the expression of one neuroblast clock transcription factor to the next in the sequence is sometimes dependent on cell division, specifically after the Hb state (Rougvie, 2005; Mettler et al., 2006). Additionally, we identified a number of genes that have roles in cell division in our microarray and RNAi screens, such as the kinetochore receptor *spdl-1 Spindly*, the cyclin-dependent kinase *cdk-1,* the cyclin D *cyd-1*, the septin *unc-61*, and the plus-end directed kinesin6-like *zen-4*.

We reasoned that the cell division that produces VD and AS neurons might be altered in *unc-55* mutants, and that this altered cell division might explain why VD neurons become competent to remodel. To test this, we observed the appearance of VD/AS neuron pairs in *unc-55* mutants, using the *unc-55* promoted mCherry marker (Fig. 2.16b). We observed no change in the appearance of VD/AS neuron pairs in *unc-55(e1170)* mutants (Fig. 3.6). Note that this reporter was not visible in the Pn.ap precursors prior to the terminal division.

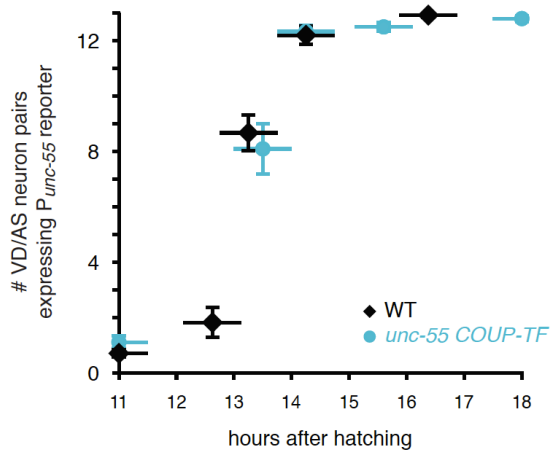

Fig 3.6. VD/AS terminal division is not delayed in *unc-55(e1170)* mutants. The *unc-55* promoter drives expression in the VD and AS neurons, visible just after the terminal division.

Analysis of the p38 MAPK *pmk-1*

Expression of the p38 MAPK *pmk-1* decreased in the *unc-55* mutant microarray, relative to wild type, suggesting that the expression of *pmk-1* is enhanced by the UNC-55 protein (Table 3.2). This puts *pmk-1* in the category with repressors of remodeling. *pmk-1* RNAi caused early dorsal puncta in L1 animals, similar to precocious remodeling or disorganized synaptogenesis phenotypes (Table 3.3). *pmk-1* RNAi also caused aberrations in VNC synapses in adult animals.

The p38 MAPK *pmk-1* plays an important role in the regulation of innate immunity (Troemel et al., 2006). *pmk-1* mutants have normal responses to the cholinesterase inhibitor aldicarb, suggesting that GABAergic and cholinergic signaling to body muscle is grossly normal in the adult (Vashlishan and Kaplan, 2008). The related p38 MAPK *pmk-3* cell-autonomously regulates the morphology of synapses during development, functioning downstream of the MAPKK *mkk-4* and the MAPKKK *dlk-1* (Nakata et al., 2005).

We obtained the mutant allele *pmk-1(km25)*. A rotation student in the lab, Mike Sussman, tested this mutant for alterations in the timing of DD remodeling. At early (11hrs) and late (18hrs) time points, *pmk-1(km25)* mutants exhibited very slightly precocious DD remodeling, which is similar to the RNAi observation (Fig. 3.7). This suggests that PMK-1 might function to prevent precocious DD remodeling.

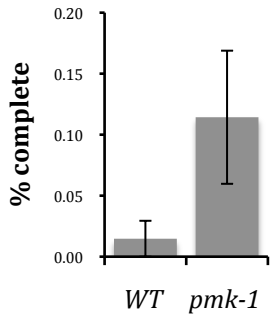

Fig 3.7. *pmk-1* mutants may have very subtle precocious DD remodeling at 11 hours post-hatching. $p < 0.05$, Chi-squared test.

Another rotation student, Peter Wang, tested the *pmk-1(km25)* mutant for suppression of *unc-55* ectopic VD remodeling by imaging ventral synapses in adult animals. *pmk-1(km25)* very slightly suppressed the *unc-55*-induced elimination of ventral synapses (Fig. 3.8). This is surprising given the decreased expression in *unc-55* mutants by microarray. We would have predicted that genes whose expression was enhanced by UNC-

55 should act as repressors of remodeling, and that mutations should, if anything, enhance VD remodeling.

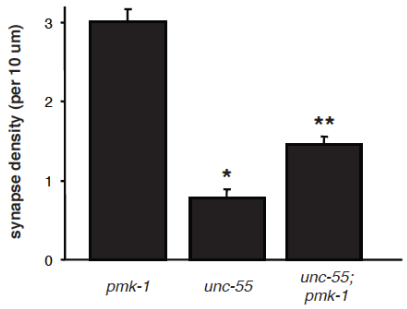

Fig 3.8. *pmk-1* slightly suppresses *unc-55* mutant VD remodeling. Synapse density was measured in adults for the indicated genotypes. (*) significantly different from wild type (not shown) $p < 0.01$. (**) different from *unc-55*, $p < 0.01$. N=40 per genotype.

Analysis of the nuclear co-repressor *gei-8*

Expression of the GEX3-interacting protein and putative nuclear co-repressor *gei-8* increased in *unc-55* mutants by microarray, suggesting that GEI-8 might promote remodeling (Table 3.1). *gei-8* contains two Myb-like DNA binding domains and an HDAC-interacting domain, similar to the vertebrate co-repressor proteins N-CoR and SMRT (Tsuboi et al., 2002). It was named for its ability to bind to GEX3 in yeast-two-hybrid assays (Tsuboi et al., 2002). These co-repressors mediate the transcriptional repression of nuclear hormone receptors by assembling complexes containing nuclear receptors and HDACs (Yamamoto et al., 2011).

gei-8 RNAi produced very strong results in both screens. In L1 animals, *gei-8* knockdown resulted in precocious dorsal synapses (Table 3.3). By the adult stage, synapses were disrupted and disorganized both dorsally and ventrally. In the *unc-55* suppression RNAi screen, *gei-8* RNAi strongly suppressed ectopic VD remodeling (Table

3.4).

Unpublished work from other groups shows that *gei-8* is expressed in neurons in the ventral nerve cord, and that *gei-8* mutants have enhanced sensitivity to the acetylcholinesterase inhibitor aldicarb (personal communications (Mikolas et al., 2009)). Increased sensitivity to aldicarb is a phenotype shared by many mutants with defects in GABA-induced muscle relaxation (Vashlishan et al., 2008).

We obtained the *gei-8(gk693)* mutant allele, which is a 1018bp deletion that takes out the ATG start site of two of three isoforms of *gei-8*. *gk693* might not be a null allele, given that a third isoform of *gei-8* could be produced, and *gk693* does not affect the HDAC-interaction domain. Mike Sussman did not detect any significant alterations in the timing of DD remodeling. Monica Thanawala did not detect significant changes in adult D neuron synapse morphology or density, though there was a trend towards a decreased density of dorsal synapses, as might be expected if DD remodeling was slightly defective. More convincingly, Peter Wang observed that *gei-8(gk693)* significantly suppressed *unc-55* ectopic VD remodeling, as determined by the density of synapses in adult ventral nerve cords (Fig. 3.9).

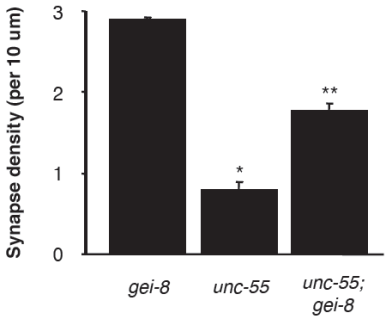

Fig 3.9. *gei-8* suppresses *unc-55* mutant VD remodeling. Synapse density was measured in adults for the indicated genotypes. (*) significantly different from wild type (not shown) $p < 0.01$. (**) different from *unc-55*, $p < 0.01$. n=40 per genotype.

Analysis of the pantothenate kinase *pnk-4*

Expression of the pantothenate kinase (PanK) homolog *pnk-4*, also known as *uvt-3*, decreased in *unc-55* mutants by microarray, suggesting that UNC-55 promotes *pnk-4* expression (Table 3.2). PanKs are involved in coenzyme A (CoA) biosynthesis (Zhou et al., 2001a). Human PanKs are implicated in the neurodegenerative disease Hallervorden-Spatz syndrome, while *Drosophila* mutants defective for the PanK homolog *fumble* are uncoordinated (Zhou et al., 2001a). *pnk-4* is expressed in ventral nerve cord neurons in *C. elegans* (McKay et al., 2003; Hunt-Newbury et al., 2007).

pnk-4 RNAi caused disruptions in dorsal and ventral synapses in adults (Table 3.3). We obtained the mutant allele *pnk-4(ok1832)* which takes out 1034bp, including part of the PanK domain. We did not detect alterations in DD remodeling, either in the RNAi screen or by imaging mutant animals (by Mike Sussman). However, Peter Wang saw that *pnk-4(ok1832)* mutations strongly suppressed ectopic *unc-55* VD remodeling (Fig. 3.10). Again, this was surprising, given that we would have predicted based on the microarray that *pnk-4* mutants would have enhanced *unc-55* phenotypes.

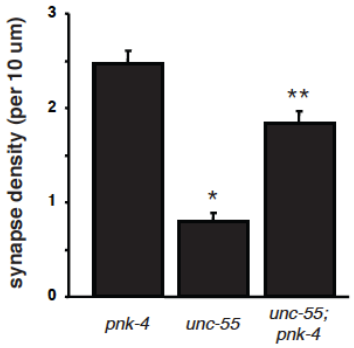

Fig 3.10. *pnk-4* strongly suppresses *unc-55* mutant VD remodeling. Synapse density was measured in adults for the indicated genotypes. (*) significantly different from wild type (not shown) $p < 0.01$. (**) different from *unc-55*, $p < 0.01$. n=40 per genotype.

DISCUSSION

UNC-55 COUP-TF acts as a cell-autonomous repressor of synaptic remodeling in *C. elegans* VD neurons. To identify novel synapse remodeling factors, we sought targets of UNC-55 regulation. We characterized gene expression changes in *unc-55* mutants using whole genome microarrays, and then performed RNAi screens to assay the function of these genes. We knocked down the top microarray hits, and scored for alterations in DD remodeling, ectopic VD remodeling, and synaptogenesis defects. This screen was successful, but plagued with high miscall rates. We also knocked down the genes up-regulated by *unc-55* mutation, and screened for suppression of ectopic *unc-55* VD remodeling.

These screens together suggested a number of avenues to pursue. We hypothesize that the neuroblast clock sequence of transcription factors may play a role in remodeling. Furthermore, we identified many genes that play roles in cell division, though we have not observed cell division defects in VD neurons in *unc-55* mutants. Finally, we obtained mutants for a few of the genes identified by the top hits RNAi screen, and tested them for alterations in DD remodeling and for suppression of *unc-55* VD remodeling. Together, these experiments suggest potential regulators of remodeling for further investigation.

Many genes regulated by UNC-55 COUP-TF

Our microarray analysis identified a number of genes differentially regulated in *unc-55* mutants. At first, the small magnitude of changes in expression level might be troubling. However, *unc-55* is expressed only in the 13 VD and 11 AS neurons. Considering that we

used whole animal lysates to test for changes in gene expression, the small expression changes are no longer surprising. Genes expressed in multiple tissues, but that are only repressed by UNC-55 in the VD neurons, would be hard to detect. In that respect, it is surprising that we were able to detect changes in *hbl-1* expression at all, given that *hbl-1* is expressed in multiple tissues. It is unlikely that we would detect second-order gene expression in the *unc-55* microarray, like *hbl-1* targets, for these reasons.

One alternative approach would be to express the polyA-binding protein PAB-1 only in VD neurons, and use that to isolate mRNA from VD neurons in wild type and *unc-55* mutant animals. Indeed, this was the approach taken by the Miller lab in a recent publication, where they expressed PAB-1 in the DD and VD neurons using the *ttr-39* promoter (Petersen et al., 2011). They then screened for *unc-55* suppressing RNAi clones among their microarray hits, published the list of genes that when knocked down could suppress VD remodeling, and characterized one gene in detail, the homeobox transcription factor *Iroquois irx-1*. Notably, we did not detect changes in expression in any of the genes that they publish in their study, although there is some similarity in gene class (we each hit a C-type lectin). This could be due to the different stages that we determined expression changes (L3 in our work versus mid L2 in their study), distortion in their RNA sample during amplification (we collect sufficient RNA from whole worm lysates that amplification is not necessary), or confounding signals from other tissues in our experiment. We can conclude that neither study completely described all of the targets of UNC-55 COUP-TF.

It is tempting to hypothesize about the roles of the genes differentially expressed in our microarray. For example, the *C. elegans* TOR-binding partner *daf-15 RAPTOR* is strongly upregulated in *unc-55* mutant sample. *daf-15* RAPTOR is a well-characterized

target of regulation by the FOXO transcription factor *daf-16* (see Appendix 2). The strength in our approach is the ability to quickly test the function of these genes, both in DD and ectopic VD remodeling.

RNAi screens suggest additional transcriptional regulators of remodeling

Our functional analysis of remodeling in DD and VD neurons highlighted the role of additional transcription factors in this process. Most conspicuously, the Kruppel-like factor *klf-1* strongly suppressed ectopic *unc-55* VD remodeling. We found that, in addition to *unc-55, hbl-1,* and *klf-1*, RNAi of many potential homologs of the neuroblast clock pathway can suppress VD remodeling. This leads to the hypothesis that this sequence of transcription factors may also regulate remodeling. Generally, in the *Drosophila* literature, each transcription factor enhances the expression of the next gene in the sequence, and represses the expression of the next+1 gene.

Remodeling shares some features with the neuroblast temporal fate specification, but is distinct in other regards. Both are developmental events that occur only at precise times in development. However, the transition from expressing one neuroblast clock gene to the next is often tied to mitosis, while D neuron remodeling occurs post-mitotically. It is also unclear whether competence to adopt a specific fate is the same thing as competence to remodel synapses. Certainly remodeling requires a number of distinct events, including ventral synapse elimination, a change in the trafficking of cargos from one side of the neuron to another, and dorsal synapse formation. However, D neurons seem to eliminate synapses contemporaneously with forming new synapses, suggesting that it is not a simple linear sequence of events. Temporal fate specification is more akin to a linear program.

We found that RNAi of *lin-29,* the homolog of *Squeeze,* the final member of the neuroblast clock TF sequence, suppressed ectopic VD remodeling. Of all the neuroblast clock homologs, *lin-29* was especially interesting because in *C. elegans lin-29* is a target of regulation by the heterochronic gene *hbl-1*, which also plays an important role in regulating remodeling (Chapter 2). At this point, it is unclear if *lin-29* is a direct target of *hbl-1* regulation, as has been described in the hypodermis, or is an indirect target, as would be inferred from homology to the fly (Abrahante et al., 2003; Lin et al., 2003). We would predict that the relationship between *hbl-1* and *lin-29* in neurons is not the same as in the hypodermis. In the hypodermis, *hbl-1* and *lin-29* mutants have opposite heterochronic phenotypes: *hbl-1* mutants exhibit precocious development, while *lin-29* mutants are delayed. By contrast, *hbl-1* and *lin-29* mutants cause similar neuronal phenotypes: both *hbl-1* and *lin-29* suppress *unc-55* mutant VD remodeling. To resolve this issue, it will be important to determine whether DD remodeling is precocious or delayed in *lin-29* mutants.

In addition to neuroblast clock transcription factors, we observed that the nuclear co-repressor *gei-8* plays an important role in remodeling. Based on sequence homology, *gei-8* is thought to recruit HDACs when bound to nuclear hormone receptors. The expression of *gei-8* slightly but significantly increases in *unc-55* mutants, and *gei-8* suppresses ectopic *unc-55* VD remodeling by RNAi and by genetic mutant. GEI-8 might antagonize UNC-55 and repress the expression of anti-remodeling genes. It would be interesting to characterize the gene expression changes in *gei-8* mutants, and see what genes are anti-correlated with the *unc-55* mutant expression array.

The homolog of the *Drosophila* gene *glass* was upregulated in the *unc-55* microarray, and RNAi of this gene suppressed VD remodeling. This gene is yet another C2H2-type zinc

finger transcription factor. *glass* plays a well-described and important role in photoreceptor differentiation.

A role for cell cycle and cell division machinery?

Multiple genes that play a role in the progression of the cell cycle and/or in cell division were differentially expressed in *unc-55* mutants. RNAi of many of these genes caused defects in DD remodeling, and/or suppressed ectopic *unc-55* VD remodeling. Specifically, we observed a role for the kinetochore receptor *spdl-1 Spindly*, the cyclin-dependent kinase *cdk-1,* the cyclin D *cyd-1*, the septin *unc-61*, and the plus-end directed kinesin6-like *zen-4*. Though some of these genes are expressed ubiquitously, some exhibit a more restricted expression pattern. *cyd-1 cyclin D* is expressed in many cells of the P lineage, which gives rise to VD and other neurons (Park and Krause, 1999).

We hypothesized that RNAi of these genes might affect the terminal division of the Pn.ap cell, which gives rise to the VD and AS neurons, and in that way might alter later differentiation of the VD neurons. However, we observed no obvious precocious or delayed appearance of the VD/AS neuron pairs (Fig. 3.6). This suggests that the mechanism by which RNAi of these genes perturbs remodeling is independent of cell division, or is related to aspects of cell division that we have not yet tested.

Both remodeling and cell division require the asymmetric localization of proteins and RNA species. Remodeling in D neurons involves a complete reversal of the polarity of the neuron. The ventral segment of the neurite that initially forms presynaptic structures becomes post-synaptic to newly born cholinergic neurons, while the dorsal segment of the neurite that is initially post-synaptic to the DA and DB cholinergic neurons forms the pre-

synaptic side of the NMJ. It is unknown whether proteins required for the establishment of polarity will be the same factors responsible for reversing an established polarity. Work by other labs has suggested that proteins important for establishing polarity in the early embryo, such as the AMPK-related Ser/Thr kinase *par-1,* and *par-4 LKB1*, also play important roles in the establishment of DD polarity in the L1 and VD polarity in the adult (Kim et al., 2009b). However, DD neurons seem to be able to remodel normally in *par-4* mutants, suggesting that *par-4* is not important for the reversal of polarity. (It is not clear whether DD neurons in *par-1* mutants can remodel.) This suggests that the machinery responsible for breaking DD polarity may be different from the initial establishment machinery.

Post-mitotic roles for the cyclin Y *cyy-1*, the cyclin-dependent kinase *pct-1*, and the cyclin-dependent kinase *cdk-5* have been described in the trafficking of synaptic components in DA9 neurons in *C. elegans* (Ou et al., 2010; Ou and Shen, 2011). Moreover, *cyy-1* and *cdk-5* play important roles in remodeling DD neurons, although *pct-1* does not seem to function in DD neurons (Park et al., 2011). *cyy-1* is important for ventral synapse elimination, while *cdk-5* is important for formation of dorsal synapses (Park et al., 2011). It would be interesting investigate the relationship between *cyy-1, cdk-5, cyd-1,* and *cdk-1*. Of course, we would need to first validate our *cyd-1* and *cdk-1* results using genetic mutants, to ensure that we aren't observing off-target RNAi effects.

METHODS

RNA sample extraction

unc-55(e1170) animals were outcrossed 12 times to wild type N2 animals. Whole animal RNA was purified from L3 stage animals, during the period when VD neurons are undergoing ectopic remodeling. Triplicate RNA samples for each genotype were prepared using Trizol extractions and Qiagen RNeasy columns. RNA quality was determined by measuring the 260/280 absorbances, as well as by the appearance of clean ribosomal bands on an EtBr gel. We were unable to detect changes in *unc-55* mRNA levels by qPCR, suggesting that *unc-55(e1170)* mRNA is not a target of nonsense-mediated decay.

Gene Expression Microarray

RNA was sent to the Harvard Medical School Quad Biopolymers Facility for full Affy processing. At their facility, RNA quality was first confirmed using an RNA 6000 Nano chip on an Agilent 2100 Bioanalyzer according to manufacturer's instructions (Agilent Technologies, Waldbronn, Germany). They performed one-cycle cDNA synthesis, cleanup of double-stranded cDNA, biotin IVT labeling of antisense cRNA, cleanup of biotinylated cRNA, and fragmentation according to Affymetrix GeneChip Expression Analysis Technical Manual instructions (P/N 702232 Rev. 2). Labeled and fragmented cRNA was hybridized to six Affymetrix GeneChip *C. elegans* Genome Arrays in a GeneChip 640 Hybridization Oven, which were then washed and stained in a GeneChip 400 Fluidics station, and scanned with a 7G GeneChip 300 Scanner. Scanned images were converted into probeset data files using Affymetrix Gene Chip Operating Software.

Microarray quality control included a few steps. We confirmed that replicates of the same genotype correlated with an $R^2>0.96$, using the least-squares regression in Rosetta Resolver v7.0 (Rosetta Biosoftware, Seattle, WA). Additionally, histograms and boxplots of the measured intensity distributions were comparable between arrays, as determined using the Bioconductor software. Scaling factors for chips were quite similar, and significant RNA degradation was not observed, using Bioconductor algorithms.

Microarray Data Processing

We analyzed the microarray data in three different ways. Using the Affy package in the Bioconductor package implemented in the R statistical computing environment (www.bioconductor.org; R version 2.4.1), we used the Robust Multichip Average (RMA) and GC-RMA normalization methodologies (Bolstad et al., 2003; Irizarry et al., 2003; Wu and Irizarry, 2004; Wu et al., 2004). These two methods consist of background subtraction and quantile normalization, but GC-RMA also takes into account different affinities of probes based on GC content. These methods have been shown by various groups to perform well, both for spiked-in controls and as compared to other methods, and are standard in the field(Bolstad et al., 2003; Rajagopalan, 2003; Millenaar et al., 2006). Following each of these two normalization methods, we used the linear modeling of microarrays (LIMMA) protocol for detecting differentially expressed genes, which uses empirical Bayesian statistics (Smyth, 2004). These calculations were implemented using Bioconductor packages (Affy package 1.12.2; GCRMA package 2.6.0; LIMMA package 2.9.8). In addition to the two Bioconductor analyses, we also used the Rosetta Resolver program

to normalize the chips and detect differentially expressed genes, and implemented the RatioBuild pipeline (Vardhanabhuti et al., 2007).

RNAi screens for remodeling defects

To assay for remodeling defects, we used the synaptic marker UNC-57 Endophilin::GFP (expressed under the D neuron promoter *unc-25 GAD*) with the Eri mutation *nre-1; lin-15b(hd126)* (Schmitz et al., 2007).

Feeding RNAi is refractory in neurons of wild type *C. elegans*. We evaluated a few RNAi-sensitive strains to find one with efficient RNAi but with little transgene silencing. We compared 1) *eri-1*, 2) *eri-1; lin-15B*, 3) *nre-1 lin-15B (hd126)*, and 4) *eri-1; lin-35* (Kennedy et al., 2004; Wang et al., 2005; Schmitz et al., 2007). Among these strains, RNAi of GFP in the neurons worked most effectively in the *nre-1 lin-15B (hd126)* background while minimizing transgene silencing. In the *eri-1; lin-15B* background, transgene silencing when the worms were fed L4440, the empty RNAi plasmid, was a significant complication.

We initially screened for many types of D neuron synapse defects. In blind pilot studies, we were able to convincingly identify positive controls that affect multiple processes, including gene expression from the *unc-25* promoter (*unc-30* transcription factor), synaptogenesis (*syd-1*, *syd-2 liprin-alpha*, and *sad-1*), temporal control of DD remodeling (*lin-14* and *hbl-1 hunchback*), and repression of VD remodeling (*unc-55 COUP-TF*) (Hallam and Jin, 1998; Zhou and Walthall, 1998; Zhen and Jin, 1999; Crump et al., 2001; Hallam et al., 2002; Dai et al., 2006; Kim et al., 2008; 2009b).

We fed worms on RNAi bacteria for two generations, then scored animals at an early L1 stage for precocious remodeling, at an L2 stage for delays in remodeling, and at the

adult stage for defects in synaptogenesis and mislocalization of VD synapses. We screened the 71 top hits from the microarray. Top hits were probesets that were hit by multiple microarray analysis algorithms, or that were hit by any algorithm with $p < 0.001$, or that were hit by RMA(split)+LIMMA which pairs each wild type and *unc-55* mutant sample that were collected on the same day instead of grouping all samples of the same genotype together (Table 3.7). RNAi clones were obtained from the Ahringer library, or from the Vidal Unique sublibrary if necessary. Each RNAi clone was scored 4 times, twice by each researcher. High false positive rates (for individual calls, 20-32% for L1 phenotypes and 35-36% for adult phenotypes) caused us to set stringent thresholds for determining hits. RNAi clones called 3 or 4 out of 4 times scored were classified as hits ($p < 0.05$ based on false positive rate, Chi-squared test; Table 3.3).

B0218.3 *pmk-1*	F11C1.6 *nhr-25*	**F54D1.6**	**T07C12.6 *sre-28***
C02F5.11 *tsp-2*	~~F12A10.7~~	~~F55H2.2 *vha-14*~~	T10H4.12 *cpr-3*
C04G2.1 *ttr-39*	~~F15B9.6~~	F56H6.5 *gmd-2*	**T15B7.16 *lgc-54***
C06A8.5 *spdl-1*	F17B5.1	~~F59C6.11~~	~~T22H9.2 *atg-9*~~
~~C06B3.3 *cyp-35C1*~~	~~F19B2.3 srw-39~~	H22K11.2	**T23F6.4 *rbd-1***
C09F12.1 *clc-1*	F22F4.2 *inx-3*	~~K01A2.4~~	**T25G12.7 *dhs-30***
C10C5.6 *daf-15*	**F25G6.7**	K02B9.1 *meg-1*	W03G9.1 *snf-1*
C14B9.6 *gei-8*	F38A5.5 *nspb-3* *	~~K02C4.2~~	W05G11.6
C17B7.5	F38A5.10 *nspb-4*	K04G2.10	**Y40B10A.1 *lbp-9***
C17C3.1	**F39C12.1**	K05F1.6	Y51A2D.4 *hmit-1.1*
C18E9.9	F40F9.2	**K05F1.7 *msp-63***	Y51A2D.9 *ttr-24*
C31A11.5 *oac-6*	F42A9.6	~~K07B1.8~~	**Y56A3A.2**
C34G6.2 *tyr-4*	**F42A10.*4 efk-1***	K11H12.4	Y57G11C.13 *arl-8*
C42D8.3 *pnk-4*	F43D2.1	~~M05D6.4~~	**Y57G11C.24 *eps-8***
C51F7.1 *frm-7*	F43G9.3	R02D5.3	~~Y119C1B.1~~
F01D5.1	F45D11.3	R09B5.9 *cnc-4*	ZC404.8 *spn-4*
F02H6.5 *sqrd-1*	~~F45D11.15~~	R09F10.6 *srh-11*	ZK637.5 *asna-1* *
F09B9.1 *oac-14*	F47G4.4	T05G5.3 *cdk-1* *	

Table 3.7. "Top hits" genes screened by RNAi for remodeling phenotypes. RNAi clones listed in **bold** were sequenced and target the appropriate gene. RNAi clones in black did not cause remodeling phenotypes, and so have not been sequence-verified. * indicates a lethal or arrest phenotype, so remodeling could not be tested. ~~Strikethrough~~ indicates RNAi clone didn't grow, didn't target correct gene when sequenced, or wasn't available.

In the second RNAi screen, the mutation *unc-55(e1170)* was also in the strain. RNAi screening was performed as described above. Animals were assigned a score, 0 to 3, based on the extent of suppression of VD remodeling, as determined by looking for ventral synapses in the adult (0 indicated no suppression of *unc-55*, 3 indicated *hbl-1*-like suppression). Each RNAi clone was scored 4 times, twice by each researcher. This initial screen produced low false positive rates for the negative controls L4440 (empty RNAi plasmid) and *unc-55*. Thresholds for calling hits were determined for each researcher based on their empirical false positive rates. The 28 RNAi clones that were hit at least 2 of 4 times, or that were assigned a strong score at least once, were selected for rescreening, and scored an additional 3 times. RNAi clones suppressed *unc-55* if they were hit 3 of 7 times ($p < 0.03$) or 4 of 7 times ($p < 0.001$, Chi-squared test based on false positive rates).

Imaging D neuron synapses

D neuron synapses were identified using *nuIs279*, which expresses UNC-57::GFP under the *unc-25 GAD* promoter. Imaging for alterations in the timing of remodeling or in the density and morphology of synapses in adult dorsal and ventral nerve cords was performed as described in Chapter 2.

Chapter 4

Concluding remarks and discussion

Transcriptional regulation of remodeling

The ability of a neuron to alter synaptic connections is an essential feature of circuit development, and, to a lesser extent, of circuit plasticity after development. Without the ability to remodel synaptic connections, neurons would be unable to change their initial synaptic partners. Following guidance of axons and dendrites to general regions, synaptic partners are chosen based on specificity factors and other cues. Regardless of how precise these decisions are, clearly situations exist when these initial synaptic partner choices are not appropriate for adult circuit function. There may be too many synaptic connections formed, or they may be with inappropriate partners. Observed examples of remodeling are discussed in the introduction. Yet neural circuit flexibility is not infinite. Neuronal circuits must also retain stability over long periods of time. Inappropriate remodeling of synaptic connections would rapidly dissolve the function of circuits. For the most part, once development is complete, neuronal circuits exhibit limited synapse formation and elimination (Grutzendler et al., 2002; Yang et al., 2009; Ziv and Ahissar, 2009).

Although neuronal activity regulates the specifics of synapse remodeling, including which synapses are eliminated and the extent of synapse formation, clearly the presence of neuronal activity alone is insufficient to explain why remodeling generally only occurs during precise time windows in development. Neurons, once remodeling is completed, do not stop receiving signals from their synaptic partners. How is the neuronal activity during remodeling different than the activity before or after remodeling? Perhaps it is not a difference in the activity signal, but in the responsiveness of the neuron to the signal. Defining the difference between neurons undergoing remodeling and those that cannot remodel has been the focus of research for many years. We propose that some of this

difference may be the selective expression of genes only during development, only in neurons in which remodeling occurs.

We describe here a number of transcriptional differences between neurons that can remodel and those that cannot. Genes whose expression is activity-dependent have been well described, including the classic examples of CREB and BDNF. Indeed, both of these activity-regulated genes have been described to play a role in the regulation of remodeling in vertebrates (Cohen and Greenberg, 2008). Yet these genes are broadly expressed, in most or perhaps all neurons. Their expression is not shut off after development. As such, their activity-dependent expression is inadequate to fully explain how remodeling occurs only during development. What is required is the expression of genes only during the time during development when remodeling occurs, only in the neurons that are undergoing remodeling, and whose expression may be regulated by activity.

We have identified a number of transcription factors that are known to regulate the timing of other developmental events. Some, like the heterochronic genes, regulate developmental timing in other tissues. Others, like the neuroblast clock, regulate the temporal cell fate of neurons. Together, our work suggests that transcription factors play an important role in regulating remodeling. Moreover, understanding the role of transcription factors, especially those known to regulate developmental timing in other contexts, will help illuminate how remodeling is regulated.

UNC-55 is a general repressor of remodeling

Previous work suggested that UNC-55 COUP-TF plays a key role in determining the difference between VD and DD neurons (Walthall et al., 1993; Walthall and Plunkett, 1995;

Zhou and Walthall, 1998; Shan et al., 2005). UNC-55 expression apparently accounts fully for the inability of VD neurons to remodel, as *unc-55* mutants have absolutely no ventral IPSCs (Fig. 2.2a-b). DD and VD neurons may both be primed for remodeling, but without the expression of genes repressed by UNC-55, VD neurons are unable to carry out this process. We and others have therefore attempted to characterize genes whose expression is regulated by UNC-55 in order to better understand remodeling (Petersen et al., 2011).

UNC-55 regulates many aspects of remodeling. Elimination of any one UNC-55 target has been insufficient to fully prevent VD remodeling. This may be due to partial elimination of function, as by RNAi knockdown or hypomorphic mutant alleles, but it also may suggest that we need to disrupt multiple factors to fully prevent remodeling. Indeed, remodeling involves multiple discrete events. For some of these events, the D neurons are pre-synaptic. Ventral pre-synaptic structures must be eliminated in the D neuron, and the post-synaptic muscle arm must disassemble. Dorsal pre-synaptic structures must be formed in the D neuron and post-synaptic muscle arms must make contact and mature. In *unc-55* mutants, both the D neuron and the muscle aspects of remodeling occur by our assays (although surprisingly not in work from other labs, which shows that UNC-49 $GABA_A$ receptor localization is unchanged in *unc-55* mutants (Petersen et al., 2011), though this conflicts with other reports (Gally and Bessereau, 2003)). As UNC-55 acts cell-autonomously in the D neurons, this suggests that the GABAergic neuron instructs the muscle in synapse formation. However, as GABA mutants have normal remodeling, whatever the neuron is secreting that instructs the muscle to form a muscle arm and a post-synapse is something other than GABA itself. This agrees with prior work which

demonstrated that UNC-49 $GABA_A$ receptor clustering in the muscle requires innervation by D neurons but not GABA signaling (Gally and Bessereau, 2003).

For other aspects of remodeling, which we have not yet discussed, the D neuron is post-synaptic: cholinergic excitation of the D neuron also changes during remodeling. Initially DA and DB neurons form synapses onto dorsal DD neurites. After remodeling, DD neurons receive VA and VB excitatory input in ventral neurites. Finally, there are hints that developmental events in other tissues are coordinated with D neuron remodeling. Other groups are currently examining the hypothesis that DD neurons drive ventral muscle contraction in the L1, and that DDs only become inhibitory after remodeling due to changes in the muscle chloride conductance. It would be interesting to investigate what happens to the remodeling of the input to D neurons when *unc-55* is mutated or misexpressed.

From transcription factors to remodeling machinery

Among UNC-55 targets should be genes that promote remodeling. We have characterized one target, *hbl-1*, and implicated many others. *hbl-1* is also a transcription factor. *hbl-1* should promote expression of pro-remodeling genes, and possibly repress the expression of anti-remodeling genes. The identification of *hbl-1* targets is therefore of particular interest to us. Based on experiments in other systems, we have a number of candidate genes, including the neuroblast clock transcription factors and the *lin-29* transcription factor. We have provided evidence that some of these genes promote VD remodeling in *unc-55* mutants. We are still far from connecting transcription factors to the machinery responsible for carrying out the process of remodeling.

One hypothesis is that, within the microarray list of genes upregulated in *unc-55* mutants, should be targets of *hbl-1* regulation. After all, *hbl-1* is upregulated on the microarray list, so the genes it regulates may be on the list as well. In support of this hypothesis, the next member of the neuroblast clock, *klf-1*, is upregulated in *unc-55* mutants by microarray. However, we detected an UNC-55 binding site within the putative *klf-1* promoter region, suggesting that *klf-1* may be a direct target of UNC-55 repression. This suggests that UNC-55 may repress the expression of *hbl-1* as well as of *hbl-1* target genes, to redundantly repress remodeling. Given the small number of cells in which UNC-55 is expressed, it would be surprising if we could detect indirect targets of UNC-55 in whole worm lysates.

Instead of mining the *unc-55* list, a better approach would be to identify *hbl-1* targets by comparing expression in wild type to *hbl-1* mutants. Others have characterized the genes that change expression following heat-shock-driven expression of *hbl-1* in all tissues (Niwa et al., 2009). One challenge will be to determine genes regulated by *hbl-1* in other tissues versus in D neurons. Unlike *unc-55*, which is expressed in a very restricted pattern, *hbl-1* is expressed broadly. *hbl-1* is even expressed in other neurons in the ventral nerve cord (Fig 2.5a, 2.6, and 2.17), which we very tentatively think may be the DB neurons, based on number, location in the nerve cord, and embryonic birth date. While targets of *hbl-1* common to both D neurons and other tissues may be relevant, targets of *hbl-1* specific to tissues other than D neurons will not be informative.

It is possible that the machinery responsible for remodeling may be only indirectly regulated by transcription. It may be that the protein complexes responsible for the execution of remodeling (the elimination of synapses, directing synaptogenesis, and

rerouting trafficking within the neuron) are regulated post-transcriptionally. The molecular machinery could be present but inactive in wild type VD neurons, and derepressed by the action of an UNC-55 target. In this case, our microarray would detect increased expression of the activator in *unc-55* mutants, but not increased expression of the machinery itself.

Some of the machinery responsible for remodeling has been recently described. Work by others has implicated the cyclin Y *cyy-1* in synapse elimination and the cyclin-dependent kinase *cdk-5* in synapse formation of remodeling DD neurons (Park et al., 2011). They demonstrate that following ventral synapse elimination, synaptic components are reused in new dorsal synapses, and that *cdk-5* is important for this reuse of synaptic proteins. Additionally, they have demonstrated the role of UNC-104 Kinesin3 in trafficking in remodeling D neurons. We have identified genes that are remarkably similar, including the cyclin D *cyd-1*, the cyclin-dependent kinase *cdk-1*, and the kinesin-6 *zen-4*. It will be interesting to determine if *cyy-1, cdk-5,* and *unc-104 kinesin* expression is regulated by UNC-55. We will need to use genetic mutants in *cyd-1, cdk-1,* and *zen-4* to ensure that we are not observing off-target RNAi and microarray effects. After validation, this will be an interesting avenue to pursue in attempting to connect transcriptional changes with the machinery performing remodeling.

Cell fate vs. remodeling

Initial characterization of UNC-55 labeled it as a determinant of cell fate, to distinguish the VD fate from the DD fate. Considering our work in light of previous papers, it is ambiguous whether VD neurons are adopting a more DD-like fate in *unc-55* mutants.

In *unc-55* mutants, VD neurons become competent to perform the remodeling that is characteristic of DD neurons. Our work implicating cell fate determinants like the neuroblast clock and the *glass* homolog, which plays a role in *Drosophila* photoreceptor cell fate, make this a serious consideration. However, since the DD and the VD neurons are so similar, even though they are born at different times from different lineages, we lack the tools to decisively distinguish these cell types by anything other than remodeling. The neuropeptide *flp-13* is selectively expressed in DD neurons only because, like *hbl-1*, its expression in VD neurons is repressed by UNC-55 (Shan et al., 2005). As a side note, *flp-13* does not seem to regulate remodeling, because mutations in *alr-1 Aristaless/Arx* cause misexpression of *flp-13* in VD neurons without altering VD synapse localization (Melkman and Sengupta, 2005). DD and VD neurons have different numbers of cell bodies, of different shape, and at different position in the anterior-posterior axis of the ventral nerve cord. By these features DDs and VDs remain distinct in *unc-55* mutants, yet these are all features that are decided before UNC-55 expression.

The role of *hbl-1* in DD neurons is not the determination of cell fate. HBL-1 levels bidirectionally regulate the timing of when remodeling occurs. Increased levels of *hbl-1*, as in *tom-1* or *mir-84* mutants, result in precocious remodeling, while decreased levels of *hbl-1*, as in *hbl-1* or *unc-13* mutants, result in delayed remodeling. Therefore, unlike *unc-55*, *hbl-1* is clearly not involved in the determination of cell fate, but instead in the execution of that fate. Other *unc-55* targets may be similarly involved in the execution of cell fate.

Remodeling in different systems

DD remodeling is a drastic example of remodeling, as the polarity of information flow within the neuron is entirely reversed. Vertebrate examples of remodeling are more subtle. In vertebrate neurons, if one synapse may be retained, an adjacent synapse may be eliminated. DD remodeling may involve a complete change in intracellular trafficking, which may be different from the more local changes in a vertebrate neuron during remodeling.

Another difference between remodeling in our system and that in vertebrate systems is that we haven't observed competition between similar neurons innervating the same target area. The frequency of IPSC events in the dorsal muscle is doubled in *unc-55* mutants (Fig. 2.2d). This suggests that remodeling VD neurons form as many dorsal synapses as DD neurons. VD neurons are forming dorsal synapses much later than DD neurons, which have already completed remodeling by L3 stage. We would predict that competition between VD and DD neurons would decrease the number of dorsal synapses formed. Competition plays an important role in remodeling in vertebrate systems (Sanes and Lichtman, 1999).

We observe an important role for activity-dependent gene expression in the regulation of remodeling. Activity-dependent gene expression has been extensively studied in vertebrates, so activity-dependent expression of transcription factors regulating remodeling could be conserved. It is not yet clear in what neurons activity plays a role to regulate remodeling, how activity levels are sensed by the DD neurons, or how transcription of *hbl-1* is regulated by activity. We have recently begun to investigate these questions (see Appendix 1). Cholinergic signaling prevents sprouting of the SAB motor

neurons that innervate the head of *C. elegans*, and sensory information is important for maintaining the morphology of sensory neurons, suggesting that activity-dependent regulation of development may also occur in other *C. elegans* neurons (Peckol et al., 1999; Zhao and Nonet, 2000).

The transcriptional machinery that allows a neuron to be competent to undergo remodeling could be conserved. Descriptions of COUP-TFI and COUP-TFII knockout mice show phenotypes that are remarkably reminiscent of what we have observed in *unc-55* mutants. Conditional COUP-TFII knockout mice have Purkinje neurons with altered dendritic branches, and reduced proliferation of granule cell precursors (Kim et al., 2009a). Double knockdown of COUP-TFI and COUP-TFII resulted in sustained neurogenesis and prolonged generation of early born neurons in the forebrain (Naka et al., 2008). Moreover, eye-specific COUP-TFI/II double knockout in mice demonstrated that COUP-TFs regulate expression of the homeodomain transcription factor Otx2 in the eye, and Otx2 is known to regulate ocular dominance formation (Sugiyama et al., 2008; Tang et al., 2010). It is less clear what the homolog of *hbl-1* in vertebrates might be, given the number of C2H2-type zinc finger transcription factors, but the current best homolog is Ikaros. Ikaros regulates temporal competence in retinal progenitor cells in the mouse (Elliott et al., 2008). The Kruppel-like gene KLF9 is regulated by neuronal activity, and is important for neurogenesis-dependent synaptic plasticity (Scobie et al., 2009). Accordingly, the transcriptional regulation of remodeling we describe may provide insight into remodeling in other systems.

Appendix 1: Determining the neuronal activity regulating remodeling

Introduction

Our experiments in Chapter 2 indicate that neuronal activity regulates the progression of remodeling by regulating *hbl-1* expression. Mutations that compromise the ability of neurons to secrete neurotransmitters or neuropeptides, *unc-13* and *unc-18*, cause significant delays in DD remodeling. Mutations that increase the release of neurotransmitter, *tom-1 tomosyn* and *slo-1 BK channel*, cause precocious DD remodeling in an HBL-1-dependent manner (Fig A.1). We have begun experiments aimed at determining the source and nature of the relevant activity. An equally important and related question, that we have not yet begun to investigate, is how this activity signal is received by the DD neurons and results in altered *hbl-1* transcription.

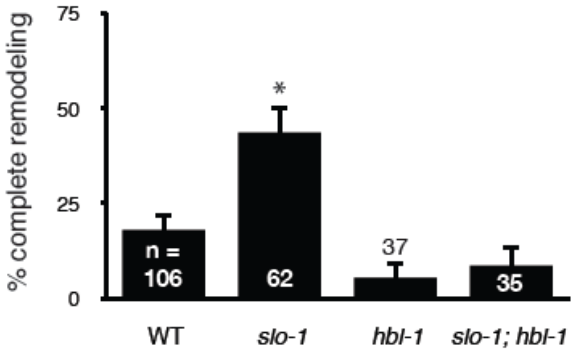

Fig A.1. Precocious remodeling in *slo-1* mutants is suppressed by *hbl-1* mutation. At 11 hours after hatching, more *slo-1* mutants have completed remodeling DD neurons than wild type (* $p<0.01$, Chi-squared test). By contrast, *hbl-1* and *hbl-1;slo-1* double mutants do not complete remodeling earlier than wild type. This is consistent with Fig. 2.22e, completion of remodeling in these mutants at 20 hours after hatching.

There are many potential sources of activity that could regulate DD remodeling. We have ruled out a role for GABAergic signaling, as mutants in *unc-25 GAD* and *unc-47 VGAT* have no alterations in DD remodeling (Fig. 2.20). Thus neither the cell-autonomous secretion of GABA by the DD neurons nor GABA release by the VD neurons as they innervate the ventral nerve cord regulates the timing of DD remodeling. Additionally, it has been reported that in *lin-6* mutants, in which post-embryonic neurons are not formed, DD neurons are capable of remodeling (White et al., 1978). However, as the *lin-6* mutant was examined at the L4 stage by electron microscopy, we cannot say whether the timing of DD remodeling was perturbed in the absence of post-embryonically born neurons.

This leaves many possibilities. Cholinergic signaling onto DD neurons might be responsible. DA and DB cholinergic neurons form synapses onto the dorsal DD process to depolarize DD neurons in the L1 stage. DD neurons in the L1 stage express cholinergic receptors, including *acr-12* (Cinar et al., 2005). Alternatively, sensory neurons in the head may be sensing the environment, and regulating remodeling in response to environmental cues. They could be regulating DD neuron remodeling through interneurons or neuropeptide signaling. DD neurons could be secreting a neuropeptide and sensing it cell-autonomously. We have yet to find conclusive evidence that supports one hypothesis over any other.

Neuropeptides

We wondered whether neuropeptides might play a role in regulating the timing of remodeling. The mutations we used to alter circuit activity, *unc-13, unc-18, tom-1 Tomosyn,*

and *slo-1 BK channel,* all alter both neurotransmitter release from synaptic vesicles and neuropeptide release from dense core vesicles.

The PC2 convertase *egl-3* proteolytically cleaves proprotein precursors in an essential step of neuropeptide biosynthesis (Kass et al., 2001). The carboxypeptidase E *egl-21* then removes basic residues from the C terminus of neuropeptide precursors after *egl-3* cleavage. In *egl-3* mutants, many neuropeptides are absent (Husson et al., 2006). In *egl-21* mutants, many FLP and NLP neuropeptides are not fully processed and are presumed to be biologically inactive (Jacob and Kaplan, 2003; Husson et al., 2007). The *egl-3* genetic locus is too close to the integration site of our D neuron synapse marker, *nuIs279* Endophilin UNC-57::GFP, to allow us to follow remodeling in *egl-3* mutants.

We looked for changes in remodeling in *egl-21 carboxypeptidase E* mutants. If mutations in *tom-1 tomosyn* and *slo-1 BK channel* enhance neuronal release of neuropeptides, then blocking neuropeptide processing using *egl-21* mutation should suppress the remodeling phenotype. However, we saw no suppression of precocious DD remodeling by *egl-21* in *slo-1* mutants (Fig. A.2). This suggests that the neuropeptides which require EGL-21 processing for bioactivity are not responsible for precocious remodeling in *slo-1* mutants.

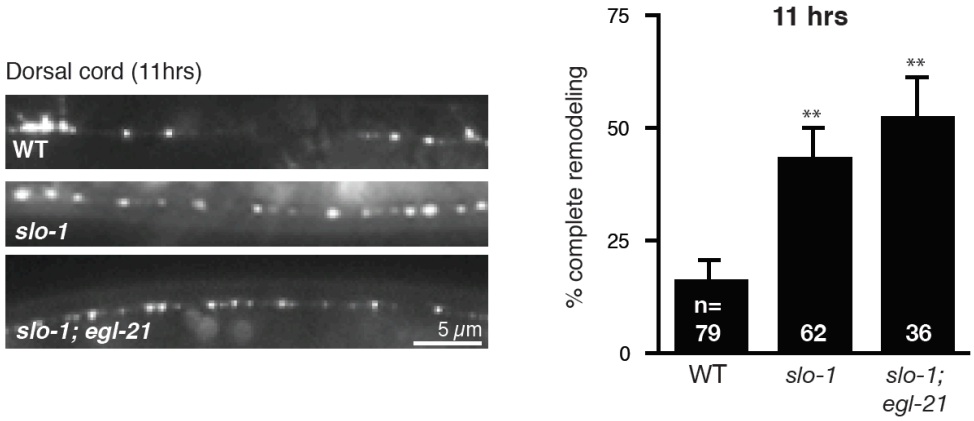

Fig A.2. ***egl-21 carboxypeptidase E*** **mutation does not suppress precocious remodeling in** ***slo-1 BK channel*** **mutants**. Completion of DD remodeling at 11 hours after hatching is followed as described in Chapter 2. ** $p < 0.001$, Chi^2 test.

Other experiments are required to determine if EGL-21-independent neuropeptides are responsible for precocious remodeling in *tom-1* and *slo-1* mutants, or if neuropeptides repress remodeling, or if neuropeptides are irrelevant for DD remodeling. These include analyzing remodeling in *egl-3* single mutants and for suppression of *tom-1* or *slo-1* precocious remodeling, looking at remodeling in *egl-21* single mutants, and looking at remodeling in mutants in which neuropeptide secretion is compromised such as *pkc-1* or *unc-31 CAPS*.

It is interesting to note that the expression of the protein kinase C *pkc-1* was upregulated in *unc-55* mutants by microarray (Table 3.1). PKC-1 is an important regulator of neuropeptide secretion (Sieburth et al., 2007). Moreover, RNAi of *pkc-1* suppressed ectopic *unc-55* VD remodeling (Table 3.4). This suggests that *pkc-1* may play an important role in the regulation of remodeling, potentially by regulating neuropeptide secretion. It will be critical to determine if *pkc-1* is functioning in the VD neurons or in other tissues.

Activation of sensory neurons

Multiple tools to selectively activate a subset of neurons have been developed. These include restricted expression of optogenetic tools, like the light activated channel-rhodopsin2 (Mattis et al., 2011). Alternatively, we could silence subsets of neurons by selectively expressing TeTx or gain-of-function versions of *egl-36 Shaw*-type potassium channels (Elkes et al., 1997). These *egl-36(gf)* mutants produce channels that are active at more negative potentials.

We chose to start by using Capsaicin-induced activation of sensory neurons expressing the TRPV1 receptor VR1 (Tobin et al., 2002). We obtained animals expressing VR1 under the *osm-6* promoter that drives expression in 56 sensory neurons, all of the ciliated neurons except the BAG and FLP pairs (Collet et al., 1998). We synchronized animals at hatching, placed newly hatched L1s on plates containing 5 uM capsaicin, and looked at the timing of remodeling at 11-12 and 19-20 hours later.

There were two significant problems with this experiment. First, we observed that capsaicin exposure for this period of time resulted in many dead animals, whether or not the animals carried the VR1 array. This is in agreement with published results that even 30 minutes of capsaicin treatment can affect wild type animals (altered thermal avoidance after 30 min capsaicin treatment: (Wittenburg and Baumeister, 1999)). This means that capsaicin treatment is likely affecting many cells, not just the neurons in which we have expressed VR1. Secondly, the presence of the P_{osm-6}::VR1 array caused delays in completion of remodeling at 19-20 hours after hatching, regardless of whether capsaicin was present or not. We hypothesize that the animals carrying the array had a general developmental

delay. We need to develop a way to express VR1 that does not alter general developmental timing.

Appendix 2: The DAF-16 FOXO transcription factor regulates DD remodeling

Introduction

Insulin signaling and the insulin receptor have been implicated in many stages of the development of the mammalian nervous system (reviewed in (Chiu and Cline, 2010)). The insulin receptor is expressed in the central nervous system, specifically in the mouse olfactory bulb, cerebral cortex, hypothalamus, hippocampus, and cerebellum. The receptor is expressed at higher levels during development than in the adult. In hippocampal neurons in culture, the insulin receptor is localized to the post-synaptic density. Insulin receptor signaling in the brain regulates spine density, synaptic plasticity, and neurite outgrowth. For example, insulin contributes to long-term depression and trafficking of AMPA and NMDA receptors. Inactivating the insulin receptor using dominant negatives or morpholinos causes defects in the experience-dependent development of the retinotectal circuit in *Xenopus* (Chiu et al., 2008). Alterations in insulin receptor function affect neuronal survival, and learning and memory (Kauffman et al., 2010). Some data suggests that the A-beta peptide produced in Alzheimers patients may bind and block insulin receptor signaling, and enhancing insulin receptor signaling has been a treatment for schizophrenia. Some work has even suggested that the expression of insulin growth factor IGF-1 is directly regulated by the UNC-55 homolog COUP-TFII in the mouse cerebellum an in cell culture (Kim et al., 2009a).

There is one insulin receptor homolog in the *C. elegans* genome, encoded by *daf-2 InsR*. DAF-2 InsR signals through an Akt/PI3K pathway to inactivate the FOXO transcription factor DAF-16 (Hu, 2007; Landis and Murphy, 2010). DAF-16 FOXO shuttles

between the cytoplasm and the nucleus in a phosphorylation-dependent manner. Activation of AKT-1 results in the phosphorylation-induced cytoplasmic localization of DAF-16 FOXO. Insulin receptor signaling through FOXO transcription factors regulates physiological processes such as responses to stress, longevity, fat storage, and reproduction in many systems (Mukhopadhyay and Tissenbaum, 2007).

In *C. elegans*, *daf-2 InsR* and *daf-16 FOXO* signaling have been shown to be important for post-embryonic muscle arm extension, a component of neuromuscular junction synapse formation. *daf-2(e1370ts) InsR* mutants had supernumerary muscle arms at 20°C (Dixon et al., 2008). This phenotype is suppressed by *daf-16 FOXO*, and DAF-16 can be rescued in either the muscle or the intestine, suggesting that signaling through DAF-16 is required non-autonomously for muscle arm extension. In addition, DAF-2 InsR and DAF-16 FOXO signaling pathways, acting in the muscle, regulate presynaptic growth controlled by the SCF^{FSN-1} E3 ubiquitin ligase (Liao and Zhen, 2008).

Rationale

We first became interested in investigating a role for insulin signaling in the regulation of remodeling based on two different microarray experiments. In the first, previous members of the Kaplan lab compared gene expression in wild type versus *tom-1 Tomosyn* mutant whole animal lysates (Dybbs et al., 2005). We noted that *hbl-1* expression increased in *tom-1 Tomosyn* mutants, when these results were analyzed by RMA+LIMMA (1.4 fold change increase, $p < 0.01$) or by GCRMA+LIMMA (2.4 fold change increase, $p < 0.002$). This agrees with what we observed using *hbl-1* reporter analysis, although the stages of animals observed (L1 versus L4) and tissues (DD neurons versus whole animal

lysate) were different (Fig. 2.21c-d). We could also detect expression changes in many targets of *daf-2 InsR* and *daf-16 FOXO* regulation as determined by microarray experiments, including *far-3, cyp-35A2, gst-4, acdh-1, gei-7, ctl-1*, *tps-2, unc-38, unc-44, jnk-1,* and *daf-16 FOXO* itself (Lee et al., 2003; McElwee et al., 2003; Murphy et al., 2003). This suggested that mutating *tom-1 Tomosyn* altered insulin signaling, perhaps by causing increased release of ligands for the DAF-2 InsR.

In the *unc-55* microarray discussed in Chapter 3, we observed increased expression of the remodeling regulator *hbl-1*. In addition, one of the genes with the most statistically significant increase in expression was the *daf-16 FOXO* target *daf-15 RAPTOR* (Table 3.1). While RNAi of *daf-15 RAPTOR* did not alter remodeling in either the top hits screen or the *unc-55* suppression screen, nevertheless this suggested that in animals with ectopic VD remodeling DAF-16 FOXO activity was altered.

Results

To determine if insulin receptor signaling regulates remodeling, we first looked at the timing of DD remodeling, as described previously (Chapters 2 & 3). At 19 hours after hatching, while most wild type animals have completed DD remodeling, *daf-2(e1370ts) InsR* mutants had slight delays in DD remodeling, and *daf-16(mgDf47) FOXO* mutants had very severe defects in remodeling (Fig. B.1).

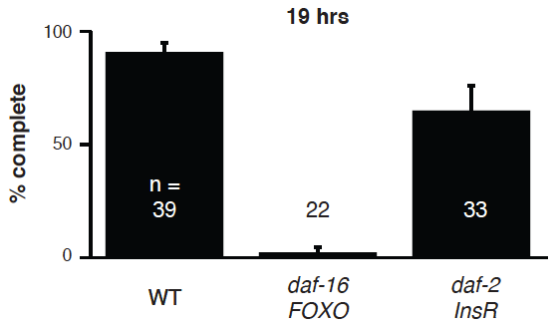

Fig B.1. DD remodeling is delayed in *daf-16 FOXO* mutants. Percent complete DD remodeling at 19 hours after hatching at 20°C. Error bars indicate SEM. Number of animals observed is indicated.

The 20°C temperature used for the remodeling assay is semi-restrictive for *daf-2(e1370ts) InsR*. At the permissive 15°C, *daf-2(e1370)* animals do not form any dauers; at the restrictive 25°C, *daf-2(e1370)* mutants become dauers constitutively; at the semi-restrictive 20°C approximately 15% of *daf-2(e1370)* enter dauer (Karp and Ambros, 2011). We hypothesized that the 20°C temperature may not be restrictive enough to affect remodeling. We repeated our remodeling assay at higher temperatures, and looked for remodeling completion at 12 hours after hatching. At 12 hours after hatching, *daf-2(e1370)* mutants did not have obvious delays in remodeling at 20°C. Note that increasing temperature speeds up the general rates of overall development, so wild type animals complete remodeling earlier at higher temperatures. We observed that at restrictive temperatures, when *daf-2 InsR* mutants are in the process of entering the alternative L2 stage called L2d that precedes dauer formation, DD remodeling is significantly delayed in *daf-2(e1370)* animals (Fig. B.2).

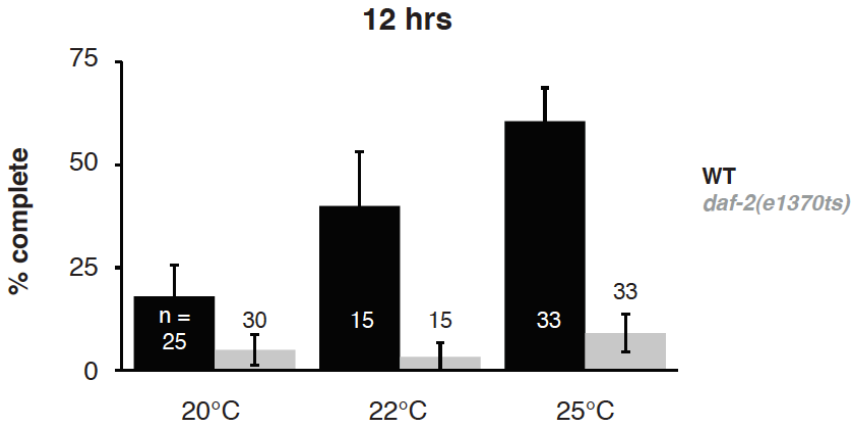

Fig B.2. Delayed remodeling in *daf-2 InsR* mutants at restrictive temperatures. Percent complete remodeling of wild type is shown in black bars, *daf-2(e1370ts)* in gray, at 12 hours after hatching at the indicated temperatures.

We have shown that increasing secretion of neurotransmitters and/or neuropeptides, by mutating either *tom-1* Tomosyn or *slo-1 BK channel*, is sufficient to drive precocious DD remodeling (Fig. 2.22a-b). Increased secretion of an insulin-like ligand in these mutant backgrounds might be responsible for this phenotype. If a ligand binding to the DAF-2 InsR is responsible for driving precocious remodeling, then *daf-2* mutations should suppress the precocious remodeling of *tom-1* or *slo-1* mutants. Therefore we looked for completion of remodeling in *tom-1; daf-2* double mutants. Unlike wild type animals where completion of remodeling increases at higher temperatures, and similar to *daf-2* mutants that do not have increased remodeling at higher temperatures, the completion of remodeling in *tom-1; daf-2* double mutants was consistent across temperatures (Fig. B.3). Even at 20°C, where the *daf-2(e1370)* mutation does not have a phenotype by itself, *daf-2(e1370)* partially suppressed the precocious *tom-1* remodeling. Given the intermediate phenotype of *daf-2; tom-1* double mutants, we cannot say whether *daf-2(e1370)* only partially suppresses the *tom-1* phenotype, or whether we are observing

the additive phenotype of two unrelated perturbations that individually cause opposite effects on remodeling.

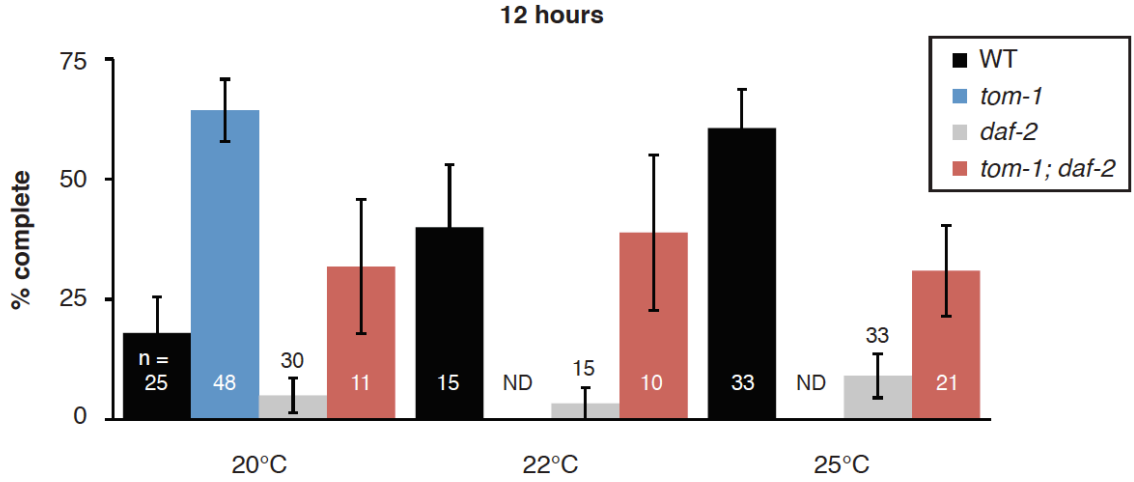

Fig B.3. *daf-2 InsR* mutation partially suppresses precocious remodeling of *tom-1* mutants. Percent complete remodeling at 12 hours after hatching at indicated temperatures.

DD remodeling is delayed, but is eventually completed in *daf-2 InsR* and *daf-16 FOXO* mutants, as determined by imaging synapse density in adults (Fig B.4). *daf-2 InsR, daf-16 FOXO,* and *hbl-1* mutants all exhibit mild defects in dorsal synapse formation (Fig B.4 and 2.7d). *hbl-1* and *daf-16 FOXO* have non-additive defects in dorsal synapse formation, but potentially additive defects in ventral synapse elimination. Thus the ventral data suggests that *hbl-1* and *daf-16* are acting in parallel pathways to promote remodeling, while the mild dorsal synaptogenesis defect suggests that they may be acting in the same pathway.

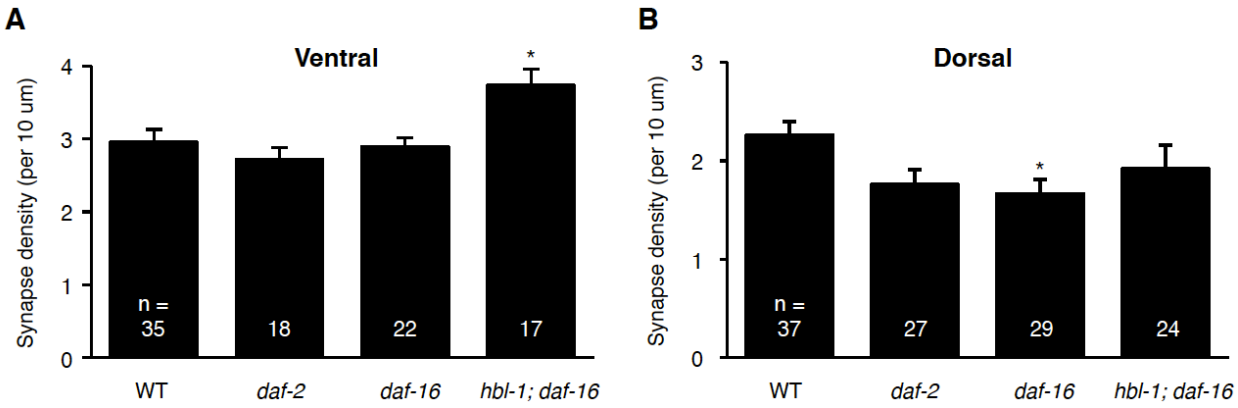

Fig B.4. Remodeling eventually completed in *daf-2 InsR* and *daf-16 FOXO* mutants. Ventral (a) and dorsal (b) imaging of synapse density to assay remodeling in *daf-2* and *daf-16* mutant adults. Mild defects in ventral synapse elimination in *hbl-1; daf-16* mutants and in dorsal synapse formation in *daf-16* are observed. Synapse density in adults, raised at 20°C. * $p < 0.01$

Mutations in *unc-55* induce ectopic remodeling in VD neurons, which can be visualized as decreased synapse density ventrally and increased dorsal synapse density dorsally. We wondered whether *daf-2 InsR* and *daf-16 FOXO* mutations would suppress the ectopic remodeling caused by *unc-55* mutation. We observed that a mutation in *daf-16 FOXO* suppressed neither the ventral synapse loss nor the dorsal synapse gain of *unc-55* (Fig B.5). A mutation in *daf-2 InsR* did not suppress the dorsal synapse increase, but did suppress the ventral synapse elimination. This suggests that a *daf-16* mutation does not play a role in VD remodeling, while by contrast a *daf-2* mutation prevents the synapse elimination component of remodeling, but does not play a role in synapse formation. These results are different from what we observed previously, where ectopic synapse formation and synapse elimination were both suppressed by *hbl-1* mutation.

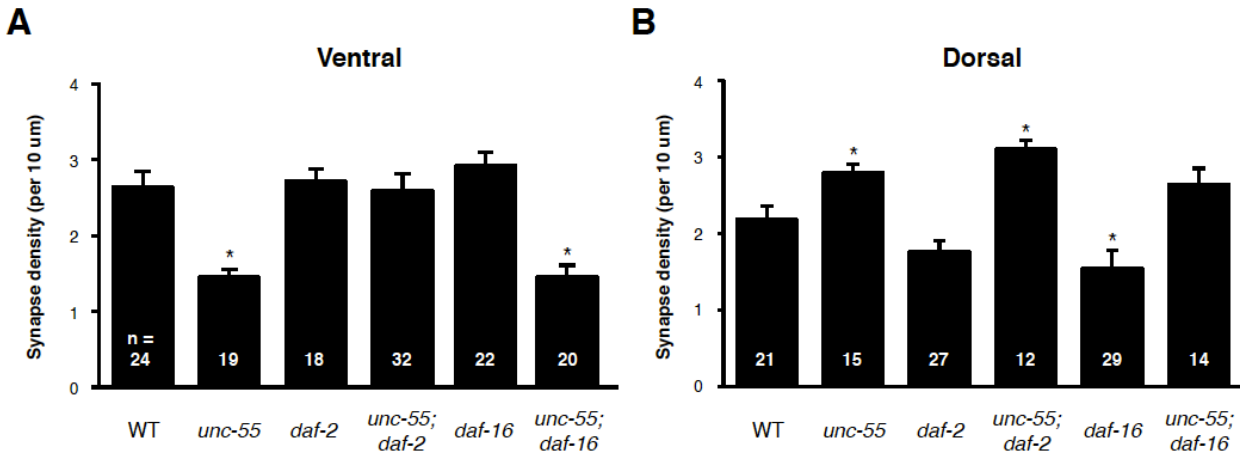

Fig B.5. *daf-2 InsR* and *daf-16 FOXO* do not suppress *unc-55* ectopic VD remodeling. Ventral (a) and dorsal (b) imaging of synapse density in adults raised at 20°C. * $p < 0.01$

Future Directions

The DAF-16 FOXO transcription factor shuttles between the nucleus and the cytoplasm, dependant on DAF-2 InsR signaling (Lee et al., 2001; Lin et al., 2001). We plan to look at DAF-16 localization in DD and VD neurons during development, in wild type, *unc-55 COUP-TF,* and *tom-1 Tomosyn* mutant backgrounds. We have developed a GFP-tagged DAF-16 expressed in the D neurons under the *unc-25* promoter to look at localization, and to test for cell-autonomous rescue of *daf-16 FOXO* delays in DD remodeling. We also plan to look for expression of a *daf-16* transcriptional reporter in the DD neurons around the time of remodeling. Further experiments to test for the relationship between *daf-2 InsR, daf-16 FOXO*, and *hbl-1* signaling pathways are required.

Appendix 3: Other regulators of remodeling

This appendix lists other genes that, when knocked down by RNAi, altered remodeling. These RNAi clones were embedded in the RNAi screens described in Chapter 3.

RESULTS

The microRNAs *let-7* and *mir-84* regulate molting by regulating expression of the nuclear hormone receptors *nhr-23* and *nhr-25* (Hayes et al., 2006). RNAi knockdown of the nuclear hormone receptor *nhr-23* resulted in larval arrest around the L2 stage. Nevertheless, we observed many L1 animals in which DD remodeling seemed to occur precociously. RNAi of *nhr-25* did not cause an arrest or a remodeling phenotype. RNAi of *nhr-64* did not cause an arrest phenotype, but did seem to alter DD remodeling.

daf-12 is known to interact with *mir-84* signaling pathways, and shares sequence homology with the *Drosophila* ecdysone receptor, which is known to regulate developmental pruning (Lee et al., 2000; Bethke et al., 2009; Hammell et al., 2009). RNAi of *daf-12* may have caused subtle defects in VD ventral synaptogenesis, or derepressed the remodeling program in VD neurons.

COUP-TF interacts with many cofactors, including the COUP-TF interacting proteins CTIP1 and 2, which are also C2H2 zinc finger transcription factors (Avram et al., 2000). Knockdown of the worm homolog, F13H6.1, resulted in precocious DD remodeling.

The pumilio homolog *puf-9* is required for the repression of the 3'UTR of *hbl-1* by the *let-7* family of microRNAs (Nolde et al., 2007). RNAi of *puf-9* enhances the phenotypes

of *let*-7 hypomorphs. RNAi of *hbl-1* can suppress *puf-9* phenotypes, but RNAi of *puf-9* does not suppress *hbl-1* phenotypes. Interestingly, RNAi of *puf-9* could suppress the ectopic VD remodeling of *unc-55* mutants. We are not yet clear where or how *puf-9* might be functioning in this context.

Appendix 4: Expression Profiling of *mir-1* mutants, *mef-2* mutants, and *mir-1;mef-2* double mutants

Overview

The muscle microRNA miR-1 regulates multiple aspects of synapse function, including acetylcholine receptor subunits and retrograde signaling via the transcription factor MEF-2 (Simon et al., 2008). To identify genes transcriptionally regulated by *mir-1* and *mef-2*, we carried out expression profiling of *mir-1* mutants, *mef-2* mutants, and *mir-1; mef-2* double mutants. We identified gene expression changes using three algorithms, RMA+LIMMA, GCRMA+LIMMA, and Rosetta Resolver.

NOTE: Some of the data collected here is published in (Simon et al., 2008).

Methods

Preparation of worms and RNA extraction were performed by Dave Simon as described (Simon et al., 2008; Simon and Kaplan, 2008). He prepared triplicate samples for N2 wild type, *mir-1* mutants, and *mef-2* mutants. Microarray experiments to determine gene expression, and computation analysis were performed as described for the *unc-55* microarrays (Chapter 3).

Microarray processing was conducted at the Biopolymers Facility at Harvard Medical School. RNA quality was first confirmed using an RNA 6000 Nano chip on an Agilent 2100 Bioanalyzer according to manufacturer's instructions (Agilent Technologies, Waldbronn, Germany). One-cycle cDNA synthesis, cleanup of double-stranded cDNA, biotin IVT labeling of antisense cRNA, cleanup of biotinylated cRNA, and fragmentation were carried out according to Affymetrix GeneChip Expression Analysis Technical Manual instructions (P/N 702232 Rev. 2). Labeled and fragmented cRNA was hybridized to Affymetrix GeneChip *C. elegans* Genome Arrays in a GeneChip 640 Hybridization Oven, which were then washed and stained in a GeneChip 400 Fluidics station, and scanned with a 7G GeneChip 3000 Scanner (Affymetrix, Inc). Scanned images were converted into probeset data files using Affymetrix Gene Chip Operating Software.

Standard quality control procedures were performed using the Affy package in Bioconductor, implemented in the R statistical computing environment (http://www.bioconductor.org; R version 2.4.1). The quality of data from replicate samples was also checked using least-squares regression ($R^2 > 0.95$) in Rosetta Resolver v7.0 (Rosetta Biosoftware, Seattle, WA). For analysis, the nine probeset data files were

normalized using the Robust Multichip Average method (RMA) and the GeneChip RMA method (GCRMA)(Irizarry et al., 2003; Wu et al., 2004; Wu and Irizarry, 2004). Replicates were combined and differentially expressed genes were identified using the Linear Models for Microarray Data approach (LIMMA) (Fig D.1)(Smyth, 2004). These calculations were implemented using Bioconductor packages (Affy package 1.12.2; GCRMA package 2.6.0; LIMMA package 2.9.8). The probeset data files were also analyzed using the integrated RatioBuild pipeline in Resolver. Genes were classified as differentially expressed if the fold change p-value was less than 0.01 using any methodology. Genes were annotated as *mir-1/mef-2* correlated or anti-correlated if they changed with $p < 0.01$ in one mutant compared to N2, and with $p < 0.05$ in the other mutant compared to N2.

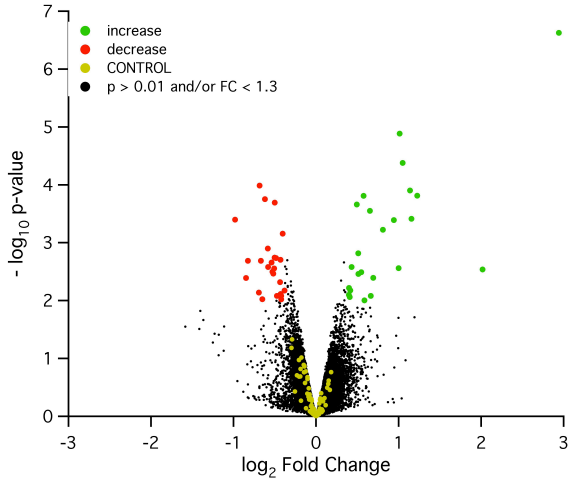

Fig D.1. Volcano plot of genes differentially expressed in *mir-1* versus N2. RMA+LIMMA analysis shown, with p<0.01 and FC>1.3 thresholds. Controls in yellow include polyA reverse transcription controls spiked into the RNA sample, hybridization spiked-in controls, and endogenous *C. elegans* maintenance genes.

Using all three analysis algorithms, setting thresholds of fold change > 1.3 and p-value < 0.01, we identified 65 probesets that increased in *mir-1* and 66 probesets that decreased in *mir-1* compared to wild type. We identified 211 probesets that increased in

mef-2 mutants and 151 probesets that decreased in *mef-2* mutants using $p < 0.01$ thresholds.

We also isolated RNA from triplicate samples of *mir-1; mef-2* double mutant animals. The RNA for the wild type, *mir-1,* and *mef-2* samples were collected and analyzed in June 2007, while the RNA for the *mir-1; mef-2* double mutant was collected and analyzed in January 2008. This resulted in differences between the samples. The signal from the three *mir-1; mef-2* arrays was brighter than for the three *mir-1* microarrays (Fig D.2).

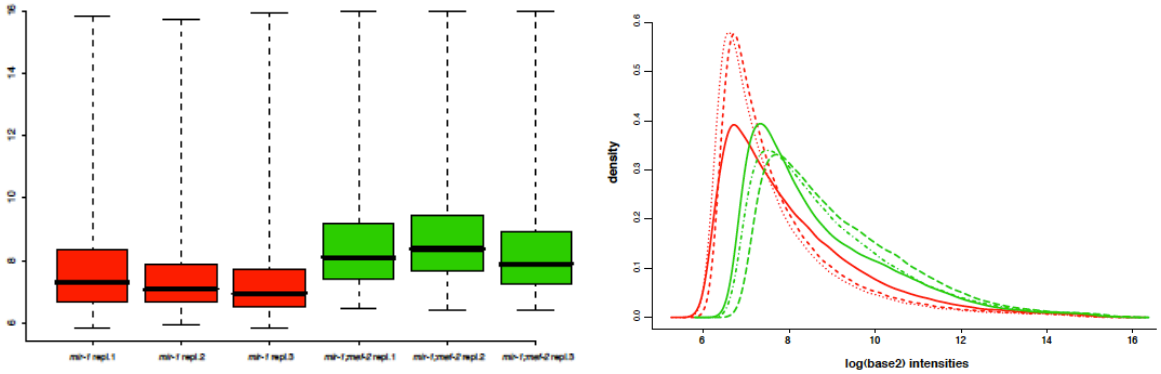

Fig D.2. Signal intensity from *mir-1* and *mir-1; mef-2* microarrays. Boxplots (left) and histograms (right) both show significant differences in raw signal intensity between *mir-1* (red) and *mir1; mef-2* (green) microarrays.

Normalization methods RMA, GCRMA, and as implemented by Rosetta Resolver all addressed these changes in signal. However, subsequent analysis indicated that polyA RT controls were significantly differentially expressed following all three analysis algorithms (RMA shown as an example, Fig D.3).

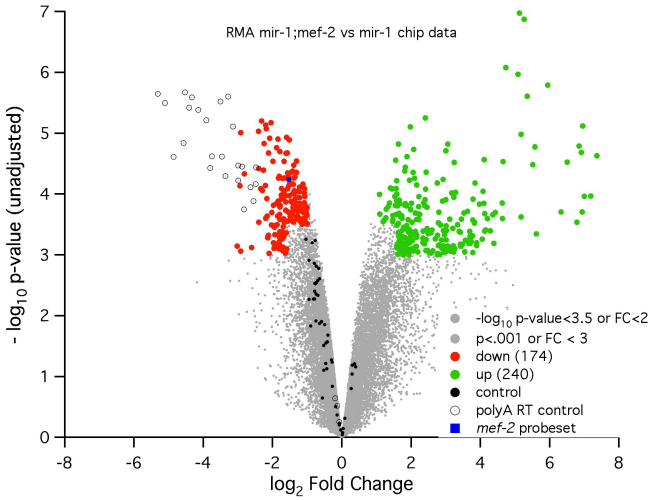

Fig D.3. Volcano plot of genes differentially expressed between *mir-1;mef-2* and *mir-1*. RMA normalization + LIMMA determination of changes in gene expression between *mir-1* and *mir-1; mef-2*.

PolyA controls (open circles) are *B. subtilis* genes absent from eukaryotic genomes, which are spiked into the RNA sample before one cycle reverse transcription. Protocols at the Quad BioPolymers Facility did not change in this period, however polyA RT controls were from different batches. Different amounts of polyA RT controls may have been spiked into the RNA samples, or reverse transcription may have been more or less efficient for different experiments. The other controls (black circles), including spiked-in hybridization controls and endogenous *C. elegans* maintenance genes (GAPDH, catalase, actin, and gly14), did not significantly change. Note that the probeset detecting *mef-2* showed significantly lower expression in the *mir-1;mef-2* double mutants compared to the *mir-1* mutants samples.

REFERENCES

Abbott, A.L., Alvarez-Saavedra, E., Miska, E.A., Lau, N.C., Bartel, D.P., Horvitz, H.R., and Ambros, V. (2005). The let-7 MicroRNA family members mir-48, mir-84, and mir-241 function together to regulate developmental timing in Caenorhabditis elegans. Developmental Cell *9*, 403–414.

Abrahante, J.E., Daul, A.L., Li, M., Volk, M.L., Tennessen, J.M., Miller, E.A., and Rougvie, A.E. (2003). The Caenorhabditis elegans hunchback-like gene lin-57/hbl-1 controls developmental time and is regulated by microRNAs. Developmental Cell *4*, 625–637.

Ahmari, S.E., Buchanan, J., and Smith, S.J. (2000). Assembly of presynaptic active zones from cytoplasmic transport packets. Nat Neurosci *3*, 445–451.

Ambros, V., and Horvitz, H.R. (1984). Heterochronic mutants of the nematode Caenorhabditis elegans. Science *226*, 409–416.

Ambros, V., and Horvitz, H.R. (1987). The lin-14 locus of Caenorhabditis elegans controls the time of expression of specific postembryonic developmental events. Genes & Development *1*, 398–414.

Arikkath, J., and Reichardt, L.F. (2008). Cadherins and catenins at synapses: roles in synaptogenesis and synaptic plasticity. Trends Neurosci *31*, 487–494.

Armentano, M., Chou, S.-J., Tomassy, G.S., Leingärtner, A., O'Leary, D.D.M., and Studer, M. (2007). COUP-TFI regulates the balance of cortical patterning between frontal/motor and sensory areas. Nat Neurosci *10*, 1277–1286.

Avram, D., Fields, A., Pretty On Top, K., Nevrivy, D.J., Ishmael, J.E., and Leid, M. (2000). Isolation of a novel family of C(2)H(2) zinc finger proteins implicated in transcriptional repression mediated by chicken ovalbumin upstream promoter transcription factor (COUP-TF) orphan nuclear receptors. J Biol Chem *275*, 10315–10322.

Bamber, B.A., Beg, A.A., Twyman, R.E., and Jorgensen, E.M. (1999). The Caenorhabditis elegans unc-49 locus encodes multiple subunits of a heteromultimeric GABA receptor. J Neurosci *19*, 5348–5359.

Bamber, B.A., Richmond, J.E., Otto, J.F., and Jorgensen, E.M. (2005). The composition of the GABA receptor at the Caenorhabditis elegans neuromuscular junction. Br. J. Pharmacol. *144*, 502–509.

Barnes, T., and Hekimi, S. (1996). THE CAT SSA TON AMA T (with apologies to SB). Worm Breeder's Gazette *14*, 26.

Ben-Ari, Y. (2002). Excitatory actions of gaba during development: the nature of the

nurture. Nat Rev Neurosci *3*, 728–739.

Bethke, A., Fielenbach, N., Wang, Z., Mangelsdorf, D.J., and Antebi, A. (2009). Nuclear hormone receptor regulation of microRNAs controls developmental progression. Science *324*, 95–98.

Bolstad, B.M., Irizarry, R.A., Astrand, M., and Speed, T.P. (2003). A comparison of normalization methods for high density oligonucleotide array data based on variance and bias. Bioinformatics *19*, 185–193.

Bosman, L.W.J., and Konnerth, A. (2009). Activity-dependent plasticity of developing climbing fiber-Purkinje cell synapses. Neuroscience *162*, 612–623.

Brenner, S. (1974). The genetics of Caenorhabditis elegans. Genetics *77*, 71–94.

Burbea, M., Dreier, L., Dittman, J.S., Grunwald, M.E., and Kaplan, J.M. (2002). Ubiquitin and AP180 regulate the abundance of GLR-1 glutamate receptors at postsynaptic elements in C. elegans. Neuron *35*, 107–120.

Caygill, E.E., and Johnston, L.A. (2008). Temporal regulation of metamorphic processes in Drosophila by the let-7 and miR-125 heterochronic microRNAs. Curr Biol *18*, 943–950.

Chattopadhyaya, B., Di Cristo, G., Wu, C.Z., Knott, G., Kuhlman, S., Fu, Y., Palmiter, R.D., and Huang, Z.J. (2007). GAD67-mediated GABA synthesis and signaling regulate inhibitory synaptic innervation in the visual cortex. Neuron *54*, 889–903.

Chiu, S.-L., and Cline, H.T. (2010). Insulin receptor signaling in the development of neuronal structure and function. Neural Dev *5*, 7.

Chiu, S.-L., Chen, C.-M., and Cline, H.T. (2008). Insulin receptor signaling regulates synapse number, dendritic plasticity, and circuit function in vivo. Neuron *58*, 708–719.

Chung, W.-S., and Barres, B.A. (2011). The role of glial cells in synapse elimination. Current Opinion in Neurobiology.

Cinar, H., Keles, S., and Jin, Y. (2005). Expression profiling of GABAergic motor neurons in Caenorhabditis elegans. Curr Biol *15*, 340–346.

Cleary, M.D., and Doe, C.Q. (2006). Regulation of neuroblast competence: multiple temporal identity factors specify distinct neuronal fates within a single early competence window. Genes & Development *20*, 429–434.

Cohen, S., and Greenberg, M.E. (2008). Communication between the synapse and the nucleus in neuronal development, plasticity, and disease. Annu. Rev. Cell. Dev. Biol. *24*, 183–209.

Collet, J., Spike, C.A., Lundquist, E.A., Shaw, J.E., and Herman, R.K. (1998). Analysis of osm-6, a gene that affects sensory cilium structure and sensory neuron function in Caenorhabditis

elegans. Genetics *148*, 187–200.

Crump, J.G., Zhen, M., Jin, Y., and Bargmann, C.I. (2001). The SAD-1 kinase regulates presynaptic vesicle clustering and axon termination. Neuron *29*, 115–129.

Dai, Y., Taru, H., Deken, S.L., Grill, B., Ackley, B., Nonet, M.L., and Jin, Y. (2006). SYD-2 Liprin-alpha organizes presynaptic active zone formation through ELKS. Nat Neurosci *9*, 1479–1487.

Ding, M., Chao, D., Wang, G., and Shen, K. (2007). Spatial regulation of an E3 ubiquitin ligase directs selective synapse elimination. Science *317*, 947–951.

Dittman, J.S., and Kaplan, J.M. (2006). Factors regulating the abundance and localization of synaptobrevin in the plasma membrane. Proc Natl Acad Sci USA *103*, 11399–11404.

Dixon, S.J., Alexander, M., Chan, K.K.M., and Roy, P.J. (2008). Insulin-like signaling negatively regulates muscle arm extension through DAF-12 in Caenorhabditis elegans. Dev Biol *318*, 153–161.

Dixon, S.J., and Roy, P.J. (2005). Muscle arm development in Caenorhabditis elegans. Development *132*, 3079–3092.

Dybbs, M., Ngai, J., and Kaplan, J.M. (2005). Using microarrays to facilitate positional cloning: identification of tomosyn as an inhibitor of neurosecretion. PLoS Genet *1*, 6–16.

Elkes, D.A., Cardozo, D.L., Madison, J., and Kaplan, J.M. (1997). EGL-36 Shaw channels regulate C. elegans egg-laying muscle activity. Neuron *19*, 165–174.

Elliott, J., Jolicoeur, C., Ramamurthy, V., and Cayouette, M. (2008). Ikaros confers early temporal competence to mouse retinal progenitor cells. Neuron *60*, 26–39.

Esquela-Kerscher, A., Johnson, S.M., Bai, L., Saito, K., Partridge, J., Reinert, K.L., and Slack, F.J. (2005). Post-embryonic expression of C. elegans microRNAs belonging to the lin-4 and let-7 families in the hypodermis and the reproductive system. Dev Dyn *234*, 868–877.

Fay, D.S., Stanley, H.M., Han, M., and Wood, W.B. (1999). A Caenorhabditis elegans homologue of hunchback is required for late stages of development but not early embryonic patterning. Dev Biol *205*, 240–253.

Fineberg, S.K., Kosik, K.S., and Davidson, B.L. (2009). MicroRNAs potentiate neural development. Neuron *64*, 303–309.

Fiore, R., Siegel, G., and Schratt, G. (2008). MicroRNA function in neuronal development, plasticity and disease. Biochim Biophys Acta *1779*, 471–478.

Frand, A.R., Russel, S., and Ruvkun, G. (2005). Functional genomic analysis of C. elegans molting. Plos Biol *3*, e312.

Frasch, M. (2008). A matter of timing: microRNA-controlled temporal identities in worms and flies. Genes & Development *22*, 1572–1576.

Fritschy, J.-M., Panzanelli, P., and Tyagarajan, S.K. (2012). Molecular and functional heterogeneity of GABAergic synapses. Cell Mol Life Sci.

Gally, C., and Bessereau, J.-L. (2003). GABA is dispensable for the formation of junctional GABA receptor clusters in Caenorhabditis elegans. J Neurosci *23*, 2591–2599.

Garner, C.C., Waites, C.L., and Ziv, N.E. (2006). Synapse development: still looking for the forest, still lost in the trees. Cell Tissue Res *326*, 249–262.

Goda, Y., and Davis, G.W. (2003). Mechanisms of synapse assembly and disassembly. Neuron *40*, 243–264.

Gracheva, E.O., Burdina, A.O., Holgado, A.M., Berthelot-Grosjean, M., Ackley, B.D., Hadwiger, G., Nonet, M.L., Weimer, R.M., and Richmond, J.E. (2006). Tomosyn inhibits synaptic vesicle priming in Caenorhabditis elegans. Plos Biol *4*, e261.

Grosshans, H., Johnson, T., Reinert, K.L., Gerstein, M., and Slack, F.J. (2005). The temporal patterning microRNA let-7 regulates several transcription factors at the larval to adult transition in C. elegans. Developmental Cell *8*, 321–330.

Grosskortenhaus, R., Pearson, B.J., Marusich, A., and Doe, C.Q. (2005). Regulation of temporal identity transitions in Drosophila neuroblasts. Developmental Cell *8*, 193–202.

Grutzendler, J., Kasthuri, N., and Gan, W.-B. (2002). Long-term dendritic spine stability in the adult cortex. Nature *420*, 812–816.

Hall, D.H., and Hedgecock, E.M. (1991). Kinesin-related gene unc-104 is required for axonal transport of synaptic vesicles in C. elegans. Cell *65*, 837–847.

Hallam, S.J., and Jin, Y. (1998). Lin-14 regulates the timing of synaptic remodelling in Caenorhabditis elegans. Nature *395*, 78–82.

Hallam, S.J., Goncharov, A., McEwen, J.M., Baran, R., and Jin, Y. (2002). SYD-1, a presynaptic protein with PDZ, C2 and rhoGAP-like domains, specifies axon identity in C. elegans. Nat Neurosci *5*, 1137–1146.

Hammell, C.M., Karp, X., and Ambros, V. (2009). A feedback circuit involving let-7-family miRNAs and DAF-12 integrates environmental signals and developmental timing in Caenorhabditis elegans. Proc Natl Acad Sci USA *106*, 18668–18673.

Hayes, G.D., Frand, A.R., and Ruvkun, G. (2006). The mir-84 and let-7 paralogous microRNA genes of Caenorhabditis elegans direct the cessation of molting via the conserved nuclear hormone receptors NHR-23 and NHR-25. Development *133*, 4631–4641.

Hensch, T.K. (2004). Critical period regulation. Annu Rev Neurosci *27*, 549–579.

Hensch, T.K. (2005). Critical period plasticity in local cortical circuits. Nat Rev Neurosci *6*, 877–888.

Hensch, T.K., Fagiolini, M., Mataga, N., Stryker, M.P., Baekkeskov, S., and Kash, S.F. (1998). Local GABA circuit control of experience-dependent plasticity in developing visual cortex. Science *282*, 1504–1508.

Holtmaat, A., and Svoboda, K. (2009). Experience-dependent structural synaptic plasticity in the mammalian brain. Nat Rev Neurosci *10*, 647–658.

Holtmaat, A.J.G.D., Trachtenberg, J.T., Wilbrecht, L., Shepherd, G.M., Zhang, X., Knott, G.W., and Svoboda, K. (2005). Transient and persistent dendritic spines in the neocortex in vivo. Neuron *45*, 279–291.

Hong, Y.K., and Chen, C. (2011). Wiring and rewiring of the retinogeniculate synapse. Current Opinion in Neurobiology *21*, 228–237.

Hu, P.J. (2007). Dauer. WormBook : the Online Review of C Elegans Biology 1–19.

Hua, J.Y., and Smith, S.J. (2004). Neural activity and the dynamics of central nervous system development. Nat Neurosci *7*, 327–332.

Huang, Z.J., and Scheiffele, P. (2008). GABA and neuroligin signaling: linking synaptic activity and adhesion in inhibitory synapse development. Current Opinion in Neurobiology *18*, 77–83.

Huang, Z.J., Kirkwood, A., Pizzorusso, T., Porciatti, V., Morales, B., Bear, M.F., Maffei, L., and Tonegawa, S. (1999). BDNF regulates the maturation of inhibition and the critical period of plasticity in mouse visual cortex. Cell *98*, 739–755.

Huh, G.S., Boulanger, L.M., Du, H., Riquelme, P.A., Brotz, T.M., and Shatz, C.J. (2000). Functional requirement for class I MHC in CNS development and plasticity. Science *290*, 2155–2159.

Hunt-Newbury, R., Viveiros, R., Johnsen, R., Mah, A., Anastas, D., Fang, L., Halfnight, E., Lee, D., Lin, J., Lorch, A., et al. (2007). High-throughput in vivo analysis of gene expression in Caenorhabditis elegans. Plos Biol *5*, e237.

Husson, S.J., Clynen, E., Baggerman, G., Janssen, T., and Schoofs, L. (2006). Defective processing of neuropeptide precursors in Caenorhabditis elegans lacking proprotein convertase 2 (KPC-2/EGL-3): mutant analysis by mass spectrometry. J Neurochem *98*, 1999–2012.

Husson, S.J., Janssen, T., Baggerman, G., Bogert, B., Kahn-Kirby, A.H., Ashrafi, K., and Schoofs, L. (2007). Impaired processing of FLP and NLP peptides in carboxypeptidase E (EGL-21)-deficient Caenorhabditis elegans as analyzed by mass spectrometry. J Neurochem *102*, 246–260.

Irizarry, R.A., Hobbs, B., Collin, F., Beazer-Barclay, Y.D., Antonellis, K.J., Scherf, U., and Speed, T.P. (2003). Exploration, normalization, and summaries of high density oligonucleotide array probe level data. Biostatistics (Oxford, England) *4*, 249–264.

Isshiki, T., Pearson, B., Holbrook, S., and Doe, C.Q. (2001). Drosophila neuroblasts sequentially express transcription factors which specify the temporal identity of their neuronal progeny. Cell *106*, 511–521.

Jacob, T.C., and Kaplan, J.M. (2003). The EGL-21 carboxypeptidase E facilitates acetylcholine release at Caenorhabditis elegans neuromuscular junctions. Journal of Neuroscience *23*, 2122–2130.

Jiang, B., Treviño, M., and Kirkwood, A. (2007). Sequential development of long-term potentiation and depression in different layers of the mouse visual cortex. J Neurosci *27*, 9648–9652.

Jin, Y., Hoskins, R., and Horvitz, H.R. (1994). Control of type-D GABAergic neuron differentiation by C. elegans UNC-30 homeodomain protein. Nature *372*, 780–783.

Jin, Y., Jorgensen, E., Hartwieg, E., and Horvitz, H.R. (1999). The Caenorhabditis elegans gene unc-25 encodes glutamic acid decarboxylase and is required for synaptic transmission but not synaptic development. J Neurosci *19*, 539–548.

Jorgensen, E.M. (2005). GABA. WormBook : the Online Review of C Elegans Biology 1–13.

Kanai, M.I., Okabe, M., and Hiromi, Y. (2005). seven-up Controls switching of transcription factors that specify temporal identities of Drosophila neuroblasts. Developmental Cell *8*, 203–213.

Kanatani, S., Yozu, M., Tabata, H., and Nakajima, K. (2008). COUP-TFII is preferentially expressed in the caudal ganglionic eminence and is involved in the caudal migratory stream. J Neurosci *28*, 13582–13591.

Karp, X., and Ambros, V. (2011). The developmental timing regulator HBL-1 modulates the dauer formation decision in Caenorhabditis elegans. Genetics *187*, 345–353.

Kass, J., Jacob, T.C., Kim, P., and Kaplan, J.M. (2001). The EGL-3 proprotein convertase regulates mechanosensory responses of Caenorhabditis elegans. Journal of Neuroscience *21*, 9265–9272.

Kauffman, A.L., Ashraf, J.M., Corces-Zimmerman, M.R., Landis, J.N., and Murphy, C.T. (2010). Insulin signaling and dietary restriction differentially influence the decline of learning and memory with age. Plos Biol *8*, e1000372.

Kennedy, S., Wang, D., and Ruvkun, G. (2004). A conserved siRNA-degrading RNase negatively regulates RNA interference in C. elegans. Nature *427*, 645–649.

Kim, B.J., Takamoto, N., Yan, J., Tsai, S.Y., and Tsai, M.-J. (2009a). Chicken Ovalbumin Upstream Promoter-Transcription Factor II (COUP-TFII) regulates growth and patterning of the postnatal mouse cerebellum. Dev Biol *326*, 378–391.

Kim, J.S.M., Hung, W., Narbonne, P., Roy, R., and Zhen, M. (2009b). C. elegans STRAD and SAD cooperatively regulate neuronal polarity and synaptic organization. Development *137*, 93–102.

Kim, J.S.M., Lilley, B.N., Zhang, C., Shokat, K.M., Sanes, J.R., and Zhen, M. (2008). A chemical-genetic strategy reveals distinct temporal requirements for SAD-1 kinase in neuronal polarization and synapse formation. Neural Dev *3*, 23.

Kneussel, M., Brandstätter, J.H., Laube, B., Stahl, S., Müller, U., and Betz, H. (1999). Loss of postsynaptic GABA(A) receptor clustering in gephyrin-deficient mice. Journal of Neuroscience *19*, 9289–9297.

Knott, G.W., Holtmaat, A., Wilbrecht, L., Welker, E., and Svoboda, K. (2006). Spine growth precedes synapse formation in the adult neocortex in vivo. Nat Neurosci *9*, 1117–1124.

Koch, I., Schwarz, H., Beuchle, D., Goellner, B., Langegger, M., and Aberle, H. (2008). Drosophila ankyrin 2 is required for synaptic stability. Neuron *58*, 210–222.

Kohsaka, H., and Nose, A. (2009). Target recognition at the tips of postsynaptic filopodia: accumulation and function of Capricious. Development *136*, 1127–1135.

Kuo, C.T., Jan, L.Y., and Jan, Y.N. (2005). Dendrite-specific remodeling of Drosophila sensory neurons requires matrix metalloproteases, ubiquitin-proteasome, and ecdysone signaling. Proc Natl Acad Sci USA *102*, 15230–15235.

Kuo, C.T., Zhu, S., Younger, S., Jan, L.Y., and Jan, Y.N. (2006). Identification of E2/E3 ubiquitinating enzymes and caspase activity regulating Drosophila sensory neuron dendrite pruning. Neuron *51*, 283–290.

Kwon, H.-B., and Sabatini, B.L. (2011). Glutamate induces de novo growth of functional spines in developing cortex. Nature *474*, 100–104.

Lai, C.S.W., Franke, T.F., and Gan, W.-B. (2012). Opposite effects of fear conditioning and extinction on dendritic spine remodelling. Nature *483*, 87–91.

Landis, J.N., and Murphy, C.T. (2010). Integration of diverse inputs in the regulation of Caenorhabditis elegans DAF-16/FOXO. Dev Dyn *239*, 1405–1412.

Lee, R.Y., Hench, J., and Ruvkun, G. (2001). Regulation of C. elegans DAF-16 and its human ortholog FKHRL1 by the daf-2 insulin-like signaling pathway. Curr Biol *11*, 1950–1957.

Lee, S.S., Kennedy, S., Tolonen, A.C., and Ruvkun, G. (2003). DAF-16 target genes that control C. elegans life-span and metabolism. Science *300*, 644–647.

Lee, T., Marticke, S., Sung, C., Robinow, S., and Luo, L. (2000). Cell-autonomous requirement of the USP/EcR-B ecdysone receptor for mushroom body neuronal remodeling in Drosophila. Neuron *28*, 807–818.

Liao, E.H., and Zhen, M. (2008). Dissertation: The F-box protein FSN-1 functions in an SCF-like Ubiquitin Ligase Complex to regulate synapse formation. 1–228.

Lin, F.-J., Qin, J., Tang, K., Tsai, S.Y., and Tsai, M.-J. (2011). Coup d'Etat: an orphan takes control. Endocr Rev *32*, 404–421.

Lin, K., Hsin, H., Libina, N., and Kenyon, C. (2001). Regulation of the Caenorhabditis elegans longevity protein DAF-16 by insulin/IGF-1 and germline signaling. Nat Genet *28*, 139–145.

Lin, S.-Y., Johnson, S.M., Abraham, M., Vella, M.C., Pasquinelli, A., Gamberi, C., Gottlieb, E., and Slack, F.J. (2003). The C elegans hunchback homolog, hbl-1, controls temporal patterning and is a probable microRNA target. Developmental Cell *4*, 639–650.

Lin, Y., Bloodgood, B.L., Hauser, J.L., Lapan, A.D., Koon, A.C., Kim, T.-K., Hu, L.S., Malik, A.N., and Greenberg, M.E. (2008). Activity-dependent regulation of inhibitory synapse development by Npas4. Nature *455*, 1198–1204.

Lonze, B.E., and Ginty, D.D. (2002). Function and regulation of CREB family transcription factors in the nervous system. Neuron *35*, 605–623.

Luo, L., and O'Leary, D.D.M. (2005). Axon retraction and degeneration in development and disease. Annu Rev Neurosci *28*, 127–156.

Marin, E.C., Watts, R.J., Tanaka, N.K., Ito, K., and Luo, L. (2005). Developmentally programmed remodeling of the Drosophila olfactory circuit. Development *132*, 725–737.

Mattis, J., Tye, K.M., Ferenczi, E.A., Ramakrishnan, C., O'Shea, D.J., Prakash, R., Gunaydin, L.A., Hyun, M., Fenno, L.E., Gradinaru, V., et al. (2011). Principles for applying optogenetic tools derived from direct comparative analysis of microbial opsins. Nat Meth *9*, 159–172.

McElwee, J., Bubb, K., and Thomas, J.H. (2003). Transcriptional outputs of the Caenorhabditis elegans forkhead protein DAF-16. Aging Cell *2*, 111–121.

McEwen, J.M., Madison, J.M., Dybbs, M., and Kaplan, J.M. (2006). Antagonistic regulation of synaptic vesicle priming by Tomosyn and UNC-13. Neuron *51*, 303–315.

McKay, S.J., Johnsen, R., Khattra, J., Asano, J., Baillie, D.L., Chan, S., Dube, N., Fang, L., Goszczynski, B., Ha, E., et al. (2003). Gene expression profiling of cells, tissues, and developmental stages of the nematode C. elegans. Cold Spring Harb Symp Quant Biol *68*, 159–169.

Melkman, T., and Sengupta, P. (2005). Regulation of chemosensory and GABAergic motor neuron development by the C. elegans Aristaless/Arx homolog alr-1. Development *132*,

1935–1949.

Mellios, N., Sugihara, H., Castro, J., Banerjee, A., Le, C., Kumar, A., Crawford, B., Strathmann, J., Tropea, D., Levine, S.S., et al. (2011). miR-132, an experience-dependent microRNA, is essential for visual cortex plasticity. Nat Neurosci *14*, 1240–1242.

Mettler, U., Vogler, G., and Urban, J. (2006). Timing of identity: spatiotemporal regulation of hunchback in neuroblast lineages of Drosophila by Seven-up and Prospero. Development *133*, 429–437.

Mikolas, P., Kostrouch, Z., and Kostrouchova, M. (2009). 868A: GEI-8: Possible nuclear hormone receptor corepressor in C. elegans. International Worm Meeting Abstract 1–1.

Millenaar, F.F., Okyere, J., May, S.T., Van Zanten, M., Voesenek, L.A.C.J., and Peeters, A.J.M. (2006). How to decide? Different methods of calculating gene expression from short oligonucleotide array data will give different results. BMC Bioinformatics *7*, 137.

Moss, E.G. (2007). Heterochronic genes and the nature of developmental time. Curr Biol *17*, R425–34.

Moss, S.J., and Smart, T.G. (2001). Constructing inhibitory synapses. Nat Rev Neurosci *2*, 240–250.

Mukhopadhyay, A., and Tissenbaum, H.A. (2007). Reproduction and longevity: secrets revealed by C. elegans. Trends in Cell Biology *17*, 65–71.

Murphy, C.T., McCarroll, S.A., Bargmann, C.I., Fraser, A., Kamath, R.S., Ahringer, J., Li, H., and Kenyon, C. (2003). Genes that act downstream of DAF-16 to influence the lifespan of Caenorhabditis elegans. Nature *424*, 277–283.

Naka, H., Nakamura, S., Shimazaki, T., and Okano, H. (2008). Requirement for COUP-TFI and II in the temporal specification of neural stem cells in CNS development. Nat Neurosci *11*, 1014–1023.

Nakata, K., Abrams, B., Grill, B., Goncharov, A., Huang, X., Chisholm, A.D., and Jin, Y. (2005). Regulation of a DLK-1 and p38 MAP kinase pathway by the ubiquitin ligase RPM-1 is required for presynaptic development. Cell *120*, 407–420.

Niwa, R., Hada, K., Moliyama, K., Ohniwa, R., Tan, Y., Olsson-Carter, K., Chi, W., Reinke, V., and Slack, F. (2009). C. elegans sym-1 is a downstream target of the hunchback-like-1 developmental timing transcription factor. Cell Cycle *8*.

Nolde, M.J., Saka, N., Reinert, K.L., and Slack, F.J. (2007). The Caenorhabditis elegans pumilio homolog, puf-9, is required for the 3'UTR-mediated repression of the let-7 microRNA target gene, hbl-1. Dev Biol *305*, 551–563.

Noutel, J., Hong, Y.K., Leu, B., Kang, E., and Chen, C. (2011). Experience-Dependent

Retinogeniculate Synapse Remodeling Is Abnormal in MeCP2-Deficient Mice. Neuron *70*, 35–42.

Oray, S., Majewska, A., and Sur, M. (2004). Dendritic Spine Dynamics Are Regulated by Monocular Deprivation and Extracellular Matrix Degradation. Neuron *44*, 1021–1030.

Ou, C.-Y., and Shen, K. (2011). Neuronal polarity in C. elegans. Devel Neurobio *71*, 554–566.

Ou, C.-Y., Poon, V.Y., Maeder, C.I., Watanabe, S., Lehrman, E.K., Fu, A.K.Y., Park, M., Fu, W.-Y., Jorgensen, E.M., Ip, N.Y., et al. (2010). Two cyclin-dependent kinase pathways are essential for polarized trafficking of presynaptic components. Cell *141*, 846–858.

Pan, F., and Gan, W.-B. (2008). Two-photon imaging of dendritic spine development in the mouse cortex. Devel Neurobio *68*, 771–778.

Park, M., and Krause, M.W. (1999). Regulation of postembryonic G(1) cell cycle progression in Caenorhabditis elegans by a cyclin D/CDK-like complex. Development *126*, 4849–4860.

Park, M., Watanabe, S., Poon, V.Y.N., Ou, C.-Y., Jorgensen, E.M., and Shen, K. (2011). CYY-1/Cyclin Y and CDK-5 Differentially Regulate Synapse Elimination and Formation for Rewiring Neural Circuits. Neuron *70*, 742–757.

Pasquinelli, A.E., and Ruvkun, G. (2002). Control of developmental timing by micrornas and their targets. Annu. Rev. Cell. Dev. Biol. *18*, 495–513.

Peckol, E.L., Zallen, J.A., Yarrow, J.C., and Bargmann, C.I. (1999). Sensory activity affects sensory axon development in C. elegans. Development *126*, 1891–1902.

Pereira, F.A., Tsai, M.J., and Tsai, S.Y. (2000). COUP-TF orphan nuclear receptors in development and differentiation. Cell Mol Life Sci *57*, 1388–1398.

Petersen, S.C., Watson, J.D., Richmond, J.E., Sarov, M., Walthall, W.W., and Miller, D.M. (2011). A transcriptional program promotes remodeling of GABAergic synapses in Caenorhabditis elegans. Journal of Neuroscience *31*, 15362–15375.

Pielage, J., Bulat, V., Zuchero, J.B., Fetter, R.D., and Davis, G.W. (2011). Hts/Adducin controls synaptic elaboration and elimination. Neuron *69*, 1114–1131.

Pielage, J., Cheng, L., Fetter, R.D., Carlton, P.M., Sedat, J.W., and Davis, G.W. (2008). A presynaptic giant ankyrin stabilizes the NMJ through regulation of presynaptic microtubules and transsynaptic cell adhesion. Neuron *58*, 195–209.

Purves, D., and Lichtman, J.W. (1980). Elimination of synapses in the developing nervous system. Science *210*, 153–157.

Rajagopalan, D. (2003). A comparison of statistical methods for analysis of high density oligonucleotide array data. Bioinformatics *19*, 1469–1476.

Reinhart, B.J., Slack, F.J., Basson, M., Pasquinelli, A.E., Bettinger, J.C., Rougvie, A.E., Horvitz, H.R., and Ruvkun, G. (2000). The 21-nucleotide let-7 RNA regulates developmental timing in Caenorhabditis elegans. Nature *403*, 901–906.

Richmond, J.E., and Jorgensen, E.M. (1999). One GABA and two acetylcholine receptors function at the C. elegans neuromuscular junction. Nat Neurosci *2*, 791–797.

Richmond, J.E., Davis, W.S., and Jorgensen, E.M. (1999). UNC-13 is required for synaptic vesicle fusion in C. elegans. Nat Neurosci *2*, 959–964.

Ritzenthaler, S., and Chiba, A. (2003). Myopodia (postsynaptic filopodia) participate in synaptic target recognition. J Neurobiol *55*, 31–40.

Ritzenthaler, S., Suzuki, E., and Chiba, A. (2000). Postsynaptic filopodia in muscle cells interact with innervating motoneuron axons. Nat Neurosci *3*, 1012–1017.

Rougvie, A.E. (2005). Intrinsic and extrinsic regulators of developmental timing: from miRNAs to nutritional cues. Development *132*, 3787–3798.

Roush, S., and Slack, F.J. (2008). The let-7 family of microRNAs. Trends in Cell Biology *18*, 505–516.

Roush, S.F., and Slack, F.J. (2009). Transcription of the C. elegans let-7 microRNA is temporally regulated by one of its targets, hbl-1. Dev Biol *334*, 523–534.

Rowland, A.M., Richmond, J.E., Olsen, J.G., Hall, D.H., and Bamber, B.A. (2006). Presynaptic terminals independently regulate synaptic clustering and autophagy of GABAA receptors in Caenorhabditis elegans. Journal of Neuroscience *26*, 1711–1720.

Sanes, J.R., and Lichtman, J.W. (1999). Development of the vertebrate neuromuscular junction. Annu Rev Neurosci *22*, 389–442.

Sanes, J.R., and Lichtman, J.W. (2001). Induction, assembly, maturation and maintenance of a postsynaptic apparatus. Nat Rev Neurosci *2*, 791–805.

Sanes, J.R., and Yamagata, M. (2009). Many paths to synaptic specificity. Annu. Rev. Cell. Dev. Biol. *25*, 161–195.

Satoh, S., Tang, K., Iida, A., Inoue, M., Kodama, T., Tsai, S.Y., Tsai, M.-J., Furuta, Y., and Watanabe, S. (2009). The spatial patterning of mouse cone opsin expression is regulated by bone morphogenetic protein signaling through downstream effector COUP-TF nuclear receptors. J Neurosci *29*, 12401–12411.

Schafer, D.P., and Stevens, B. (2010). Synapse elimination during development and disease: immune molecules take centre stage. Biochem. Soc. Trans *38*, 476.

Schmitz, C., Kinge, P., and Hutter, H. (2007). Axon guidance genes identified in a large-scale RNAi screen using the RNAi-hypersensitive Caenorhabditis elegans strain nre-1(hd20) lin-

15b(hd126). Proc Natl Acad Sci USA *104*, 834–839.

Scobie, K.N., Hall, B.J., Wilke, S.A., Klemenhagen, K.C., Fujii-Kuriyama, Y., Ghosh, A., Hen, R., and Sahay, A. (2009). Krüppel-like factor 9 is necessary for late-phase neuronal maturation in the developing dentate gyrus and during adult hippocampal neurogenesis. J Neurosci *29*, 9875–9887.

Shan, G., Kim, K., Li, C., and Walthall, W.W. (2005). Convergent genetic programs regulate similarities and differences between related motor neuron classes in Caenorhabditis elegans. Dev Biol *280*, 494–503.

Shapira, M., Zhai, R.G., Dresbach, T., Bresler, T., Torres, V.I., Gundelfinger, E.D., Ziv, N.E., and Garner, C.C. (2003). Unitary assembly of presynaptic active zones from Piccolo-Bassoon transport vesicles. Neuron *38*, 237–252.

Shen, K., and Bargmann, C.I. (2003). The immunoglobulin superfamily protein SYG-1 determines the location of specific synapses in C. elegans. Cell *112*, 619–630.

Shen, K., Fetter, R.D., and Bargmann, C.I. (2004). Synaptic specificity is generated by the synaptic guidepost protein SYG-2 and its receptor, SYG-1. Cell *116*, 869–881.

Sieburth, D., Madison, J.M., and Kaplan, J.M. (2007). PKC-1 regulates secretion of neuropeptides. Nat Neurosci *10*, 49–57.

Simon, D.J., and Kaplan, J.M. (2008). Dissertation: microRNA Regulation of Synapse Function in C. elegans. 1–159.

Simon, D.J., Madison, J.M., Conery, A.L., Thompson-Peer, K.L., Soskis, M., Ruvkun, G.B., Kaplan, J.M., and Kim, J.K. (2008). The MicroRNA miR-1 Regulates a MEF-2-Dependent Retrograde Signal at Neuromuscular Junctions. Cell *133*, 903–915.

Smyth, G.K. (2004). Linear models and empirical bayes methods for assessing differential expression in microarray experiments. Statistical Applications in Genetics and Molecular Biology *3*, Article3.

Sokol, N.S., Xu, P., Jan, Y.-N., and Ambros, V. (2008). Drosophila let-7 microRNA is required for remodeling of the neuromusculature during metamorphosis. Genes & Development *22*, 1591–1596.

Stevens, B., Allen, N.J., Vazquez, L.E., Howell, G.R., Christopherson, K.S., Nouri, N., Micheva, K.D., Mehalow, A.K., Huberman, A.D., Stafford, B., et al. (2007). The classical complement cascade mediates CNS synapse elimination. Cell *131*, 1164–1178.

Sugiyama, S., Di Nardo, A.A., Aizawa, S., Matsuo, I., Volovitch, M., Prochiantz, A., and Hensch, T.K. (2008). Experience-dependent transfer of Otx2 homeoprotein into the visual cortex activates postnatal plasticity. Cell *134*, 508–520.

Sugiyama, S., Prochiantz, A., and Hensch, T.K. (2009). From brain formation to plasticity: insights on Otx2 homeoprotein. Dev. Growth Differ. *51*, 369–377.

Sulston, J.E. (1976). Post-embryonic development in the ventral cord of Caenorhabditis elegans. Philos Trans R Soc Lond, B, Biol Sci *275*, 287–297.

Tang, K., Xie, X., Park, J.-I., Jamrich, M., Tsai, S., and Tsai, M.-J. (2010). COUP-TFs regulate eye development by controlling factors essential for optic vesicle morphogenesis. Development *137*, 725–734.

Thummel, C.S. (2001). Molecular mechanisms of developmental timing in C. elegans and Drosophila. Developmental Cell *1*, 453–465.

Tobin, D., Madsen, D., Kahn-Kirby, A., Peckol, E., Moulder, G., Barstead, R., Maricq, A., and Bargmann, C. (2002). Combinatorial expression of TRPV channel proteins defines their sensory functions and subcellular localization in C. elegans neurons. Neuron *35*, 307–318.

Tognini, P., Putignano, E., Coatti, A., and Pizzorusso, T. (2011). Experience-dependent expression of miR-132 regulates ocular dominance plasticity. Nat Neurosci *14*, 1237–1239.

Tomassy, G.S., De Leonibus, E., Jabaudon, D., Lodato, S., Alfano, C., Mele, A., Macklis, J.D., and Studer, M. (2010). Area-specific temporal control of corticospinal motor neuron differentiation by COUP-TFI. Proc Natl Acad Sci USA *107*, 3576–3581.

Trachtenberg, J.T., Chen, B.E., Knott, G.W., Feng, G., Sanes, J.R., Welker, E., and Svoboda, K. (2002). Long-term in vivo imaging of experience-dependent synaptic plasticity in adult cortex. Nature *420*, 788–794.

Tripodi, M., Filosa, A., Armentano, M., and Studer, M. (2004). The COUP-TF nuclear receptors regulate cell migration in the mammalian basal forebrain. Development *131*, 6119–6129.

Troemel, E.R., Chu, S.W., Reinke, V., Lee, S.S., Ausubel, F.M., and Kim, D.H. (2006). p38 MAPK regulates expression of immune response genes and contributes to longevity in C. elegans. PLoS Genet *2*, e183.

Tsai, S.Y., and Tsai, M.J. (1997). Chick ovalbumin upstream promoter-transcription factors (COUP-TFs): coming of age. Endocr Rev *18*, 229–240.

Tsuboi, D., Qadota, H., Kasuya, K., Amano, M., and Kaibuchi, K. (2002). Isolation of the interacting molecules with GEX-3 by a novel functional screening. Biochem Biophys Res Commun *292*, 697–701.

Urban, J., and Mettler, U. (2006). Connecting temporal identity to mitosis: the regulation of Hunchback in Drosophila neuroblast lineages. Cell Cycle *5*, 950–952.

Vardhanabhuti, S., Blakemore, S.J., Clark, S.M., Ghosh, S., Stephens, R.J., and Rajagopalan, D.

(2007). A comparison of statistical tests for detecting differential expression using Affymetrix oligonucleotide microarrays. Omics *10*, 555–566.

Vashlishan, A.B., and Kaplan, J.M. (2008). Dissertation: Identification and Characterization of Genes that Regulate GABA synapses. 1–167.

Vashlishan, A.B., Madison, J.M., Dybbs, M., Bai, J., Sieburth, D., Ch'ng, Q., Tavazoie, M., and Kaplan, J.M. (2008). An RNAi Screen Identifies Genes that Regulate GABA Synapses. Neuron *58*, 346–361.

Waites, C.L., Craig, A.M., and Garner, C.C. (2005). Mechanisms of vertebrate synaptogenesis. Annu Rev Neurosci *28*, 251–274.

Walsh, M.K., and Lichtman, J.W. (2003). In vivo time-lapse imaging of synaptic takeover associated with naturally occurring synapse elimination. Neuron *37*, 67–73.

Walthall, W.W. (1990). Metamorphic-like changes in the nervous system of the nematode Caenorhabditis elegans. J Neurobiol *21*, 1085–1091.

Walthall, W.W., and Plunkett, J.A. (1995). Genetic transformation of the synaptic pattern of a motoneuron class in Caenorhabditis elegans. J Neurosci *15*, 1035–1043.

Walthall, W.W., Li, L., Plunkett, J.A., and Hsu, C.Y. (1993). Changing synaptic specificities in the nervous system of Caenorhabditis elegans: differentiation of the DD motoneurons. J Neurobiol *24*, 1589–1599.

Wang, D., Kennedy, S., Conte, D., Kim, J.K., Gabel, H.W., Kamath, R.S., Mello, C.C., and Ruvkun, G. (2005). Somatic misexpression of germline P granules and enhanced RNA interference in retinoblastoma pathway mutants. Nature *436*, 593–597.

Wang, Z.W., Saifee, O., Nonet, M.L., and Salkoff, L. (2001). SLO-1 potassium channels control quantal content of neurotransmitter release at the C. elegans neuromuscular junction. Neuron *32*, 867–881.

Watts, R.J., Hoopfer, E.D., and Luo, L. (2003). Axon pruning during Drosophila metamorphosis: evidence for local degeneration and requirement of the ubiquitin-proteasome system. Neuron *38*, 871–885.

Watts, R.J., Schuldiner, O., Perrino, J., Larsen, C., and Luo, L. (2004). Glia engulf degenerating axons during developmental axon pruning. Curr Biol *14*, 678–684.

Weimer, R.M., Richmond, J.E., Davis, W.S., Hadwiger, G., Nonet, M.L., and Jorgensen, E.M. (2003). Defects in synaptic vesicle docking in unc-18 mutants. Nat Neurosci *6*, 1023–1030.

White, J., Southgate, E., Thomson, J.N., and Brenner, S. (1986). The structure of the nervous system of the nematode Caenorhabditis elegans: the mind of a worm. Philos Trans R Soc Lond, B, Biol Sci *314*, 1–340.

White, J.G., Albertson, D.G., and Anness, M.A. (1978). Connectivity changes in a class of motoneurone during the development of a nematode. Nature *271*, 764–766.

White, J.G., Southgate, E., Thomson, J.N., and Brenner, S. (1976). The structure of the ventral nerve cord of Caenorhabditis elegans. Philos Trans R Soc Lond, B, Biol Sci *275*, 327–348.

Wittenburg, N., and Baumeister, R. (1999). Thermal avoidance in Caenorhabditis elegans: an approach to the study of nociception. Proc Natl Acad Sci USA *96*, 10477–10482.

Wu, X., Fu, Y., Knott, G., Lu, J., Di Cristo, G., and Huang, Z.J. (2012). GABA Signaling Promotes Synapse Elimination and Axon Pruning in Developing Cortical Inhibitory Interneurons. Journal of Neuroscience *32*, 331–343.

Wu, Z., and Irizarry, R.A. (2004). Preprocessing of oligonucleotide array data. Nat. Biotechnol. *22*, 656–8; author reply 658.

Wu, Z., Irizarry, R., Gentleman, R., and Martinez-Murillo, F. (2004). A Model-Based Background Adjustment for Oligonucleotide Expression Arrays. Journal of the American Statistical Association.

Xu, H.-T., Pan, F., Yang, G., and Gan, W.-B. (2007). Choice of cranial window type for in vivo imaging affects dendritic spine turnover in the cortex. Nat Neurosci *10*, 549–551.

Yamagata, M., and Sanes, J.R. (2008). Dscam and Sidekick proteins direct lamina-specific synaptic connections in vertebrate retina. Nature *451*, 465–469.

Yamamoto, H., Williams, E.G., Mouchiroud, L., Cantó, C., Fan, W., Downes, M., Héligon, C., Barish, G.D., Desvergne, B., Evans, R.M., et al. (2011). NCoR1 is a conserved physiological modulator of muscle mass and oxidative function. Cell *147*, 827–839.

Yang, G., Pan, F., and Gan, W.-B. (2009). Stably maintained dendritic spines are associated with lifelong memories. Nature *462*, 920–924.

Zelhof, A.C., Yao, T.P., Chen, J.D., Evans, R.M., and McKeown, M. (1995). Seven-up inhibits ultraspiracle-based signaling pathways in vitro and in vivo. Mol Cell Biol *15*, 6736–6745.

Zhao, H., and Nonet, M.L. (2000). A retrograde signal is involved in activity-dependent remodeling at a C. elegans neuromuscular junction. Development *127*, 1253–1266.

Zhen, M., and Jin, Y. (1999). The liprin protein SYD-2 regulates the differentiation of presynaptic termini in C. elegans. Nature *401*, 371–375.

Zhou, B., Westaway, S.K., Levinson, B., Johnson, M.A., Gitschier, J., and Hayflick, S.J. (2001a). A novel pantothenate kinase gene (PANK2) is defective in Hallervorden-Spatz syndrome. Nat Genet *28*, 345–349.

Zhou, C., Tsai, S.Y., and Tsai, M.J. (2001b). COUP-TFI: an intrinsic factor for early regionalization of the neocortex. Genes & Development *15*, 2054–2059.

Zhou, H.M., and Walthall, W. (1997). Dissertation: Characterization of unc-55, a Gene Involved in Synaptic Differentiation of the Motorneurons in Caenorhabditis elegans. 112.

Zhou, H.M., and Walthall, W.W. (1998). UNC-55, an orphan nuclear hormone receptor, orchestrates synaptic specificity among two classes of motor neurons in Caenorhabditis elegans. J Neurosci *18*, 10438–10444.

Ziv, N.E., and Ahissar, E. (2009). Neuroscience: New tricks and old spines. Nature *462*, 859–861.

Ziv, N.E., and Garner, C.C. (2004). Cellular and molecular mechanisms of presynaptic assembly. Nat Rev Neurosci *5*, 385–399.